

Příloha 1

Urban T, Waldauf P, Krajčová A, Jiroutková K, Halačová M, Džupa V, Janoušek L, Pokorná E, Duška F.

Kinetic characteristics of propofol-induced inhibition of electron-transfer chain and fatty acid oxidation in human and rodent skeletal and cardiac muscles.

PLoS One. 2019 Oct 4;14(10):e0217254. doi: 10.1371/journal.pone.0217254. PMID: 31584947; PMCID: PMC6777831. IF 2.740

RESEARCH ARTICLE

Kinetic characteristics of propofol-induced inhibition of electron-transfer chain and fatty acid oxidation in human and rodent skeletal and cardiac muscles

Tomáš Urban¹, Petr Waldauf¹, Adéla Krajčová¹, Kateřina Jiroutková¹, Milada Halačová¹, Valér Džupa², Libor Janoušek³, Eva Pokorná⁴, František Duška^{1*}

1 OXYLAB – Mitochondrial Physiology Lab: Charles University, 3rd Faculty of Medicine and FNKV University Hospital, Prague, Czech Republic, **2** Department of Orthopaedics and Traumatology, Charles University, 3rd Faculty of Medicine and FNKV University Hospital, Prague, Czech Republic, **3** Transplantation Surgery Department, Institute for Clinical and Experimental Medicine, Prague, Czech Republic, **4** Department of Organ Recovery and Transplantation Databases, Institute for Clinical and Experimental Medicine, Prague, Czech Republic

* frantisek.duska@lf3.cuni.cz

OPEN ACCESS

Citation: Urban T, Waldauf P, Krajčová A, Jiroutková K, Halačová M, Džupa V, et al. (2019) Kinetic characteristics of propofol-induced inhibition of electron-transfer chain and fatty acid oxidation in human and rodent skeletal and cardiac muscles. PLoS ONE 14(10): e0217254. <https://doi.org/10.1371/journal.pone.0217254>

Editor: Yidong Bai, University of Texas Health Science Center at San Antonio, UNITED STATES

Received: May 5, 2019

Accepted: September 20, 2019

Published: October 4, 2019

Copyright: © 2019 Urban et al. This is an open access article distributed under the terms of the [Creative Commons Attribution License](https://creativecommons.org/licenses/by/4.0/), which permits unrestricted use, distribution, and reproduction in any medium, provided the original author and source are credited.

Data Availability Statement: Raw dataset is accessible in a public repository at <https://data.mendeley.com/datasets/h8jdkws4sv/draft?a=8421ed20-277e-44de-b6c4-5281fd55a6dc>.

Funding: The study was supported by Agentura pro zdravotnický výzkum (abbreviated AZV, translated as Grant agency for Healthcare Research), grant No 16-28663A.

Competing interests: The authors have declared that no competing interests exist.

Abstract

Introduction

Propofol causes a profound inhibition of fatty acid oxidation and reduces spare electron transfer chain capacity in a range of human and rodent cells and tissues—a feature that might be related to the pathogenesis of Propofol Infusion Syndrome. We aimed to explore the mechanism of propofol-induced alteration of bioenergetic pathways by describing its kinetic characteristics.

Methods

We obtained samples of skeletal and cardiac muscle from Wistar rat ($n = 3$) and human subjects: *vastus lateralis* from hip surgery patients ($n = 11$) and myocardium from brain-dead organ donors ($n = 10$). We assessed mitochondrial functional indices using standard SUI protocol and high resolution respirometry in fresh tissue homogenates with or without short-term exposure to a range of propofol concentration (2.5–100 $\mu\text{g/ml}$). After finding concentrations of propofol causing partial inhibition of a particular pathways, we used that concentration to construct kinetic curves by plotting oxygen flux against substrate concentration during its stepwise titration in the presence or absence of propofol. By spectrophotometry we also measured the influence of the same propofol concentrations on the activity of isolated respiratory complexes.

Results

We found that human muscle and cardiac tissues are more sensitive to propofol-mediated inhibition of bioenergetic pathways than rat's tissue. In human homogenates, palmitoyl carnitine-driven respiration was inhibited at much lower concentrations of propofol than that required for a reduction of electron transfer chain capacity, suggesting FAO inhibition

mechanism different from downstream limitation or carnitine-palmitoyl transferase-1 inhibition. Inhibition of Complex I was characterised by more marked reduction of V_{max} , in keeping with non-competitive nature of the inhibition and the pattern was similar to the inhibition of Complex II or electron transfer chain capacity. There was neither inhibition of Complex IV nor increased leak through inner mitochondrial membrane with up to 100 $\mu\text{g/ml}$ of propofol. If measured in isolation by spectrophotometry, propofol 10 $\mu\text{g/ml}$ did not affect the activity of any respiratory complexes.

Conclusion

In human skeletal and heart muscle homogenates, propofol in concentrations that are achieved in propofol-anaesthetized patients, causes a direct inhibition of fatty acid oxidation, in addition to inhibiting flux of electrons through inner mitochondrial membrane. The inhibition is more marked in human as compared to rodent tissues.

Introduction

Propofol is a short-acting hypnotic agent, which is reportedly administered to 100 millions of patients each year and which had been on the WHO list of most essential drugs for more than 10 years[1]. However, in last three decades, fatal complications of propofol administration were reported and defined as Propofol infusion syndrome (PRIS)[2,3]. The syndrome typically includes metabolic acidosis, arrhythmias, ECG changes, hyperlipidaemia, fever, hepatomegaly, rhabdomyolysis, cardiac and/or renal failure. Risk of developing PRIS increases with higher dose and duration of infusion[4], and several studies in animals[5–9] and humans[10], [11–13] suggest that this syndrome might be an extreme manifestation in susceptible individuals of propofol inhibitory effect on fatty acid oxidation (FAO) and/or electron-transfer chain. Vanlander et al. in a study on rodents[14] first brought evidence for a hypothesis, that due to structural similarity of propofol and Coenzyme Q (CoQ), at least some effects of propofol on bioenergetics are caused by the inhibition of CoQ-dependent electron transfer pathways. Other mechanisms are possible, too, including metabolic rearrangement at translational level [15,16]. It is unknown whether increased concentration of substrates can overcome propofol-induced inhibition, a feature that would point towards competition of propofol with the respective substrate, or whether the presence of propofol influences the maximum flux through the ETC, which would point towards inhibition outside the substrate-binding sites of the enzymes or an interruption of electron flux through the respiratory chain, such as at the level of CoQ.

The insight into the mechanisms of propofol toxicity was mostly obtained from experiments in animals and it is currently unknown whether effects of propofol can be reproduced in human tissues. In this study, we assessed propofol-effect on energy metabolism in skeletal and heart muscle in humans and rats. We aimed to (1.) clarify the inter-species differences in the effect of propofol and (2.) elucidate the Michaelis-Menten characteristics of propofol-induced inhibition of metabolic pathways that will have been found to be inhibited by propofol. In order to maximise biological plausibility of our results, we performed our key experiments on tissue homogenates containing mitochondrial networks in cytosolic context[17].

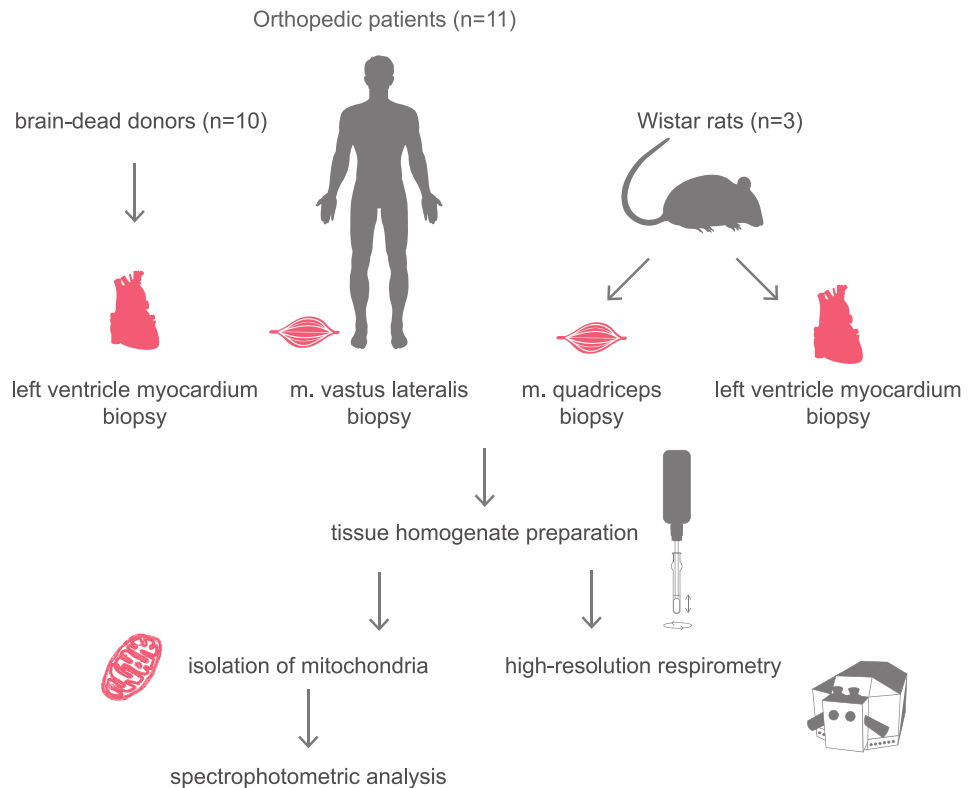


Fig 1. Study protocol overview.

<https://doi.org/10.1371/journal.pone.0217254.g001>

Methods

Overview of study design

Firstly, by using respirometry in fresh homogenates of skeletal and cardiac muscle of rat and man, we have determined the concentrations of propofol, which are able to inhibit electron transfer chain and its particular complexes. Secondly, by using the concentration found to cause a submaximal inhibition we performed substrate-titration experiments and described Michael-Menten characteristics of such an inhibition. Lastly, we isolated mitochondria and used spectrophotometry to determine direct effect of propofol on respiratory complexes in isolation. Overall study design is shown in [Fig 1](#).

Skeletal and heart muscle samples

All experiments were performed *ex vivo*, with all the respirometry measurement being done on fresh tissue homogenates. Human skeletal muscle biopsies were obtained from *m. vastus lateralis* (~300 mg) from metabolically healthy volunteers (n = 11, 4 males, 7 females, aged 63±10 years) undergoing hip replacement surgery at Department of Orthopaedic Surgery in FNKV University Hospital in Prague. We excluded both patients receiving propofol anaesthesia during surgery and patients with history of mitochondrial disorder, diabetes mellitus or any other metabolic disease except treated stable hypothyroidism. Human heart muscle

biopsies (~ 100 mg) were taken from left ventricle myocardium from brain-dead donors (n = 10), whose hearts were not suitable for transplantation due to donor age over 50 years or due to logistical reasons, at the Transplant Centre of Institute of Clinical and Experimental Medicine in Prague, Czech Republic. All skeletal muscle donors gave a prospective written informed consent. In brain dead donors, organ retrieval consent process was performed in accordance with Czech legal and ethical requirements and the need for specific informed consent for this study was waived by Research Ethics Board Fakultni Nemocnice Kralovske Vinohrady on 2nd November 2016 (Decision EK-VP/49/0/2016), which also reviewed and approved the protocol of the study. Detailed characteristics of brain-dead donor subjects are in Table A in [S1 File](#). None of the brain-dead donors had an unstable cardiac disease, 2 subjects have had documented stable coronary artery disease, one subject had had aortic valve replaced many years before death.

Rat muscle tissue samples (~ 100–200 mg) were obtained from male Wistar rats (n = 3, aged 8±2 months). Rats were obtained from Welfare of Laboratory Animals from The National Institute of Public Health. The rats were anesthetized via inhalation of diethyl ether and sacrificed by decapitation. Tissue samples were retrieved immediately before homogenisation from skeletal muscle *m. quadriceps femoris* and left ventricle myocardium. The design of this part of the protocol was reviewed and approved by the Committee for Protection and Care of Animals Used in Medical Research of the National Institute of Public Health.

Preparation of tissue homogenates

Human and rodent muscle biopsy samples were put in pre-cooled biopsy preservation and relaxing medium (BIOPS) consisting of 2.77 mM CaK₂EGTA, 7.23 mM K₂EGTA, 5.77 mM Na₂ATP, 6.56 mM MgCl₂ x 6 H₂O, 20 mM taurine, 15 mM Na₂Phosphocreatine, 20 mM imidazole, 0.5 mM dithiothreitol and 50 mM MES hydrate (pH adjusted to 7.1 at 4°C)[18]. Skeletal and heart muscle homogenates were prepared according to the protocols previously described by our research group^{14,17} and in the step-by-step protocol in [S1 File](#) and also in protocols.io with [dx.doi.org/10.17504/protocols.io.3z9gp96](https://doi.org/10.17504/protocols.io.3z9gp96).

Briefly, in skeletal muscle samples, the connective and adipose tissue was removed using scissors and forceps under microscope and muscle sample was gently blotted by sterile cotton gauze, weighted on the analytical scale and cut into fine fragments. Tissue fragments were diluted in glass grinder in the respiration medium (K medium) containing 80 mM KCl, 10 mM Tris HCl, 5mM KH₂PO₄, 3 mM MgCl₂, 1 mM EDTA, 0.5 mg/mL BSA (pH adjusted to 7.4 at 24 °C) to obtain 10 and 2.5% tissue solution (~ 100 mg of human and ~ 25 mg of rat skeletal muscle tissue /per 1 mL of K medium, respectively). Tissue fragments were then homogenized by 5–6 slow strokes up and down with 2 mL Potter-Elvehjem Teflon/glass homogenizer (clearance 0.25 mm; Wheaton™, Millville, USA) driven by electric motor homogenizer (750 rpm; HEi-Torque Value 100, Heidolph, Germany)[17].

Heart muscle homogenates were prepared similarly[19]. After removal of connective tissue and fat, fresh myocardium fragments were diluted in medium MiR05: 0.5 mM EGTA, 3 mM MgCl₂ x 6 H₂O, 60 mM lactobionic acid, 20 mM taurine, 10 mM KH₂PO₄, 20 mM HEPES, 110 mM sucrose and 1 g/L of BSA (pH adjusted to 7.1 at 24°C) to obtain 2.5 and 1% tissue solution of human and rat heart muscle, respectively. Then the process of homogenization was two-step: tissue fragments were firstly manually homogenized by 10–12 initial strokes up and down with a glass loose pestle (large clearance 0.114 ± 0.025 mm; Wheaton™, Millville, USA) in the glass Dounce grinder[19] subsequently homogenized with electro motor homogenizer, with final technique as for skeletal muscle above. Finally, crude homogenate was filtered through polyamide mesh (SILK & PROGRESS s.r.o., Czech Republic) in order to remove the

remaining connective tissue. All the steps were performed on ice. Integrity of outer mitochondrial membrane was verified by measuring the change of oxygen flux at the presence of ADP after addition of cytochrome c. In all experiments, the increments were <15%.

High resolution respirometry

All functional studies were performed using high resolution respirometry Oxygraph-2k (O2k; Oroboros Instruments, Innsbruck, Austria). The method is based on monitoring oxygen concentration with a polarographic oxygen electrode in two closed chambers allowing for 2 parallel measurements. Oxygen flux is calculated as the negative derivative of oxygen concentration [20,21] which is continually measured during sequential addition of substrates, uncouplers or inhibitors. In our experiments, we performed all initial steps including washing the chamber and calibration of O2k according to the manufacturer's recommendations [22]. Oxygen solubility factor was set up to 0.93 and 0.92 for K medium and MiR05, respectively. Changes of respiration were recorded and analysed by Datlab software (Datlab Version 7.0, Oroboros Instruments, Innsbruck, Austria). See [S1 File](#) for detailed methodology.

Reagents preparation

All reagents were purchased from Sigma-Aldrich (St. Louis, USA). Substrates were dissolved in distilled water (pH adjusted to 7.0). Uncouplers and inhibitors were dissolved in DMSO. Propofol (2,6-diisopropylphenol) stock (10 mg/mL) was prepared fresh before each measurement by dilution in 10% ethanol.

Substrate-uncoupler-inhibitor-titration (SUIT) protocols for dose-finding studies

In the dose-finding studies, we tested a range of propofol concentrations, from those resembling propofol levels in human plasma during anaesthesia and sedation (2.5; 5 and 10 µg/mL) [23,24] to supra-physiological concentrations used in previous animal studies (25; 50 and 100 µg/mL) [5–7,25]. Propofol or the respective concentration of control vehicle (ethanol) were injected directly into the chamber and both measurements were performed simultaneously.

Global mitochondrial functional indices. In the first two experiments, we assessed the influence of propofol on global bioenergetic parameters.

Inhibition of electron transfer chain (ETC). Firstly, we used a sequential addition of 2.5 mM malate (mal) plus 15 mM glutamate (glut), 1 mM ADP, 10 µM cytochrome c, 10 mM succinate (suc), 1 µM oligomycin, 0.8 and 1.5 µM FCCP (for skeletal muscle and heart muscle homogenates, resp.) followed by final injection of increasing concentrations of either propofol or vehicle. This protocol allowed us to assess possible propofol-induced inhibition of ETC in ADP-stimulated respiration. *Uncoupling of inner mitochondrial membrane (Leak).* Secondly, we looked at possible uncoupling of inner mitochondrial membrane and changed the protocol as follows: addition of 2.5 mM malate plus 15 mM glutamate, 1 mM ADP, 10 µM cytochrome c, 10 mM succinate and 1 µM oligomycin was followed by final titration of propofol concentrations to induce uncoupling (Fig 2).

Respiration linked to individual complexes. In experiments 3–5 we focused on propofol-induced changes in complexes I, II and IV (CI, CII and CIV) of the ETC that were assessed by high resolution respirometry in muscle tissue homogenates. These experiments were performed by firstly using specific inhibitor for the complementary complex that could also feed electrons to ETC (5 mM malonate [CII inhibitor], 3.5 µM rotenone [CI inhibitor] and 4 µM antimycin A [CIII inhibitor], respectively). Then we added substrates of the complex that was

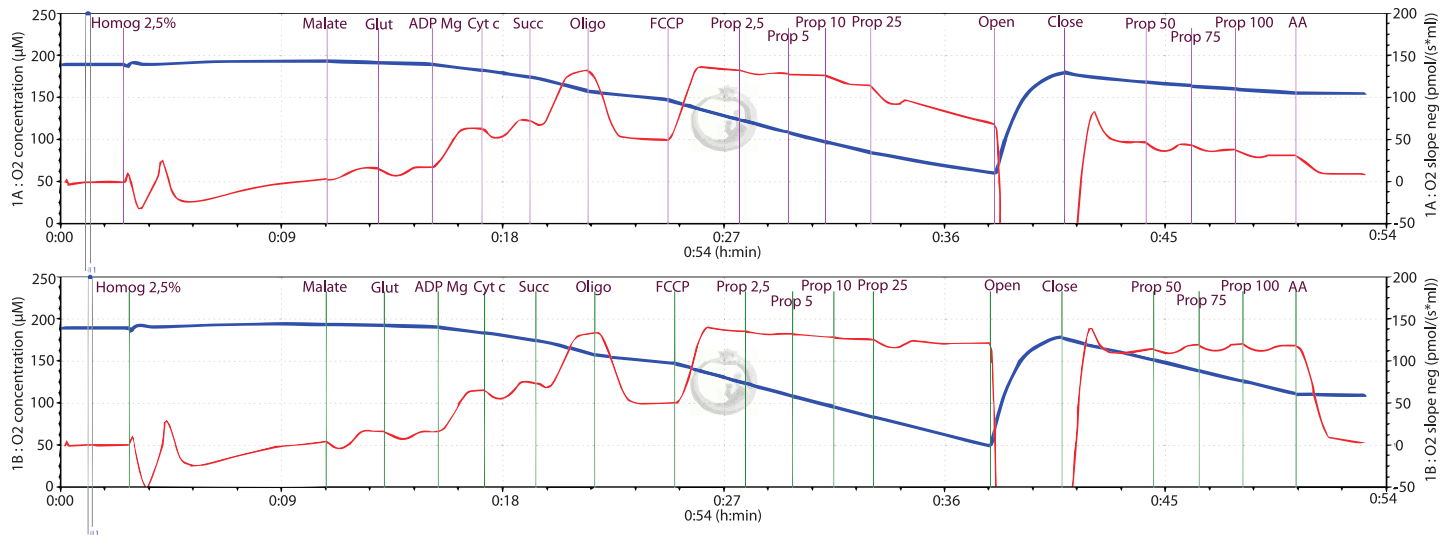


Fig 2. Example of SUIT high resolution respirometry protocol. The two measurements performed in the presence of propofol ($\mu\text{g}/\text{ml}$) or vehicle (ethanol) as control.

<https://doi.org/10.1371/journal.pone.0217254.g002>

measured: 2.5 mM Mal and 15 mM Glut for CI, 10 mM Suc for CII, and 10 mM ascorbate plus 0.2 mM TMPD for CIV. The specific substrates were followed by 1 mM ADP and 10 μM Cyt c. Lastly, we titrated propofol or the vehicle in the parallel chamber.

Fatty acid oxidation (FAO). Initially, 2.5 mM Mal was used as a sparkler followed by 1 mM ADP. Respiration was then stimulated by addition of 25 μM of palmitoyl-carnitine (heated to 70°C). Lastly, propofol was added in a step-wise manner to observe its potential influence on FAO.

Kinetic characteristics experiments

Because we found propofol to inhibit CI-driven respiration and FAO in concentrations that are clinically relevant, for these pathways we performed substrate titrations in parallel, in control chamber and in the presence of a fixed concentration of propofol (10 $\mu\text{g}/\text{ml}$ in rodents and 2.5 and 10 $\mu\text{g}/\text{ml}$ in humans). For CI-linked respiration we inhibited CII by malonate, added ADP, Cyt c, and propofol after which we started to add Mal/Glu in a stepwise manner (0.025/0.15; 0.1/0.3; 0.25/1.5; 1/3; 2.5/15 mM). In analogy, to study propofol-induced FAO inhibition we first added Mal and ADP, then propofol and then titrated palmitoyl-carnitine (0.1; 0.25; 1; 2.5; 10; 25 μM). Oxygen flux was expressed as % of respiration in the control chamber and plotted against substrate concentration.

Spectrophotometric analyses of isolated respiratory complexes

In order to assess effects of propofol on isolated complexes I, II, III and IV, we used classical spectrophotometric method on frozen homogenates as described by Spinazzi et al[26]. We performed parallel assays of samples containing 10 $\mu\text{g}/\text{ml}$ of propofol, the solvent (ethanol 0.5%) and fresh media. For measuring of *CI activity*, we used solution of 0.05 M potassium phosphate buffer, 3 mg/ml BSA, 0.3 mM KCN, 0.1 mM NADH, added isolated mitochondria and measured it in 96 well plate. We used parallel measurement with and without addition of 10 μM rotenone, read the baseline at 340 nm for 2 minutes and started reaction by injection ubiquinone, with absorbance 340 nm duration time of 2 minutes. For *CII activity*

measurement we used solution of 0.05 M potassium phosphate buffer, 1 mg/ml BSA, 0.3 mM KCN, 20 mM Suc and added isolated mitochondria. Baseline was read at 600 nm for 3 minutes then we started the reaction with 12.5 mM decyl ubiquinone, checking specificity with 1 M malonate. For measurement *complex III* activity we used solution of 0.05 M potassium phosphate buffer, 75 μ M oxidized Cyt c, 0.1 mM EDTA, 2.5% Tween-20 and isolated mitochondria. Read baseline at 550 nm for 2 minutes and start the reaction with 10 mM decyl ubiquinone and check specificity with 10 mM KCN. *Activity of CIV* was measured with solution of 0.05 M potassium phosphate buffer, 60 μ M reduced Cyt c then the baseline was read at 550 nm for 2 minutes. Reaction was start by adding isolated mitochondria and the specificity was checked by adding 0.3 mM KCN in one of the measurements.

Statistics

Data from dose-finding were processed using linear mixed effect model (LMEM). In the fixed part, the model consists of a dependent continuous parameter (e.g. oxygen flux) and a categorical independent parameter (e.g. propofol concentration, species human vs rodent). In the random part, there was a random intercept (ID of a patient) and correlation matrix of residuals, if statistically significant (as assessed by likelihood ratio test). For kinetic characterization of propofol inhibition of complex I-linked respiration and FAO, we used mixed effect multilevel non-linear regression for finding the best fit into Michaelis-Menten equation, from which we calculated K_m and V_{max} . For all statistical analyses we used software Stata 15.1 (Stata Corp., LLC, U.S.A.).

Results

Effect of propofol on bioenergetics in cytosolic context

Propofol, in a concentration-dependent manner, inhibited oxygen fluxes driven by substrates for CI and palmitoyl-carnitine, respiratory chain capacity (RCC) and to a lesser extent of oxygen fluxes driven by substrate for CII (Fig 3). Skeletal muscle of both man and rat seemed to be more sensitive to inhibition of CI-driven respiration by propofol than myocardium. Human tissues seemed to be more sensitive than rodents. The inhibition of FAO and CI-driven respiration was observed at concentrations of propofol seen in plasma of anaesthetized patients, i.e. 2.5 and 10 μ g/ml. Apparently, there was no significant effect of propofol on CIV-driven respiration or on the leak of electrons through inner mitochondrial membrane.

In light of this we selected CI-driven and palmitoyl carnitine-driven respirations for kinetic studies, in which we use 10 μ g/ml of propofol for rodent and 2.5 and 10 μ g/ml of propofol for human tissues.

Kinetic characteristics of inhibition by propofol

Energy substrates were titrated with or without the presence of propofol and pre- and post-inhibition of V_{max} and K_m , were compared. (See Figs 2 and 4). Propofol influenced kinetic parameters of CI-driven respiration in human, but not rat muscle tissues: it reduced V_{max} and to a lesser, but still significant extend, the K_m . Human skeletal muscle V_{max} value was significantly affected even from the lowest concentration of 2.5 μ g/ml of propofol (Fig 4A and 4B). With regards to FAO, even the lower concentration (2.5 μ g/ml) of propofol significantly reduced both K_m and V_{max} in both human skeletal muscle and heart tissues. The higher concentration (10 μ g/ml) also tended to reduce V_{max} in rat tissues, but the reduction was only significant in skeletal muscle (Fig 4C and 4D).

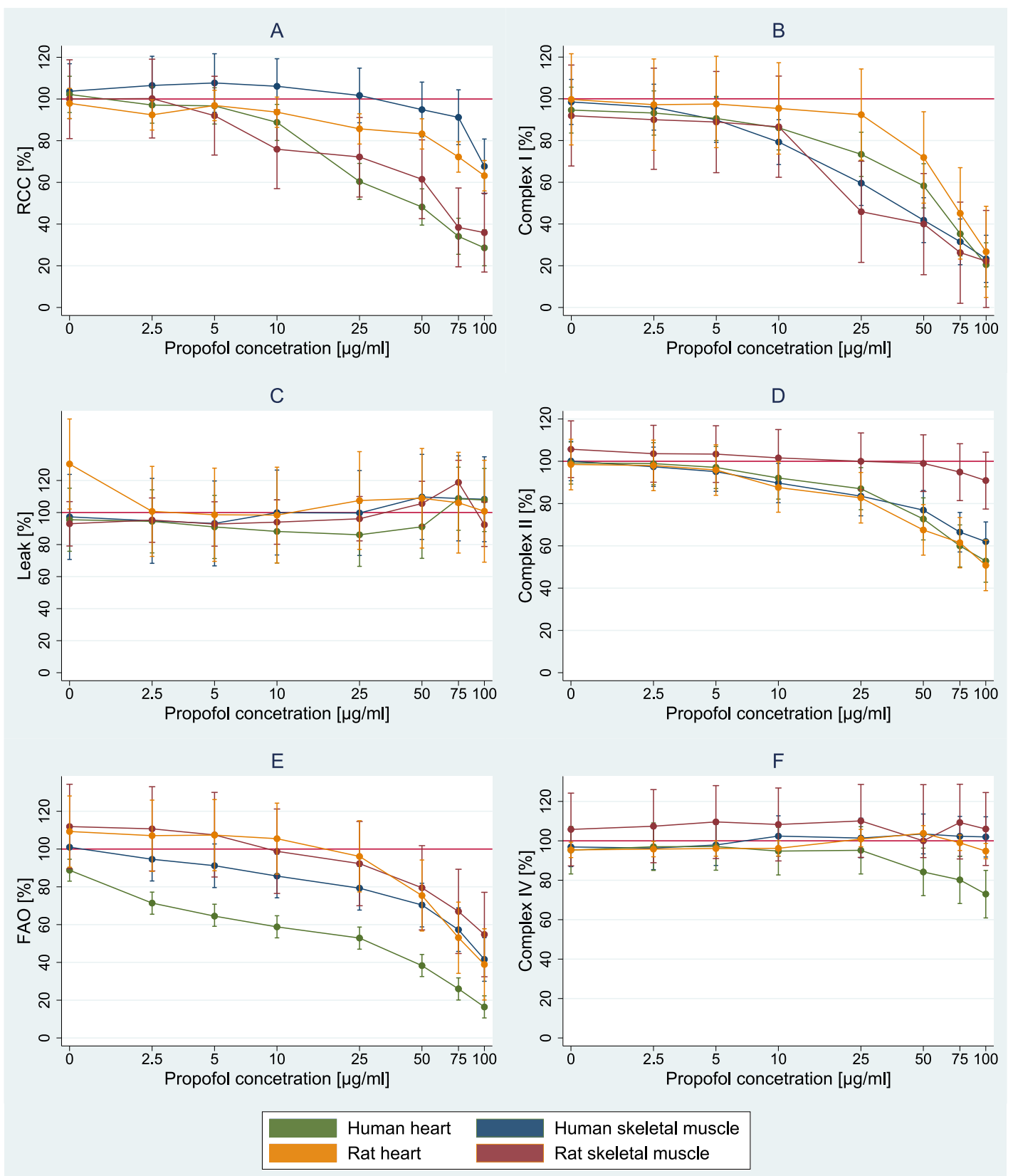


Fig 3. Prediction of difference of respiratory parameters against control at different concentration of propofol. Graph A—respiration chain capacity, graph B—complex I, graph C—LEAK, graph D—complex II, graph E—FAO, graph F—complex IV.

<https://doi.org/10.1371/journal.pone.0217254.g003>

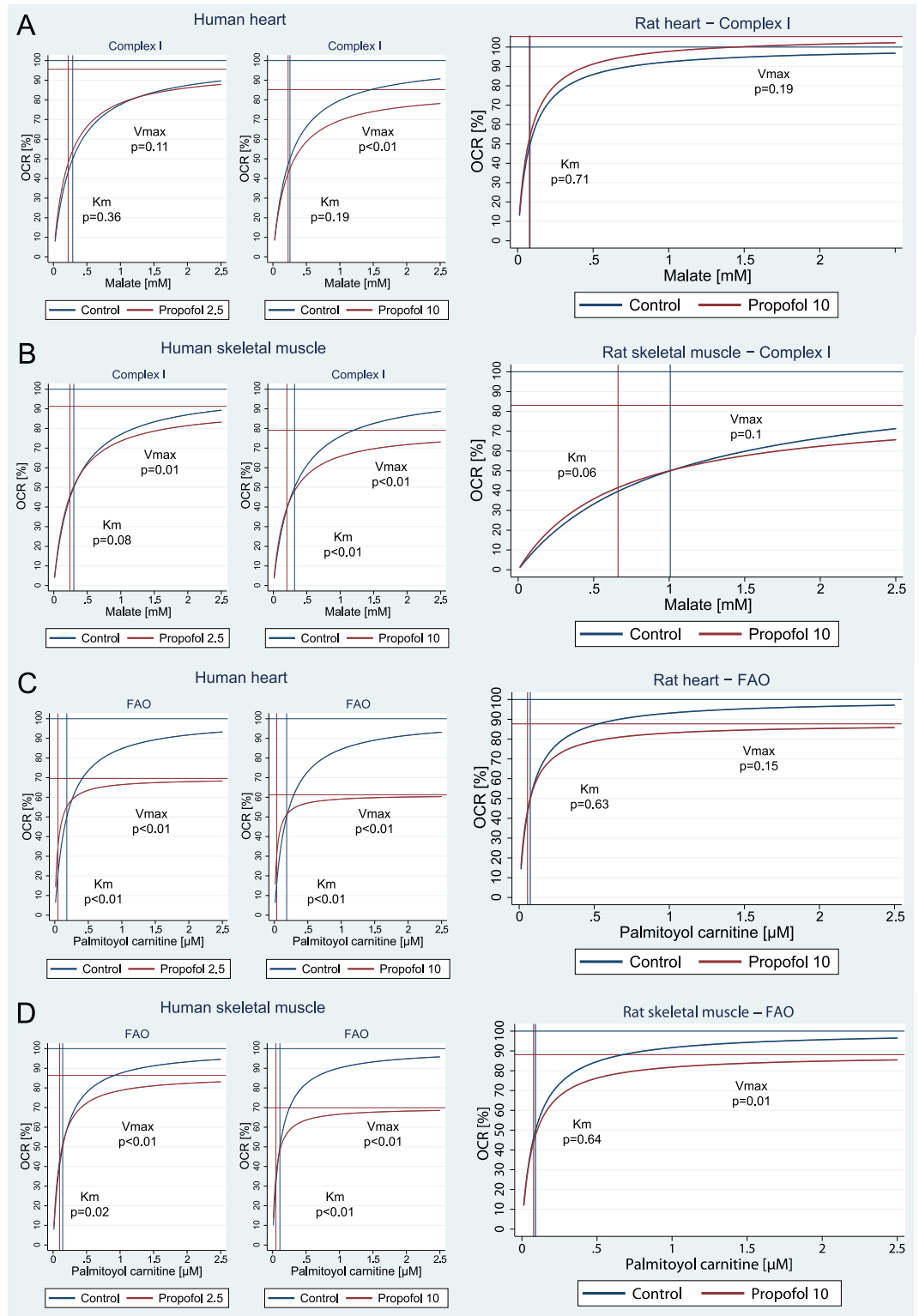


Fig 4. Kinetics of inhibition by 2.5 µg/ml and 10 µg/ml of propofol in human muscle homogenates (left and middle figures), and by 10 µg/ml in rat muscle homogenates (right figure). A = Complex I in heart tissue. B = Complex I in skeletal muscle. C = FAO in heart tissue. D = FAO in skeletal muscle. Based on multi-level linear regression model of independent measurements in all subjects. Note: FAO = fatty acid oxidation, OCR = oxygen consumption rate.

<https://doi.org/10.1371/journal.pone.0217254.g004>

Effects of propofol on isolated complexes

Of note there was no significant inhibition by 10 $\mu\text{g/ml}$ of propofol of any of the complexes if measured in isolation by spectrophotometry (See Figure A in [S1 File](#)).

Discussion

To our knowledge this is the first study that investigates the effects of clinically relevant concentration of propofol on cellular bioenergetics in human skeletal and heart muscles obtained from volunteers and brain-dead organ donors. The main finding of our study is that human skeletal and cardiac muscle tissues are more sensitive to bioenergetic effects of propofol when directly compared to rodent samples. Palmitoyl-carnitine driven respiration (FAO) is particularly more sensitive to low concentrations of propofol in humans compared to rats ([Fig 3E](#)). In addition, we have found that in our model of short-term exposure to propofol, the pattern of inhibition differs between CI-driven respiration and FAO.

In our experiments, we measured the rate of oxygen consumption during substrate titration in the presence or absence of propofol. Had propofol competed at the binding site of any substrate or intermediate, thus creating a bottleneck in the reaction, increasing the concentration of substrate would have led to the same maximal reaction velocity (V_{max}), but indeed the concentration at which 50% V_{max} is achieved (i.e. K_m) would have been higher. On the contrary, had propofol inhibited the rate-limiting enzyme a non-competitive way (e.g. by binding outside the binding site or draining electrons from the ETC as proposed[14]), K_m would remain unchanged and only V_{max} would decrease. The patterns we have observed for CI-driven respiration and FAO are different. CI-driven respiration in human skeletal muscle is inhibited by much lower propofol concentrations compared to those that are able to influence overall capacity of ETC (see [Fig 3A and 3B](#)). K_m remains unaffected and only a reduction of V_{max} is seen (see [Fig 4B](#)), in keeping with a non-competitive nature of the inhibition. Because the activity of isolated complexes was unaffected by the same concentration of propofol (10 $\mu\text{g/ml}$), inhibition of CI-driven respiration could be explained by propofol reducing electron flux outside binding sites of the enzymes, such as reducing downstream flow of electrons by interfering with Coenzyme Q. On the contrary, FAO respiration was affected differently by propofol: both V_{max} and K_m were reduced ([Fig 4C and 4D](#)) suggesting a pattern of mixed or uncompetitive inhibition. Because FAO was inhibited even by concentrations $< 5 \mu\text{g/ml}$ ([Fig 3E](#)) which are not high enough to cause any measurable reduction of ETC capacity ([Fig 3A](#)) or CII substrate-driven respiration ([Fig 3D](#)), the reduction of downstream flux of electrons by propofol can be effectively ruled out as the only cause of FAO inhibition. Propofol has long been thought to inhibit carnitine-palmitoyl transferase I (CPT-1) after Wolf [11] reported in the blood of a child with PRIS a significant elevation of acyl-CoA including malonyl-CoA, the main physiological inhibitor of CAP-1 and in turn the main regulator of fatty acids transport into the mitochondrial matrix. Of note, CAP-1 converts acyl-CoA to acyl-carnitine and in this experiment, we used palmitoyl-carnitine as the substrate. In turn, the observed inhibition of FAO cannot be explained by effects of propofol on CPT-1 as often reported[27,28]. According to our data, the inhibition of FAO by propofol in human skeletal and cardiac muscle cell must occur between CPT-2 and entry of electrons from FAO into ETC via Complex II, and not at the level of CPT-1.

Our results complement the finding of Branca et al.[5] and Rigoulet et al.[8], who found inhibition of ETC capacity in isolated rat liver, mostly due to inhibition of Complex I. In keeping with our results, rat heart mitochondria were found to be more resistant to the inhibitory effects of propofol as the effects of propofol were only seen with concentrations $> 55 \mu\text{g/ml}$ ($> 300 \mu\text{mol/l}$)[6]. Rare in vivo studies in guinea pigs [29] or rat [14] demonstrated—in line

with our results—the inhibitory effect of propofol in ranges of 9–36 $\mu\text{g/ml}$ (50–200 $\mu\text{mol/l}$) [29] or >4.5 $\mu\text{g/ml}$ (>25 $\mu\text{mol/l}$) [14], respectively, whilst isolated respiratory complexes were also unaffected by the same concentration of propofol [14]. Vanlander et al. was also able to mitigate propofol toxicity by adding Coenzyme Q to tissue homogenate [14]. The kinetic characteristics of inhibition of CI-driven respiration in human tissues observed in this study is in keeping with Coenzyme Q hypothesis.

The major strength of our work is that we directly measured the effects of propofol on human tissues that are clinically affected by PRIS, such as skeletal muscle (rhabdomyolysis) or myocardium (heart failure, arrhythmias). Native human hearts are very difficult to obtain, and we used hearts retrieved from brain-dead organ donors to perform our experiments. We experimented with concentrations of propofol that are found in blood of patients sedated or anaesthetized with propofol (2–11 $\mu\text{g/ml}$) [24] and used biologically plausible bioenergetic model of mitochondria in their cytosolic context [17]. The finding of the differences between human and rodent tissues exposed to propofol we consider very important for the interpretation of the experiments in animal models of PRIS [5,7,14,26,29,30]. On the other hand, the use of muscle homogenates only allows short term experimental exposure [17], which may not allow sufficient time for incorporation of propofol into the inner mitochondrial membrane [14] or affect gene expression [15,16]. Also, measuring parameters from the classic enzyme kinetics (such as V_{max} or K_{m}) may not be fully appropriate in systems that are likely multi-compartmental and complex, such as bioenergetic pathways in mitochondria. Moreover, variable age of experimental animals we used might have affected our results, too.

In conclusion, we demonstrated for the first time in fresh human skeletal muscle and cardiac tissue homogenates the inhibition by propofol of electron transfer chain and fatty acid oxidation. We have shown that human tissues are more sensitive to propofol than rat and that fatty acid oxidation in humans is very sensitive to an inhibition by propofol and occurs at much lower concentrations, before any observable reduction of electron flux through ETC. Kinetic characteristics of fatty acid oxidation suggest a different mechanism of inhibition from previously proposed CTP-1 inhibition. Non-competitive nature of the inhibition of Complex I substrate-driven respiration is consistent with the hypothesis that propofol effects on mitochondria are mediated by its interference with Coenzyme Q.

Supporting information

S1 File. Study methods, results and characteristics of subjects.
(DOCX)

Acknowledgments

We thank to all the volunteers who agreed to participate in this study and grieved families of organ donors for their gift of life. Dr Zdeněk Drahotka provided invaluable advice and Přemysl Kunčický and Jiří Bukovský helped to carry out pilot experiments.

Author Contributions

Conceptualization: František Duška.

Formal analysis: Tomáš Urban, Petr Waldauf, Milada Halačová.

Investigation: Tomáš Urban, Adéla Krajčová, Kateřina Jiroutková, František Duška.

Project administration: František Duška.

Resources: Valér Džupa, Libor Janoušek, Eva Pokorná.

Visualization: František Duška.

Writing – original draft: Tomáš Urban, Adéla Krajčová, Kateřina Jiroutková, František Duška.

References

1. Madera Sharline, Shipman William and R N. Application to Add Propofol to the Model List of Essential Medicines. *J Chem Inf Model*. 2013; 53: 1689–1699.
2. Wong JM. Propofol infusion syndrome. *Am J Ther*. 2010; 17(5): 487–91. <https://doi.org/10.1097/MJT.0b013e3181ed837a> PMID: 20844346
3. Vasile B, Rasulo F, Candiani A, Latronico N. The pathophysiology of propofol infusion syndrome: A simple name for a complex syndrome. *Intensive Care Med*. 2003; 29(9): 1417–25. <https://doi.org/10.1007/s00134-003-1905-x> PMID: 12904852
4. Krajčová A, Waldauf P, Anděl M, Duška F. Propofol infusion syndrome: a structured review of experimental studies and 153 published case reports. *Crit Care*. 2015; 19: 398. <https://doi.org/10.1186/s13054-015-1112-5> PMID: 26558513
5. Branca D, Roberti MS, Lorenzin P, Vincenti E S G. Influence of the anesthetic 2,6-diisopropylphenol on the oxidative phosphorylation of isolated rat liver mitochondria. *Biochem Pharmacol*. 1991; 42(1): 87–90. [https://doi.org/10.1016/0006-2952\(91\)90684-w](https://doi.org/10.1016/0006-2952(91)90684-w) PMID: 2069600
6. Branca D, Vincenti E S G. Influence of the anesthetic 2,6-diisopropylphenol (propofol) on isolated rat heart mitochondria. *Comp Biochem Physiol C Pharmacol Toxicol Endocrinol*. 1995; 110(1): 41–5. [https://doi.org/10.1016/0742-8413\(94\)00078-O](https://doi.org/10.1016/0742-8413(94)00078-O) PMID: 7749602
7. Branca D, Roberti MS, Vincenti E S G. Uncoupling effect of the general anesthetic 2,6-diisopropylphenol in isolated rat liver mitochondria. *Arch Biochem Biophys*. 1991; 290(2): 517–21. [https://doi.org/10.1016/0003-9861\(91\)90575-4](https://doi.org/10.1016/0003-9861(91)90575-4) PMID: 1656882
8. Rigoulet M, Devin A, Avéret N, Vandais B, Guérin B. Mechanisms of inhibition and uncoupling of respiration in isolated rat liver mitochondria by the general anesthetic 2,6-diisopropylphenol. *Eur J Biochem*. 1996; 241(1): 280–5. <https://doi.org/10.1111/j.1432-1033.1996.0280t.x> PMID: 8898917
9. Tong XX, Kang Y, Liu FZ, Zhang WS L J. [Effect of prolonged infusion of propofol on the liver mitochondria respiratory function in rabbits]. *Sichuan Da Xue Xue Bao Yi Xue Ban*. 2010; 41(6): 1021–3. PMID: 21265107
10. Krajčová A, Løvsletten NG, Waldauf P, Frič V, Elkalaf M, Urban T, et al. Effects of Propofol on Cellular Bioenergetics in Human Skeletal Muscle Cells. *Crit Care Med*. 2017; 46(3): e206–e212. <https://doi.org/10.1097/CCM.0000000000002875> PMID: 29240609
11. Wolf A, Weir P, Segar P, Stone J. Impaired fatty acid oxidation in propofol infusion syndrome Relation between occurrence of type 1 diabetes and asthma. *Lancet*. 2001; 357(9256): 606–7.
12. Wolf AR, Potter F. Propofol infusion in children: When does an anesthetic tool become an intensive care liability? *Paediatr Anaesth*. 2004; 14(6): 435–8. <https://doi.org/10.1111/j.1460-9592.2004.01332.x> PMID: 15153202
13. Withington DE, Decell MK, Al Ayed T. A case of propofol toxicity: Further evidence for a causal mechanism. *Paediatr Anaesth*. 2004; 14(6): 505–8. <https://doi.org/10.1111/j.1460-9592.2004.01299.x> PMID: 15153216
14. Vanlander AV, Okun JG, De Jaeger A, Smet J, De Lattre E, De Paepe B, et al. Possible pathogenic mechanism of propofol infusion syndrome involves coenzyme Q. *Anesthesiology*. 2015; 122(2): 343–52. <https://doi.org/10.1097/ALN.0000000000000484> PMID: 25296107
15. Sumi C, Okamoto A, Tanaka H, Nishi K, Kusunoki M, Shoji T, et al. Propofol induces a metabolic switch to glycolysis and cell death in a mitochondrial electron transport chain-dependent manner. *PLoS One*. 2018; 13(2): e0192796. <https://doi.org/10.1371/journal.pone.0192796> PMID: 29447230
16. Sumi C, Okamoto A, Tanaka H, Kusunoki M, Shoji T, Uba T, et al. Suppression of mitochondrial oxygen metabolism mediated by the transcription factor HIF-1 alleviates propofol-induced cell toxicity. *Sci Rep*. 2018; 8(1): 8987. <https://doi.org/10.1038/s41598-018-27220-8> PMID: 29895831
17. Ziak J, Krajcova A, Jiroutkova K, Nemcova V, Dzupa V, Duska F. Assessing the function of mitochondria in cytosolic context in human skeletal muscle: Adopting high-resolution respirometry to homogenate of needle biopsy tissue samples. *Mitochondrion*. 2015; 21: 106–12. <https://doi.org/10.1016/j.mito.2015.02.002> PMID: 25701243
18. Fontana-Ayoub, M Fasching M, Gnaiger E. http://wiki.oroboros.at/images/3/3c/MiPNet03.02_Chemicals-Media.pdf. In: Mitochondrial physiology network. 2016 pp. 1–10.

19. Krajčová A, Megvint D, Urban T, Waldauf P, Hlavička J, Budera P, et al. High resolution respirometry to assess function of mitochondria in native homogenates of human heart muscle. *Circ Res* (under Rev. 2018;).
20. Dykens JA, Will Y. *Drug-Induced Mitochondrial Dysfunction*. John Wiley & Sons, Inc.; 2008. <https://doi.org/10.1002/9780470372531>
21. Lanza I, Nair K. Functional assessment of isolated mitochondria in vitro. *Methods Enzym*. 2009; 457: 349–72. [https://doi.org/10.1016/S0076-6879\(09\)05020-4](https://doi.org/10.1016/S0076-6879(09)05020-4) PMID: 19426878
22. Gnaiger E. https://www.researchgate.net/profile/Erich_Gnaiger/publication/267851204_Oxygen_Solubility_in_Experimental_Media/links/553dd3eb0cf29b5ee4bce1d6/Oxygen-Solubility-in-Experimental-Media.pdf. In: *Mitochondrial physiology network*. 2010 pp. 1–12.
23. Herregods L, Rolly G, Versichelen L, Rosseel MT. Propofol combined with nitrous oxide-oxygen for induction and maintenance of anaesthesia. *Anaesthesia*. 1987; 42(4): 360–5. <https://doi.org/10.1111/j.1365-2044.1987.tb03975.x> PMID: 3496022
24. Casati A, Fanelli G, Casaletti E, Colnaghi E, Cedrati V, Torri G. Clinical assessment of target-controlled infusion of propofol during monitored anesthesia care. *Can J Anaesth*. 1999; 46(3): 235–9. <https://doi.org/10.1007/BF03012602> PMID: 10210047
25. Rigoulet M, Devin A, Avéret N, Vandais B, Guérin B. Mechanisms of inhibition and uncoupling of respiration in isolated rat liver mitochondria by the general anesthetic 2,6-diisopropylphenol. *Eur J Biochem*. 1996; 241: 280–5. <https://doi.org/10.1111/j.1432-1033.1996.0280t.x> PMID: 8898917
26. Spinazzi M, Casarin A, Pertegato V, Salviati L, Angelini C. Assessment of mitochondrial respiratory chain enzymatic activities on tissues and cultured cells. *Nat Protoc*. 2012; 7(6): 1235–46. <https://doi.org/10.1038/nprot.2012.058> PMID: 22653162
27. Diedrich DA, Brown DR. Analytic Reviews: Propofol Infusion Syndrome in the ICU. *J Intensive Care Med*. 2011; 26(2): 59–72. <https://doi.org/10.1177/0885066610384195> PMID: 21464061
28. Vollmer JP, Haen S, Wolburg H, Lehmann R, Steiner J, Reddersen S, et al. Propofol Related Infusion Syndrome: Ultrastructural Evidence for a Mitochondrial Disorder. *Crit Care Med*. 2018; 46(1): e91–e94. <https://doi.org/10.1097/CCM.0000000000002802> PMID: 29252954
29. Schenkman KA, Yan S. Propofol impairment of mitochondrial respiration isolated perfused guinea pig hearts determined by reflectance spectroscopy. *Crit Care Med*. 2000; 28(1): 172–7. <https://doi.org/10.1097/00003246-200001000-00028> PMID: 10667518
30. Campos S, Félix L, Venâncio C, Antunes L, Peixoto F. Decrease of state III mitochondrial respiration by prolonged infusion of propofol vehicle in rabbit liver. *Eur J Anaesthesiol*. 2013; 30: 154–154. <https://doi.org/10.1097/00003643-201306001-00479>

Příloha 2

Gojda J, Waldauf P, Hrušková N, Blahutová B, Krajčová A, **Urban T**, Tůma P, Řasová K, Duška F.

Lactate production without hypoxia in skeletal muscle during electrical cycling: Crossover study of femoral venous-arterial differences in healthy volunteers.

PLoS One. 2019 Mar 1;14(3):e0200228. doi: 10.1371/journal.pone.0200228. PMID: 30822305; PMCID: PMC6396965. IF 2.740

RESEARCH ARTICLE

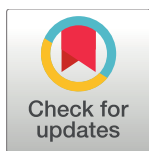
Lactate production without hypoxia in skeletal muscle during electrical cycling: Crossover study of femoral venous-arterial differences in healthy volunteers

Jan Gojda^{1,2}*, Petr Waldauf¹, Natálie Hrušková³, Barbora Blahutová³, Adéla Krajčová^{1,2}, Tomáš Urban¹, Petr Tůma⁴, Kamila Řasová³, František Duška¹

1 Department of Anaesthesia and Intensive Care Medicine, Kralovske Vinohrady University Hospital and The Third Faculty of Medicine, Charles University, Prague, Czech Republic, **2** 2nd Department of Internal Medicine, Kralovske Vinohrady University Hospital and The Third Faculty of Medicine, Charles University, Prague, Czech Republic, **3** Department of Rehabilitation, Kralovske Vinohrady University Hospital and The Third Faculty of Medicine, Charles University, Prague, Czech Republic, **4** Department of Hygiene, The Third Faculty of Medicine, Charles University, Prague, Czech Republic

* These authors contributed equally to this work.

* jan.gojda@lf3.cuni.cz



OPEN ACCESS

Citation: Gojda J, Waldauf P, Hrušková N, Blahutová B, Krajčová A, Urban T, et al. (2019) Lactate production without hypoxia in skeletal muscle during electrical cycling: Crossover study of femoral venous-arterial differences in healthy volunteers. PLoS ONE 14(3): e0200228. <https://doi.org/10.1371/journal.pone.0200228>

Editor: Stephen E. Alway, University of Tennessee Health Science Center College of Graduate Health Sciences, UNITED STATES

Received: June 19, 2018

Accepted: February 11, 2019

Published: March 1, 2019

Copyright: © 2019 Gojda et al. This is an open access article distributed under the terms of the [Creative Commons Attribution License](https://creativecommons.org/licenses/by/4.0/), which permits unrestricted use, distribution, and reproduction in any medium, provided the original author and source are credited.

Data Availability Statement: All relevant data are within the paper and its Supporting Information file.

Funding: The study was supported by Ministry of Health of the Czech Rep. grant AZV 16-28663A (<http://www.zvcr.cz/en>). The funder had no role in study design, data collection and analysis, decision to publish, or preparation of the manuscript.

Abstract

Background

Aim of the study was to compare metabolic response of leg skeletal muscle during functional electrical stimulation-driven unloaded cycling (FES) to that seen during volitional supine cycling.

Methods

Fourteen healthy volunteers were exposed in random order to supine cycling, either volitional (10-25-50 W, 10 min) or FES assisted (unloaded, 10 min) in a crossover design. Whole body and leg muscle metabolism were assessed by indirect calorimetry with concomitant repeated measurements of femoral venous-arterial differences of blood gases, glucose, lactate and amino acids.

Results

Unloaded FES cycling, but not volitional exercise, led to a significant increase in across-leg lactate production (from -1.1 ± 2.1 to 5.5 ± 7.4 mmol/min, $p < 0.001$) and mild elevation of arterial lactate (from 1.8 ± 0.7 to 2.5 ± 0.8 mM). This occurred without widening of across-leg veno-arterial (VA) O_2 and CO_2 gaps. Femoral SvO_2 difference was directly proportional to VA difference of lactate ($R^2 = 0.60$, $p = 0.002$). Across-leg glucose uptake did not change with either type of exercise. Systemic oxygen consumption increased with FES cycling to similarly to 25W volitional exercise ($138 \pm 29\%$ resp. $124 \pm 23\%$ of baseline). There was a net uptake of branched-chain amino acids and net release of Alanine from skeletal muscle, which were unaltered by either type of exercise.

Competing interests: The authors have declared that no competing interests exist.

Conclusions

Unloaded FES cycling, but not volitional exercise causes significant lactate production without hypoxia in skeletal muscle. This phenomenon can be significant in vulnerable patients' groups.

Introduction

Functional electrical stimulation-assisted cycling (FES cycling) is a method originally developed over 30 years ago for patients with spinal cord injury [1]. It uses computer-driven electrical pulses delivered by transcutaneous electrodes and directly activating muscle contractions, independently on functionality of the physiological pathway between upper motoneuron and the neuromuscular junctions. The method is now commercially available in the form of both stationary and mobile devices [2], used by patients with a wide range of conditions incl. spinal cord injury [3], stroke [4,5], and multiple sclerosis [6]. FES cycling was demonstrated to improve cardiovascular fitness, insulin sensitivity [7] bone density and muscle strength [2,8]. In recent years, FES-cycling has become particularly attractive for sedated critically ill patients. Early mobilization is the only intervention, which can partially prevent the development of intensive care unit-acquired weakness [9–14]—the major long-term consequence in the survivors of protracted critical illness [15,16]. Muscle atrophy [17,18] and dysfunction [18] occur very early in the critically ill and FES cycling can help to deliver exercise before the patient can co-operate with a physiotherapist [19].

Although FES cycling seems to be feasible in intensive care unit patients [19], before its effect on meaningful clinical outcomes can be tested in the critically ill and other vulnerable patients groups, important physiological questions need to be addressed. Metabolic efficacy (i.e. power output divided by metabolic cost) of the FES cycling is typically very low, around 5–10%, as compared to 25–40% in volitional cycling [20–22]). This is likely due to non-physiological pattern of muscle activation, where large muscle groups are activated simultaneously rather than small well-coordinated units [2,23]. Despite FES cycling increases cardiac output [24] and leg blood flow to the same extent [25] or even more [26] than volitional cycling and consequently oxygen delivery to the muscle should be normal, there are features suggesting early switch to anaerobic metabolism: early fatigue [23,27], rapid intramyocellular glycogen depletion [28], increase of respiratory quotient (RQ) >1 [20] and even a mild increase in arterial lactate levels [29]. Increased lactate production could be caused by microcirculation impairment during electrically stimulated asynchronous contraction [30] or by a mismatch between glycogenolysis activated by electrical stimulation [31] and pyruvate oxidation.

Nonetheless, a direct evidence of the presence of anaerobic metabolism in skeletal muscle during FES cycling is lacking. In addition, whilst the influence of volitional resistance exercise on amino acid metabolism has been extensively studied [32–36] there is no such data for FES cycling, although one study demonstrated activation of anabolic signalling in electrically stimulated gastrocnemius muscle in a rat [31]. These questions may be particularly relevant before FES-assisted exercise is introduced to critically ill patients, who are in profound protein catabolism and may be less able to clear lactate from systemic circulation.

In light of this we conducted a crossover study of volitional and FES supine cycling in healthy postprandial volunteers, where we combined indirect calorimetry with across-leg venous-arterial (VA) difference studies. We hypothesized that FES-cycling as compared to light volitional exercise would lead to increased production of lactate in correlation with

widening of VA-CO₂ gap (as the measure of anaerobic metabolism), and with increased amino-acid efflux from skeletal muscle during exercise.

Materials and methods

Study subjects

Our experimental group consisted of 14 young (31±8 years), non-obese (23.7±3.7kg/m²) healthy volunteers (gender M/F = 11/3). University Hospital Kralovske Vinohrady's Research Ethics Board reviewed the protocol and approved the study. Prior to the enrolment, all subjects gave their written informed consent in accordance with the Declaration of Helsinki.

Overview of study design

The study was performed during two visits performed 1 week apart. Subjects were asked to attend the visit at 08:00 AM after an overnight fast. In between these visits, the subjects were advised to take their usual diet and avoid strenuous exercise. During the first visit, the volunteers underwent a physical examination and body composition measurement. After 30 min bed rest, their energy expenditure was measured using indirect calorimetry with a ventilated canopy system. Afterwards, in each subject's VO_{2MAX} was determined on a cycle ergometer with stepwise load by 25 W increments until exhaustion. During the second visit, subjects were given a standardized breakfast containing 70 g of carbohydrates, 10 g protein and 15 g of fat. Afterwards, femoral vein and radial artery were cannulated. After 30 min rest, the subjects were exposed in random order to one of two supine exercise protocols, separated by 3 hours rest. Both protocols begun with baseline measurements (AV difference studies and calorimetry) followed by 5 min of passive cycling. Then, the subjects either performed three 10 min cycles of volitional cycling (at 10, 25 and 50 W, respectively) separated by 5 min of passive cycling (Group A), or FES cycling (Group B). The exercise protocols are outlined in Fig 1.

Methods

Indirect calorimetry and body composition assessment. Resting energy expenditure and RQ were measured after overnight (12 h) fast and 30 min bedrest using canopy as a mixing chamber with 10 sec sampling (Quark RMR device, Cosmed, Italy). To determine peak oxygen uptake (VO_{2max}) exhaustive exercise test was performed in each subject on an electromagnetically braked bicycle ergometer Ergoline Ebike (Ergoline GmbH, Germany). After 5 min warm-up period, a workload of 50W was initiated and increased by 25 W every minute continuously until fatigue despite the verbal encouragement. Oxygen uptake was measured using mask, breath-by-breath, 10 sec sampling period (Quark RMR device, Cosmed, Italy). ECG was monitored continuously. Gas analysers (container 5% CO₂, 16% O₂ and room air) and flow analyser were calibrated prior to each measurement. Body fat was assessed using bioimpedance analysis (NutriGuard 2000, Bodystat, Germany).

Cannulations. Femoral vein was cannulated 2–3 cm below inguinal ligament under ultrasound guidance. In order to avoid the admixture of blood from saphenous and pelvic veins [37], a single-lumen central venous catheter (B-Braun, Germany) was inserted retrogradely to the depth of 10–15 cm so that the tip was deep in the femoral muscular compartment. For arterial sampling, we used a 22 F catheter (BBraun, Germany) inserted into the radial artery.

Cycling protocols. For both volitional and FES cycling we used RT-300 bikes (Restorative Therapies Ltd., USA) and the exercise was performed in supine position. *Volitional cycling* consisted of three 10 min intervals of active cycling: 10W (13 revolutions/min, resistance 7 N/m), 25W (31 revolutions/minute, 7.6 N/m), 50W (35 revolutions/min, and resistance 13.4 N/

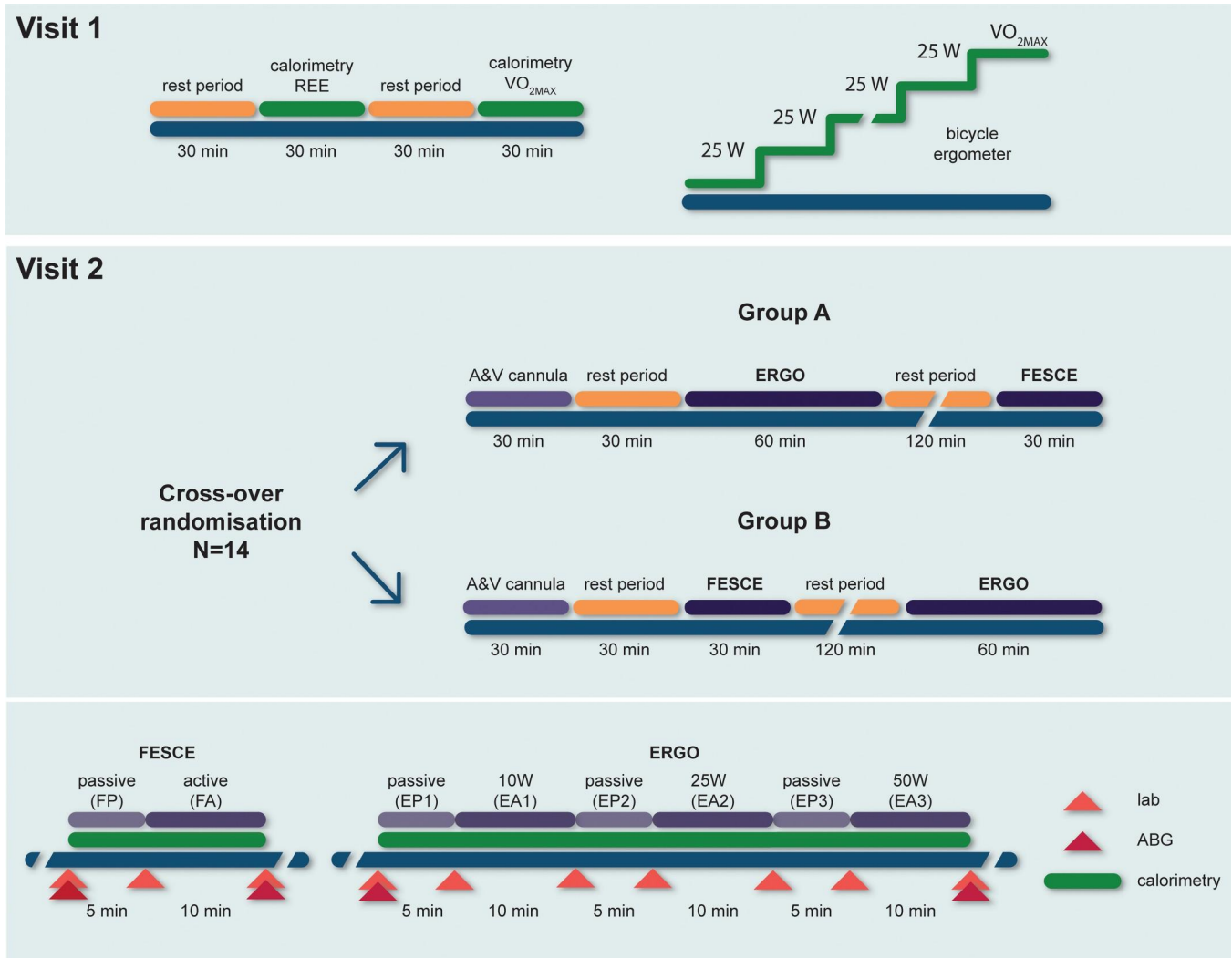


Fig 1. Overview of study design. Arrows designate arterial and venous blood sampling times. Note: ERGO = volitional cycling, FESCE = functional electrical stimulation cycling. Details of exercise are shown in the inset at the bottom.

<https://doi.org/10.1371/journal.pone.0200228.g001>

m). These period were preceded (warm up) and separated by 5 min of passive cycling at 25 revolutions/min. *FES cycling*: Three pairs of transcutaneous electrodes (3 x 4", Restorative Therapies, Ltd., USA) electrodes were applied on each leg over quadriceps, hamstrings and gluteus maximus muscles, as per manufacturer’s instructions. Prior to electrode placement, we measured the thickness of fat layer between the skin and muscle by ultrasound. After 5 min passive warm up (25 revolutions/min), the target speed was changed to 30 revolutions/min and stimulation gradually (1%/s) started to achieve 25 mA. Then, in each subject, the stimulation current was gradually increased to reach subjectively tolerated maximum. Oxygen uptake was measured continuously in both volitional and FES assisted cycling using mask breath-by-breath system (Quark RMR device, Cosmed, Italy). Gas analysers (container 5% CO₂, 16% O₂ and room air) and flow analyser were calibrated prior to each measurement.

Laboratory methods. Arterial and venous blood samples were analysed for blood gases, lactate and haemoglobin using POCT analyser Cobas b221 (Roche Diagnostics Limited, USA). For other analysis blood samples were centrifuged and frozen at -80°C until analysed. Serum

creatine kinase and myoglobin was measured in a certified institutional laboratory (Cobas system, Roche Diagnostics Ltd., USA). Serum amino acid concentration in arterial/venous blood was analysed using capillary electrophoresis as described [38].

Calculations and statistics

Metabolic efficacy. Metabolic efficacy of volitional cycling was calculated as power output divided by the increase of energy expenditure [2]. Veno-arterial gap in the total content of carbon dioxide (ctCO₂ gap) was calculated according to equations used in ABL 900 Analyser (by Radiometer, Copenhagen, Denmark).

$$\text{ctCO}_2(\text{B}) = 9.286 \times 10^{-3} \times \text{pCO}_2 \times \text{ctHb} \times [1 + 10^{(\text{pH}_{\text{ERY}} - \text{pK}_{\text{ERY}})}] + \text{ctCO}_2(\text{P}) \times \left(1 - \frac{\text{ctHb}}{21.0}\right)$$

where ctCO₂ (B) = CO₂ content in blood in mmol/L; ctCO₂ (P) = CO₂ content in plasma in mmol/L and equals to 0.23 x pCO₂ + cHCO₃⁻(P); pCO₂ is partial pressure in kPa, ctHb = haemoglobin content in mmol/L. ctCO₂(P). pH_{ERY} = estimated intracellular pH in red blood cells, which equals to 7.19+0.77 x (pH-7.4)+0.035 x (1-SO₂), where SO₂ is haemoglobin saturation with oxygen; and finally pK_{ERY} is a negative decadic logarithm of bicarbonate dissociation constant:

$$\text{pK}_{\text{ERY}} = 6.125 - \log\{1 + 10^{[\text{pH}_{\text{ERY}} - 7.84 - (0.06 \times \text{SO}_2)]}\}$$

Blood flow. In both FES and volitional cycling, leg oxygen uptake represents a relatively fixed proportion (76±8% and 78±9%, respectively) of whole-body oxygen uptake [39]. Therefore, an index of blood flow through the leg was calculated as whole-body oxygen consumption divided by the difference of oxygen content in arterial and femoral-venous blood. Blood oxygen content was calculated in mmol/L as 0.00983 * pO₂ + SO₂[%]/100 * Hb * 0.06206 * (1-CO-Hb [%])/100 - metHb[%], where SO₂ is saturation of haemoglobin with oxygen [%], Hb is haemoglobin [mmol/L], CO-Hb and met-Hb are fractions of carbonyl and methemoglobin, respectively, and pO₂ is partial pressure of oxygen [kPa].

Statistics. We used linear mixed effect model for 2x2 crossover design processed with software Stata 15 (Stata Corp., LLC, U.S.A.) [40,41]. The model consists of fixed and random part. In the fixed part, the model contained following parameters: (1) Sequence, i.e. order in which subject performed volitional and FES cycling protocols. Had this parameter been significant, a carry-over effect would have been present; (2) Period, basal vs. active, a parameter exploring the effect of the exercise, regardless whether volitional or FES; (3) Treatment, exploits the difference between volitional and FES cycling; and (4) Interaction Period#Treatment exploits whether FES cycling differs from volitional cycling during exercise period. Random part of the model contains subject number in order to take into account repeated measurements. Binary data are showed as frequency + %, continuous data as means ± SD. P value <0.05 was considered as significant. Whenever another test was used we specified this in the text. Sample size determination was performed prior commencement of the protocols with VA lactate difference as a primary outcome.

Results

Characteristics, tolerability and signs of muscle damage

All 14 subjects finished the protocol without adverse events; baseline (visit 1) calorimetry data are available for 13 subjects only due to a technical problem. Baseline characteristics are

outlined in Table 1. Sequence parameter of linear mixed effect model was not significant in any of analysed parameters ($p = 0.14\text{--}0.94$), so we assume no carry over effect from previous cycling protocol.

Maximum tolerated stimulation current of FES was 45 ± 13 mA (range 25–67 mA). Although FES cycling caused a degree of discomfort, post-exercise serum myoglobin remained within reference range (<85 ng/mL) in all subjects (33 ± 15 pg/mL, range 21–74). Nonetheless, there was a positive correlation between maximal stimulation current and post-exercise serum myoglobin (Spearman's $R^2 = 0.57$, $p = 0.002$).

Metabolic efficacy of volitional vs. FES cycling

Metabolic efficacy of volitional cycling was $39.2\pm 5.6\%$. Unloaded FES cycling led to an increase of metabolic rate to $138\pm 29\%$ from baseline, which was comparable to the increase with 25 W volitional exercise ($124\pm 23\%$). See Fig 2. Energy gain from anaerobic glycolysis was negligible or negative for volitional cycling and 5.0 ± 6.2 W for FES cycling.

Blood flow index

At rest before volitional and FES cycling, blood flow index was 6.6 ± 2.4 vs. 6.3 ± 3.4 ($p = 0.57$), and increased significantly ($p < 0.01$) and similarly ($p = 0.77$) to 160% and 165% of baseline after volitional and FES exercise.

Exploring muscle metabolism during FES cycling

VA differences of both O_2 and CO_2 contents (ctO_2 and $ctCO_2$) tended to widen with volitional exercise (Fig 3A and 3B), whilst the opposite trend was seen for FES cycling. In line, there was no change in oxygen saturation of haemoglobin in femoral venous blood neither with volitional exercise (from $63.9\pm 12.7\%$ to $64.3\pm 8.7\%$), whilst there was an increase after FES cycling (from 62.6 ± 11.3 to $70.3\pm 8.7\%$; $p = 0.02$). Across-leg respiratory exchange ratio (i.e. the ratio between VA differences of CO_2 and O_2 contents) although different at baseline (Fig 3C) tended to increase with volitional cycling, but this change was not significant. There was no change from baseline in across-leg glucose uptake of glucose (FES -5.5 ± 3.9 to -5.9 ± 3.6 mmol/min; volitional -7.0 ± 3.6 to -6.9 ± 6.1 mmol/min). Whole body RQ increased with FES cycling (0.88 ± 0.02 to 0.95 ± 0.02 , $p = 0.001$, but did not change with volitional exercise (0.87 ± 0.02 to 0.85 ± 0.02 , $p = 0.55$; See Fig 3D) and only FES cycling led to an increase in across-leg lactate VA differences and production (from -1.1 ± 2.1 to 5.5 ± 7.4 mmol/min, $p < 0.001$ vs. from -0.9 ± 1.1 to -0.4 ± 1.2 mmol/min, $p = 0.70$ Fig 3E) with very high inter-individual variability (See

Table 1. Baseline characteristics of study subjects.

Parameter	Mean \pm SD	N
Age (years)	31 \pm 8	14
Sex (M/F)	11/3	14
BMI (kg/m ²)	23.7 \pm 3.7	14
Body fat (%)	14 \pm 6	14
REE (kcal/day)	1901 \pm 356	13
RQ at rest	0.90 \pm 0.10	13
VO ₂ MAX (ml/kg/min)	41 \pm 6	13

Note: BMI = body mass index, REE = resting energy expenditure, RQ = respiratory quotient, VO_{2max} = peak oxygen consumption. Baseline data from one subject are unavailable due to technical problem with the machine.

<https://doi.org/10.1371/journal.pone.0200228.t001>

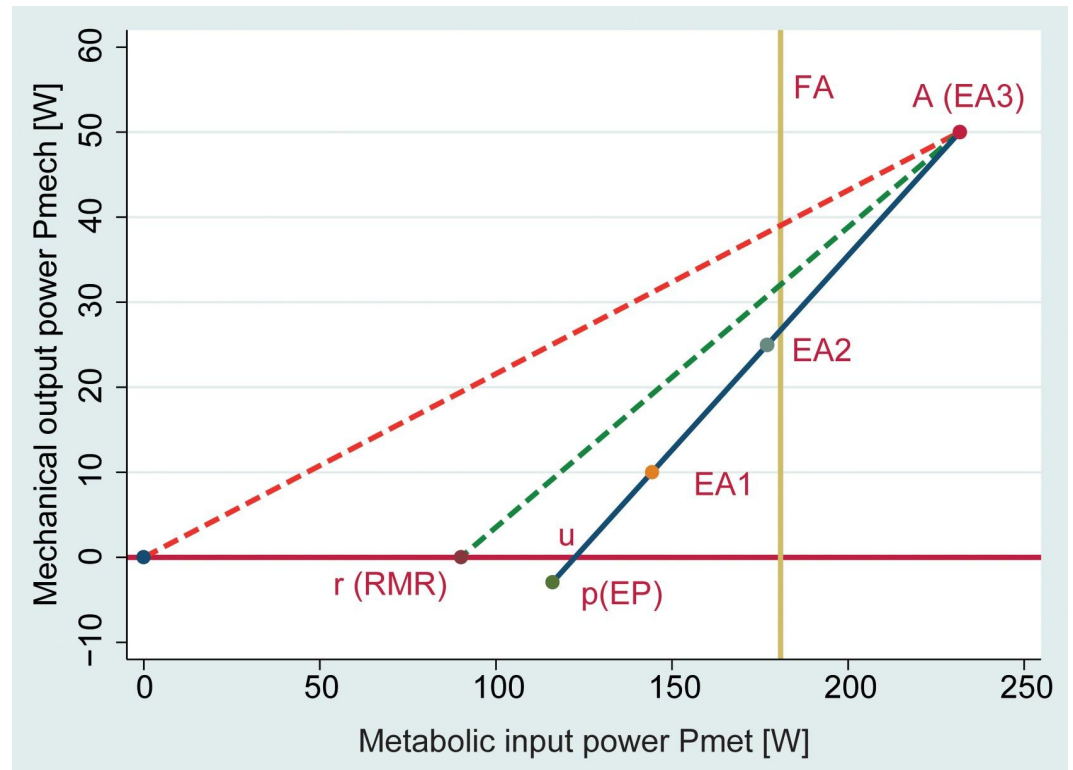


Fig 2. Hunt's diagram [2,22] outlining the efficacy of volitional exercise relative to metabolic cost of unloaded FES cycling (yellow line). Note: Metabolic efficiency is the gradient of the line joining the active cycling operating point (A) to one of the baseline conditions: u is unloaded cycling; r is rest, p is passive cycling.

<https://doi.org/10.1371/journal.pone.0200228.g002>

Fig 3F). Systemic arterial lactate levels remained normal after volitional cycling (from 1.6 ± 0.6 mmol/l to 0.9 ± 2.1 mmol/l, $p = 0.887$), and increased after FES cycling (from 1.6 ± 0.7 mmol/l to 2.3 ± 0.8 mmol/l, $p < 0.001$).

Analysing lactate production

With FES cycling, there was a significant positive correlation between VA lactate difference and femoral venous haemoglobin saturation with oxygen (Spearman's $R^2 = 0.6$, $p = 0.002$, Fig 3G). Lactate producers had smaller veno-arterial difference in CO_2 content of the blood ($R^2 = 0.3$, $p = 0.046$, Fig 3H), effectively ruling out oxygen delivery problem. Subjects with femoral VA lactate difference > 0.5 mmol/L ("lactate producers", $n = 5$, see Fig 3F) were compared with the rest of the group ($n = 9$) but no difference was found besides lactate having higher RQ at baseline (0.94 ± 0.06 vs., 0.86 ± 0.07 , $p = 0.034$). Of note, stimulation current used during FES cycling was not different in lactate producers (42 ± 10 vs. 44 ± 16 mA, $p = 0.87$).

Amino acid metabolism

As expected in postprandial volunteers, at baseline resting skeletal muscle was taking up branched-chain amino acids (BCAAs) whilst producing Alanine (Ala). Skeletal muscle only produced Glutamine (Gln) at baseline in the volitional cycling group, otherwise the change was not significantly different from zero (Fig 4). Neither type of exercise led to a significant change of amino acid metabolism, but it is apparent from Fig 4 that with volitional cycling there was a trend to an increase in Ala production and a decrease of glutamine production,

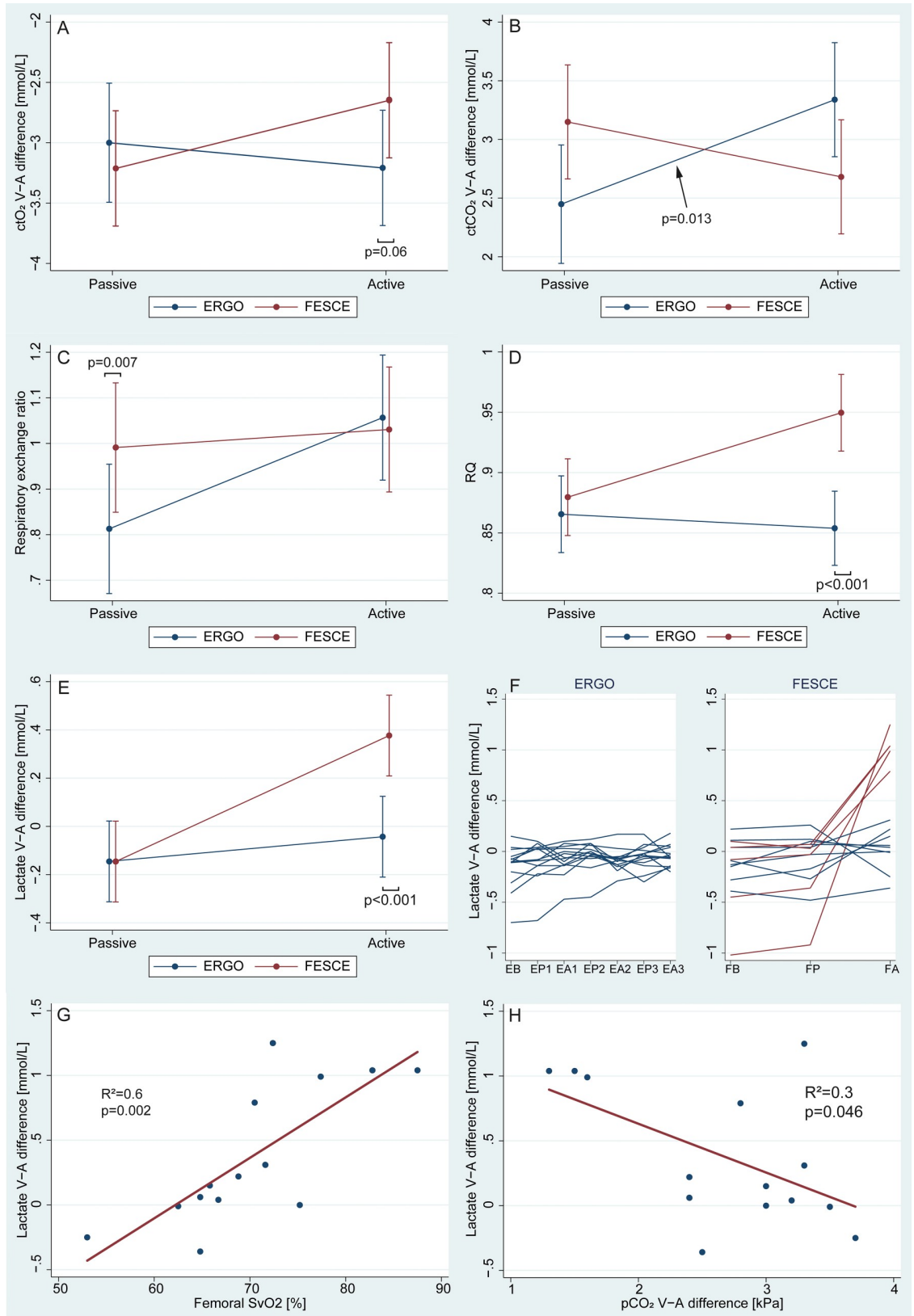


Fig 3. Venous-arterial (VA) differences studies. Lactate VA difference is derived from multiplying femoral VA differences of concentrations and calculated leg blood flow. See text for further details. Linear regression was used in G and H. Note: ctO_2 and $ctCO_2$ = total blood content of oxygen and carbon dioxide; RQ = whole body respiratory quotient; SvO_2 = femoral venous saturation of haemoglobin with oxygen. ERGO = volitional cycling; FESCE = functional electrical stimulation-assisted cycling; Passive period vs Active FES/50W volitional period.

<https://doi.org/10.1371/journal.pone.0200228.g003>

whilst after FES cycling no such a trend was apparent (across-leg amino acid exchange remained unaffected). Uptake of BCAAs continued and did not change with either type of exercise ($p = 0.83$ and $p = 0.86$).

Discussion

The major finding of our study is that unloaded supine FES cycling leads to lactate production without signs of muscle hypoperfusion, as low blood flow through exercising limbs would have caused femoral venous haemoglobin desaturation (Esaki et al., 2005; Sun et al., 2016) and widening of VA- CO_2 gap [42], which were not observed in our subjects. Moreover, there was a significant positive correlation between across-leg lactate production and femoral venous oxygenation, suggesting that subjects producing lactate did so whilst extracting less oxygen from (and producing less CO_2 into) the local circulation. There was a marked interindividual variability in metabolic response to FES cycling: some subjects responded to FES similarly to volitional cycling, whilst others produced so much lactate that it elevated systemic (arterial) lactate concentrations well above the normal range. We have not found any convincing characteristics of the subjects producing lactate during FES, although they seemed to be oxidizing more carbohydrates at baseline. Notably there was no correlation between the amplitude of stimulation current used and the production of lactate.

Tissue dysoxia and femoral venous desaturations are known to accompany lactate production during high intensity volitional exercise (i.e. $>$ approx. 60% $VO_{2\text{ MAX}}$) [43, 44, 45], at which oxidative phosphorylation becomes oxygen dependent. At lower exercise intensities, there is a concomitant lactate production in fast twitch glycolytic muscle fibres and consumption in slow twitch fibres [46] and—as seen in our subjects—during a steady low intensity volitional exercise, skeletal muscle may become a net lactate consumer [47].

The most obvious explanation of FES-driven lactate production would be tissue dysoxia, occurring despite adequate flow of oxygenated blood through major vessels. Non-physiological asynchronous contractions of large muscle units activated by FES [2,23] could have caused an inhomogeneous perfusion at the level of microcirculation, with hypoxic regions and units with luxurious perfusion acting as functional AV shunts. The increase in whole-body RQ with FES cycling, would support the presence of some degree of anaerobic metabolism, but it could also be explained by impaired fatty acid oxidation with the preference of carbohydrate substrates [39] or by primary increased ventilation. The major argument against microcirculatory impairment and anaerobic lactate generation is the absence of widening of venous-arterial CO_2 gap. Carbon dioxide is produced also anaerobically and released from bicarbonate as the consequence of buffering acid load in hypoxic tissue, and because CO_2 diffuses rapidly even from poorly perfused tissue, VA- CO_2 gap is regarded as a very sensitive marker of tissue hypoxia caused by impaired microvascular flow [48]. Not only VA CO_2 gap was not widened after FES cycling, but it was inversely proportional to lactate production. Moreover, the $138 \pm 29\%$ increase in the whole body oxygen consumption after FES-cycling observed by us and others [49] would also argue against major oxygen delivery problem.

Lactate production without tissue dysoxia may occur as a result of the dysbalance between pyruvate production from glycolysis and its conversion to acetyl-CoA and oxidation in tricarboxylic acid cycle [46,47]. Muscle contraction instantly triggers, via the increase in $Ca^{2+}_{[TC]}$,

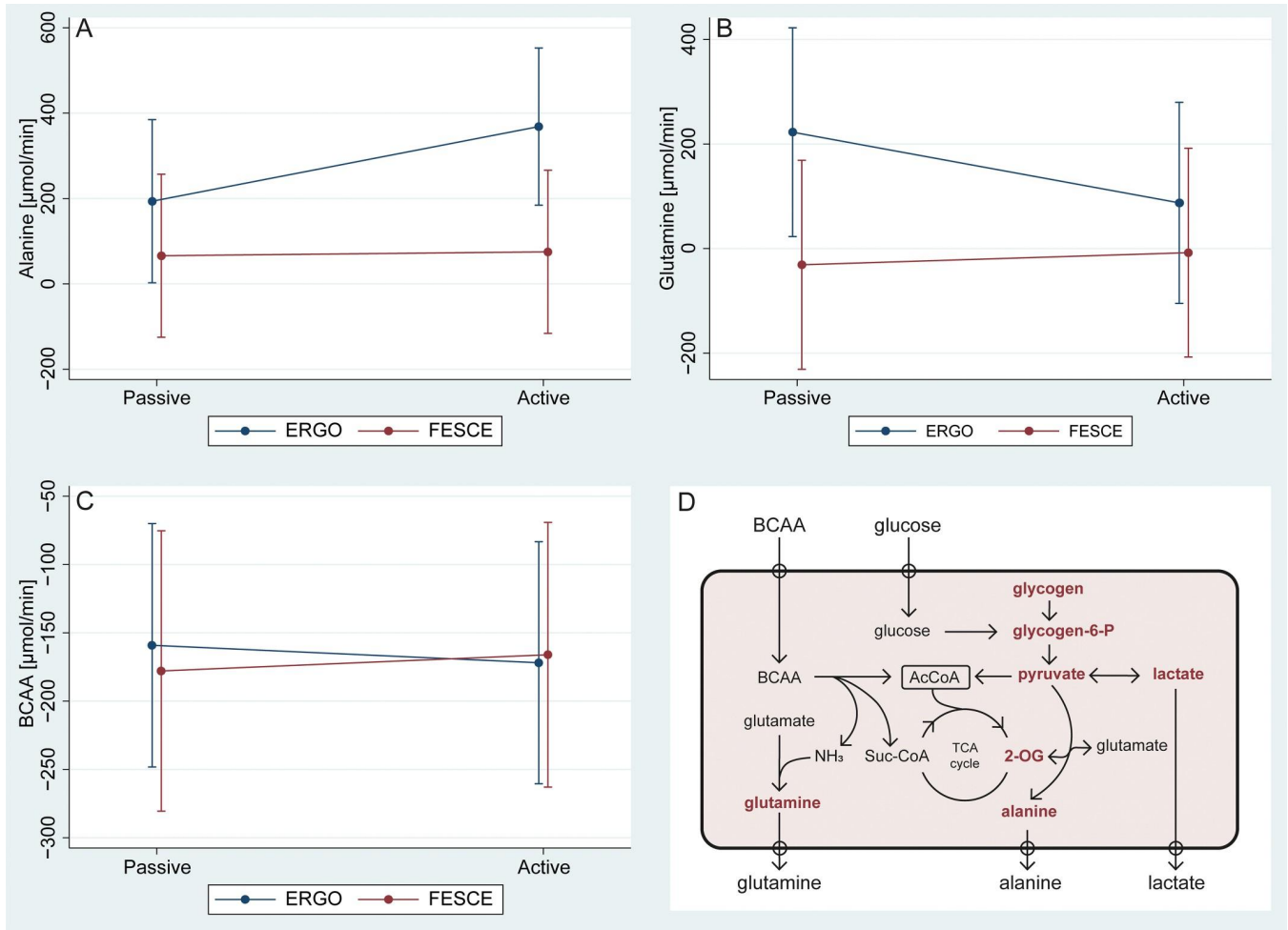


Fig 4. Amino acid metabolism during volitional and FES cycling. Values are derived from multiplying femoral VA differences of concentrations and calculated leg blood flow. Note: BCAA = branched-chain amino acids (i.e. the sum of Valine, Leucine, and Isoleucine); ERGO = volitional cycling; FESCE = functional electrical stimulation-assisted cycling; Passive period vs Active FES/50W volitional period. TCA = tricarboxylic acid cycle, 2-OG = 2-oxoglutarate.

<https://doi.org/10.1371/journal.pone.0200228.g004>

glycogenolysis and glycolysis, producing pyruvate. Sudden increase in cytosolic pyruvate concentration shifts the near-equilibrium reaction: $\text{Pyruvate} + \text{Glutamate} \leftrightarrow \text{Alanine} + \text{2-oxoglutarate}$, rightwards. Alanine is increasingly released during exercise and 2-oxoglutarate is believed to increase the functional capacity of tricarboxylic acid cycle [50] allowing for increase in oxidative ATP production. BCAAs uptake in skeletal muscle continues or even increases during exercise, providing carbons for oxidative pathways and nitrogen for Alanine and Glutamine formation (Fig 4D). Although non-significant, we have observed some trends to these responses after volitional cycling, but no rearrangement at all of amino acid metabolism was seen with FES exercise. Glycolytic compartment is known to respond much faster compared to oxidative phosphorylation and a rapid increase in cytosolic pyruvate concentration could lead to lactate release from cells even in the absence of tissue hypoxia [46]. Moreover, FES cycling compared to volitional exercise is known to activate glycogenolysis and glycolysis disproportionately faster than oxidative pathways [20,39]. In light of this, our data are consistent with aerobic lactate generation due to a dysbalance between pyruvate generation from glycogenolysis and glycolysis and its oxidation in citric acid cycle. Indeed, skeletal muscle is not a

metabolically homogenous tissue [47] and FES may preferentially trigger muscle contraction in glycolytic fast twitch fibres, whilst lactate oxidizing slow fibres may have been less sensitive to electrical stimulation. The sensitivity of different muscle fibres to external stimulation is unknown and remains to be studied, but a higher sensitivity of fast twitch fibres would be in keeping with the finding, that a long-term external electrical stimulation of a denervated muscle restores its mass and contractile power, but not fatigability [51].

From clinical point of view we found important the absence of venous haemoglobin desaturation during FES-cycling as decreased central venous saturation impairs systemic oxygenation in patients with a degree of intrapulmonary shunt. Mild lactic acidosis could be of concern in patients with impaired lactate clearance (e.g. liver failure). Unloaded FES cycling led to VO_2 response comparable to 25W volitional exercise, which would represent a very significant exercise load for critically ill patients, who tend to have even higher metabolic cost for a given power output [52] and only tolerated cycling at 3–6 W in one study [52]. Lastly, although the absence of laboratory signs of muscle damage and amino acid release is reassuring, the positive association of post-exercise serum myoglobin with stimulation current amplitude suggest a risk of muscle damage from the use of stimulation currents above 70mA, which are often needed to elicit visible contractions in sedated critically ill patient, perhaps due to their impaired muscle excitability [16].

The major weakness of our study is that we have not used direct measurements of leg blood flow and tissue oxygenation. We only use indirect indices, which prevents us from drawing any conclusions about the influence of FESCE on blood flow, which might have been altered, eg. by altered function of muscle pump. However, effects of FES exercise on leg blood flow are known [17,25] and the main finding of the study, i.e. lactate production without evidence of tissue hypoxia, can be supported by across-leg VA differences alone. Muscle tissue oxygen concentrations are known to be closely reflected by femoral venous oxygen content [43,53].

In conclusion, we have demonstrated that 10 min of supine FES cycling in healthy volunteers leads to production of lactate without features suggestive oxygen consumption/delivery mismatch, which are known to accompany lactate production during high intensity voluntary exercise [42,43]. Despite a significant increase in systemic oxygen consumption (proportional to 25W of volitional exercise) and unaltered across-leg glucose uptake with FES cycling, we have not observed the rearrangement of amino acid metabolism towards anaplerosis.

Supporting information

S1 Table. Dataset spreadsheet.
(XLSX)

Acknowledgments

The authors thank to Jana Potočková, Šárka Gregorová, Šárka Vosalová for technical assistance and to all healthy volunteers, who decided to participate in this study.

Author Contributions

Conceptualization: Jan Gojda, Kamila Řasová, František Duška.

Data curation: Petr Waldauf, František Duška.

Formal analysis: Jan Gojda, Petr Tůma, Kamila Řasová, František Duška.

Funding acquisition: František Duška.

Investigation: Jan Gojda, Petr Waldauf, Natália Hrušková, Barbora Blahutová, Adéla Krajčová, Tomáš Urban, Petr Tůma.

Methodology: Jan Gojda, Petr Waldauf, Barbora Blahutová, Tomáš Urban, Petr Tůma, František Duška.

Project administration: Jan Gojda, Natália Hrušková, Barbora Blahutová.

Resources: Kamila Řasová, František Duška.

Software: Petr Waldauf, Natália Hrušková, Barbora Blahutová, Adéla Krajčová, Petr Tůma.

Supervision: Kamila Řasová, František Duška.

Validation: Jan Gojda, František Duška.

Visualization: Petr Waldauf.

Writing – original draft: Jan Gojda, František Duška.

Writing – review & editing: Jan Gojda, Petr Waldauf, Adéla Krajčová, Tomáš Urban, Kamila Řasová, František Duška.

References

1. Glaser RM. Physiologic aspects of spinal cord injury and functional neuromuscular stimulation. *Cent Nerv Syst Trauma*. 1986; 3: 49–62. Available: <http://www.ncbi.nlm.nih.gov/pubmed/3524868> PMID: 3524868
2. Hunt KJ, Fang J, Saengsuwan J, Grob M, Laubacher M. On the efficiency of FES cycling: a framework and systematic review. *Technol Health Care*. 2012; 20: 395–422. <https://doi.org/10.3233/THC-2012-0689> PMID: 23079945
3. Szecsi J, Schiller M. FES-propelled cycling of SCI subjects with highly spastic leg musculature. *NeuroRehabilitation*. 2009; 24: 243–53. <https://doi.org/10.3233/NRE-2009-0475> PMID: 19458432
4. Lo H-C, Hsu Y-C, Hsueh Y-H, Yeh C-Y. Cycling exercise with functional electrical stimulation improves postural control in stroke patients. *Gait Posture*. 2012; 35: 506–10. <https://doi.org/10.1016/j.gaitpost.2011.11.017> PMID: 22153770
5. Peri E, Ambrosini E, Pedrocchi A, Ferrigno G, Nava C, Longoni V, et al. Can FES-Augmented Active Cycling Training Improve Locomotion in Post-Acute Elderly Stroke Patients? *Eur J Transl Myol*. PAGE-Press; 2016; 26: 6063. <https://doi.org/10.4081/ejtm.2016.6063> PMID: 27990234
6. Szecsi J, Schlick C, Schiller M, Pöllmann W, Koenig N, Straube A. Functional electrical stimulation-assisted cycling of patients with multiple sclerosis: Biomechanical and functional outcome—A pilot study. *J Rehabil Med*. 2009; 41: 674–680. <https://doi.org/10.2340/16501977-0397> PMID: 19565162
7. Mohr T, Dela F, Handberg A, Biering-Sørensen F, Galbo H, Kjaer M. Insulin action and long-term electrically induced training in individuals with spinal cord injuries. *Med Sci Sports Exerc*. 2001; 33: 1247–52. Available: <http://www.ncbi.nlm.nih.gov/pubmed/11474322> PMID: 11474322
8. Young W. Electrical Stimulation and Motor Recovery. *Cell Transplant*. 2015; 24: 429–446. <https://doi.org/10.3727/096368915X686904> PMID: 25646771
9. Morris PE, Herridge MS. Early intensive care unit mobility: future directions. *Crit Care Clin*. Elsevier; 2007; 23: 97–110. <https://doi.org/10.1016/j.ccc.2006.11.010> PMID: 17307119
10. Schweickert WD, Kress JP. Implementing Early Mobilization Interventions in Mechanically Ventilated Patients in the ICU. *Chest*. 2011; 140: 1612–1617. <https://doi.org/10.1378/chest.10-2829> PMID: 22147819
11. Choong K, Koo KKY, Clark H, Chu R, Thabane L, Burns KEA, et al. Early Mobilization in Critically Ill Children. *Crit Care Med*. 2013; 41: 1745–1753. <https://doi.org/10.1097/CCM.0b013e318287f592> PMID: 23507722
12. TEAM Study Investigators, Hodgson C, Bellomo R, Berney S, Bailey M, Buhr H, et al. Early mobilization and recovery in mechanically ventilated patients in the ICU: a bi-national, multi-centre, prospective cohort study. *Crit Care*. 2015; 19: 81. <https://doi.org/10.1186/s13054-015-0765-4> PMID: 25715872
13. Pawlik AJ. Early Mobilization in the Management of Critical Illness. *Crit Care Nurs Clin North Am*. 2012; 24: 481–490. <https://doi.org/10.1016/j.ccell.2012.05.003> PMID: 22920471

14. Friedrich O, Reid MB, Van den Berghe G, Vanhorebeek I, Hermans G, Rich MM, et al. The Sick and the Weak: Neuropathies/Myopathies in the Critically Ill. *Physiol Rev. American Physiological Society*; 2015; 95: 1025–109. <https://doi.org/10.1152/physrev.00028.2014> PMID: 26133937
15. Herridge MS, Tansey CM, Matté A, Tomlinson G, Diaz-Granados N, Cooper A, et al. Functional Disability 5 Years after Acute Respiratory Distress Syndrome. *N Engl J Med*. 2011; 364: 1293–1304. <https://doi.org/10.1056/NEJMoa1011802> PMID: 21470008
16. Kress JP, Hall JB. ICU-Acquired Weakness and Recovery from Critical Illness. *N Engl J Med*. 2014; 370: 1626–1635. <https://doi.org/10.1056/NEJMra1209390> PMID: 24758618
17. Levine S, Nguyen T, Taylor N, Friscia ME, Budak MT, Rothenberg P, et al. Rapid Disuse Atrophy of Diaphragm Fibers in Mechanically Ventilated Humans. *N Engl J Med*. 2008; 358: 1327–1335. <https://doi.org/10.1056/NEJMoa070447> PMID: 18367735
18. Parry SM, Puthuchearu ZA. The impact of extended bed rest on the musculoskeletal system in the critical care environment. *Extrem Physiol Med. BioMed Central*; 2015; 4: 16. <https://doi.org/10.1186/s13728-015-0036-7> PMID: 26457181
19. Parry SM, Berney S, Warrillow S, El-Ansary D, Bryant AL, Hart N, et al. Functional electrical stimulation with cycling in the critically ill: A pilot case-matched control study. *J Crit Care*. 2014; 29: 695.e1–695.e7. <https://doi.org/10.1016/j.jcrc.2014.03.017> PMID: 24768534
20. Duffell LD, de N. Donaldson N, Newham DJ. Why is the Metabolic Efficiency of FES Cycling Low? *IEEE Trans Neural Syst Rehabil Eng*. 2009; 17: 263–269. <https://doi.org/10.1109/TNSRE.2009.2016199> PMID: 19258202
21. Hunt KJ, Hosmann D, Grob M, Saengsuwan J. Metabolic efficiency of volitional and electrically stimulated cycling in able-bodied subjects. *Med Eng Phys*. 2013; 35: 919–925. <https://doi.org/10.1016/j.medengphy.2012.08.023> PMID: 23253953
22. Hunt KJ, Ferrario C, Grant S, Stone B, McLean AN, Fraser MH, et al. Comparison of stimulation patterns for FES-cycling using measures of oxygen cost and stimulation cost. *Med Eng Phys. Elsevier*; 2006; 28: 710–8. <https://doi.org/10.1016/j.medengphy.2005.10.006> PMID: 16298543
23. Downey RJ, Merad M, Gonzalez EJ, Dixon WE. The Time-Varying Nature of Electromechanical Delay and Muscle Control Effectiveness in Response to Stimulation-Induced Fatigue. *IEEE Trans Neural Syst Rehabil Eng*. 2017; 25: 1397–1408. <https://doi.org/10.1109/TNSRE.2016.2626471> PMID: 27845664
24. Kjaer M, Perko G, Secher NH, Boushel R, Beyer N, Pollack S, et al. Cardiovascular and ventilatory responses to electrically induced cycling with complete epidural anaesthesia in humans. *Acta Physiol Scand. Blackwell Publishing Ltd*; 1994; 151: 199–207. <https://doi.org/10.1111/j.1748-1716.1994.tb09738.x> PMID: 7942055
25. Kim CK, Strange S, Bangsbo J, Saltin B. Skeletal muscle perfusion in electrically induced dynamic exercise in humans. *Acta Physiol Scand. Blackwell Publishing Ltd*; 1995; 153: 279–287. <https://doi.org/10.1111/j.1748-1716.1995.tb09864.x> PMID: 7625181
26. Scremin OU, Cuevas-Trisan RL, Scremin AM, Brown C V, Mandelkern MA. Functional electrical stimulation effect on skeletal muscle blood flow measured with H₂(15)O positron emission tomography. *Arch Phys Med Rehabil*. 1998; 79: 641–6. Available: <http://www.ncbi.nlm.nih.gov/pubmed/9630142> PMID: 9630142
27. Tepavac D, Schwirtlich L. Detection and prediction of FES-induced fatigue. *J Electromyogr Kinesiol*. 1997; 7: 39–50. Available: <http://www.ncbi.nlm.nih.gov/pubmed/20719690> PMID: 20719690
28. Kim CK, Bangsbo J, Strange S, Karpakka J, Saltin B. Metabolic response and muscle glycogen depletion pattern during prolonged electrically induced dynamic exercise in man. *Scand J Rehabil Med*. 1995; 27: 51–8. Available: <http://www.ncbi.nlm.nih.gov/pubmed/7792551> PMID: 7792551
29. Glaser RM. *Physiology of Functional Electrical Stimulation-Induced Exercise: Basic Science Perspective. Neurorehabil Neural Repair. Sage PublicationsSage CA: Thousand Oaks, CA*; 1991; 5: 49–61. <https://doi.org/10.1177/136140969100500106>
30. Gater DR, McDowell SM, Abbas JJ. *Electrical Stimulation: A Societal Perspective. Assist Technol. Taylor & Francis Group*; 2000; 12: 85–91. <https://doi.org/10.1080/10400435.2000.10132012> PMID: 11067581
31. Tsutaki A, Ogasawara R, Kobayashi K, Lee K, Kouzaki K, Nakazato K. Effect of intermittent low-frequency electrical stimulation on the rat gastrocnemius muscle. *Biomed Res Int. Hindawi*; 2013; 2013: 480620. <https://doi.org/10.1155/2013/480620> PMID: 23936807
32. Dreyer HC, Fujita S, Cadenas JG, Chinkes DL, Volpi E, Rasmussen BB. Resistance exercise increases AMPK activity and reduces 4E-BP1 phosphorylation and protein synthesis in human skeletal muscle. *J Physiol. Wiley-Blackwell*; 2006; 576: 613–24. <https://doi.org/10.1113/jphysiol.2006.113175> PMID: 16873412

33. Hulston CJ, Wolsk E, Grondhal TS, Yfanti C, Van Hall G. Protein Intake Does Not Increase Vastus Lateralis Muscle Protein Synthesis during Cycling. *Med Sci Sport Exerc.* 2011; 43: 1635–1642. <https://doi.org/10.1249/MSS.0b013e31821661ab> PMID: 21364482
34. Biolo G, Maggi SP, Williams BD, Tipton KD, Wolfe RR. Increased rates of muscle protein turnover and amino acid transport after resistance exercise in humans. *Am J Physiol Metab.* 1995; 268: E514–E520. <https://doi.org/10.1152/ajpendo.1995.268.3.E514> PMID: 7900797
35. Holm L, van Hall G, Rose AJ, Miller BF, Doessing S, Richter EA, et al. Contraction intensity and feeding affect collagen and myofibrillar protein synthesis rates differently in human skeletal muscle. *Am J Physiol Metab.* 2010; 298: E257–E269. <https://doi.org/10.1152/ajpendo.00609.2009> PMID: 19903866
36. Dideriksen K, Reitelseder S, Holm L. Influence of Amino Acids, Dietary Protein, and Physical Activity on Muscle Mass Development in Humans. *Nutrients.* 2013; 5: 852–876. <https://doi.org/10.3390/nu5030852> PMID: 23486194
37. van Hall G, González-Alonso J, Sacchetti M, Saltin B. Skeletal muscle substrate metabolism during exercise: methodological considerations. *Proc Nutr Soc.* 1999; 58: 899–912. Available: <http://www.ncbi.nlm.nih.gov/pubmed/10817157> PMID: 10817157
38. Tüma P. Rapid determination of globin chains in red blood cells by capillary electrophoresis using INST-Coated fused-silica capillary. *J Sep Sci.* 2014; 37: 1026–1032. Available: <http://dx.doi.org/10.1002/jssc.201400044> PMID: 24677638
39. Kjær M, Dela F, Sørensen FB, Secher NH, Bangsbo J, Mohr T, et al. Fatty acid kinetics and carbohydrate metabolism during electrical exercise in spinal cord-injured humans. *Am J Physiol Integr Comp Physiol.* American Physiological SocietyBethesda, MD; 2001; 281: R1492–R1498. <https://doi.org/10.1152/ajpregu.2001.281.5.R1492> PMID: 11641120
40. Jones B, Kenward MG. Chapter 5: Analysis of continuous data. In: Design and analysis of cross-over trials [Internet]. Available: <http://researchonline.lshtm.ac.uk/2537976/>
41. Soulele K, Macheras P, Silvestro L, Rizea Savu S, Karalis V. Population pharmacokinetics of fluticasone propionate/salmeterol using two different dry powder inhalers. *Eur J Pharm Sci.* 2015; 80: 33–42. <https://doi.org/10.1016/j.ejps.2015.08.009> PMID: 26296862
42. Vallet B, Teboul J-L, Cain S, Curtis S. Venoarterial CO(2) difference during regional ischemic or hypoxic hypoxia. *J Appl Physiol.* 2000; 89: 1317–1321. <https://doi.org/10.1152/jappl.2000.89.4.1317> PMID: 11007564
43. Sun Y, Ferguson BS, Rogatzki MJ, McDonald JR, Gladden LB. Muscle Near-Infrared Spectroscopy Signals versus Venous Blood Hemoglobin Oxygen Saturation in Skeletal Muscle. *Med Sci Sport Exerc.* 2016; 48: 2013–2020. <https://doi.org/10.1249/MSS.0000000000001001> PMID: 27635772
44. Esaki K, Hamaoka T, Rådegran G, Boushel R, Hansen J, Katsumura T, et al. Association between regional quadriceps oxygenation and blood oxygen saturation during normoxic one-legged dynamic knee extension. *Eur J Appl Physiol.* 2005; 95: 361–370. <https://doi.org/10.1007/s00421-005-0008-5> PMID: 16096839
45. Gladden LB. Lactate metabolism: a new paradigm for the third millennium. *J Physiol.* Wiley-Blackwell; 2004; 558: 5–30. <https://doi.org/10.1113/jphysiol.2003.058701> PMID: 15131240
46. Gladden LB. Lactate metabolism: a new paradigm for the third millennium. *J Physiol.* Wiley-Blackwell; 2004; 558: 5–30. <https://doi.org/10.1113/jphysiol.2003.058701> PMID: 15131240
47. Brooks GA. Intra- and extra-cellular lactate shuttles. *Med Sci Sports Exerc.* 2000; 32: 790–9. Available: <http://www.ncbi.nlm.nih.gov/pubmed/10776898> PMID: 10776898
48. Mallat J, Lemyze M, Meddour M, Pepy F, Gasan G, Barrailler S, et al. Ratios of central venous-to-arterial carbon dioxide content or tension to arteriovenous oxygen content are better markers of global anaerobic metabolism than lactate in septic shock patients. *Ann Intensive Care.* Springer; 2016; 6: 10. <https://doi.org/10.1186/s13613-016-0110-3> PMID: 26842697
49. Hettinga DM, Andrews BJ. Oxygen consumption during functional electrical stimulation-assisted exercise in persons with spinal cord injury: implications for fitness and health. *Sports Med.* 2008; 38: 825–38. Available: <http://www.ncbi.nlm.nih.gov/pubmed/18803435> PMID: 18803435
50. Wagenmakers AJ. Muscle amino acid metabolism at rest and during exercise: role in human physiology and metabolism. *Exerc Sport Sci Rev.* 1998; 26: 287–314. Available: <http://www.ncbi.nlm.nih.gov/pubmed/9696993> PMID: 9696993
51. Ashley Z, Sutherland H, Russold MF, Lanmüller H, Mayr W, Jarvis JC, et al. Therapeutic stimulation of denervated muscles: The influence of pattern. *Muscle Nerve.* 2008; 38: 875–886. <https://doi.org/10.1002/mus.21020> PMID: 18563723
52. Hickmann CE, Roeseler J, Castanares-Zapatero D, Herrera EI, Mongodin A, Laterre P-F. Energy expenditure in the critically ill performing early physical therapy. *Intensive Care Med.* 2014; 40: 548–555. <https://doi.org/10.1007/s00134-014-3218-7> PMID: 24477456

53. Mathewson KW, Haykowsky MJ, Thompson RB. Feasibility and reproducibility of measurement of whole muscle blood flow, oxygen extraction, and VO_2 with dynamic exercise using MRI. *Magn Reson Med*. 2015; 74: 1640–1651. <https://doi.org/10.1002/mrm.25564> PMID: 25533515

Příloha 3

Krajčová A, Løvsletten NG, Waldauf P, Frič V, Elkalaf M, **Urban T**, Anděl M, Trnka J, Thoresen GH, Duška F.

Effects of Propofol on Cellular Bioenergetics in Human Skeletal Muscle Cells.

Crit Care Med. 2018 Mar;46(3):e206-e212. doi: 10.1097/CCM.0000000000002875. PMID: 29240609. IF 6.971

Effects of Propofol on Cellular Bioenergetics in Human Skeletal Muscle Cells

Adéla Krajčová, MD^{1,2,3}; Nils Gunnar Løvsletten, MSci Pharm⁴; Petr Waldauf, MD¹; Vladimír Frič, MD⁵; Moustafa Elkalaf, MBBCh, PhD^{2,3}; Tomáš Urban¹; Michal Anděl, MD, CSc²; Jan Trnka, MD, PhD^{2,3}; G. Hege Thoresen, MD, PhD⁴; František Duška, MD, PhD¹

Objectives: Propofol may adversely affect the function of mitochondria and the clinical features of propofol infusion syndrome suggest that this may be linked to propofol-related bioenergetic failure. We aimed to assess the effect of therapeutic propofol concentrations on energy metabolism in human skeletal muscle cells.

Design: In vitro study on human skeletal muscle cells.

Settings: University research laboratories.

Subjects: Patients undergoing hip surgery and healthy volunteers.

Interventions: Vastus lateralis biopsies were processed to obtain cultured myotubes, which were exposed to a range of 1–10 µg/mL propofol for 96 hours.

Measurements and Main Results: Extracellular flux analysis was used to measure global mitochondrial functional indices, glycoly-

¹Department of Anaesthesia and Intensive Care of Královské Vinohrady University Hospital and The Third Faculty of Medicine, OXYLAB-Laboratory for Mitochondrial Physiology, Charles University, Prague, Czech Republic.

²Centre for Research on Diabetes, Metabolism and Nutrition of Third Faculty of Medicine, Charles University, Prague, Czech Republic.

³Laboratory for Metabolism and Bioenergetics, The Third Faculty of Medicine, Charles University, Prague, Czech Republic.

⁴Department of Pharmaceutical Biosciences, School of Pharmacy, University of Oslo, Oslo, Norway.

⁵Department of Orthopaedics and Traumatology, Královské Vinohrady University Hospital and The Third Faculty of Medicine, Charles University, Prague, Czech Republic.

Supplemental digital content is available for this article. Direct URL citations appear in the printed text and are provided in the HTML and PDF versions of this article on the journal's website (<http://journals.lww.com/ccmjournal>).

Supported, in part, by grants GAUK 270915, PRVOUK P 31/P 33, PROGRES Q 36/Q 37, and AZV 16-28663A.

Dr. Krajčová disclosed that material for the laboratory work was supported from funding grants (UNCE, PROGRES Q36/Q37, PRVOUK P31/P33, AZV 16-28663A, GAUK 270915). Dr. Anděl's institution received funding from Charles University Institutional Program Prvok P 31 and Charles University Grant Nr 270 915, and he received funding from Sanofi Diabetes, Lilly, Novo Nordisk, Astra Zeneca, Merck, BMS, Sanofi Diabetes, GSK, and MSD. Dr. Trnka's institution received funding from Charles University. The remaining authors have disclosed that they do not have any potential conflicts of interest.

For information regarding this article, E-mail: adela.krajcova@lf3.cuni.cz

Copyright © 2017 by the Society of Critical Care Medicine and Wolters Kluwer Health, Inc. All Rights Reserved.

DOI: 10.1097/CCM.0000000000002875

sis, fatty acid oxidation, and the functional capacities of individual complexes of electron transfer chain. In addition, we used [1-¹⁴C] palmitate to measure fatty acid oxidation and spectrophotometry to assess activities of individual electron transfer chain complexes II–IV. Although cell survival and basal oxygen consumption rate were only affected by 10 µg/mL of propofol, concentrations as low as 1 µg/mL reduced spare electron transfer chain capacity. Uncoupling effects of propofol were mild, and not dependent on concentration. There was no inhibition of any respiratory complexes with low dose propofol, but we found a profound inhibition of fatty acid oxidation. Addition of extra fatty acids into the media counteracted the propofol effects on electron transfer chain, suggesting inhibition of fatty acid oxidation as the causative mechanism of reduced spare electron transfer chain capacity. Whether these metabolic in vitro changes are observable in other organs and at the whole-body level remains to be investigated.

Conclusions: Concentrations of propofol seen in plasma of sedated patients in ICU cause a significant inhibition of fatty acid oxidation in human skeletal muscle cells and reduce spare capacity of electron transfer chain in mitochondria. (*Crit Care Med* 2018; 46:e206–e212)

Key Words: fatty acid oxidation; mitochondrial dysfunction; propofol; propofol infusion syndrome; skeletal muscle

Propofol infusion syndrome (PRIS) is a rare, but potentially fatal complication of propofol administration characterized by presence of unexplained metabolic acidosis, arrhythmias, Brugada-like pattern on the electrocardiogram, cardiac and/or renal failure, rhabdomyolysis, hyperkalemia, hepatomegaly and hyperlipidemia (1–7). The pathogenesis of PRIS is still unknown; experimental studies performed on animal models and clinical features of PRIS (8–10) are suggestive of its mitochondrial origin (11–18). According to the animal in vitro studies, propofol is thought to act as an inhibitor of the electron transport chain (11, 13, 14, 16) and probably a mild uncoupler of the inner mitochondrial membrane (12, 14). However, these effects were only observed after a very short exposure of nonhuman cells to propofol concentrations in the

order of magnitude higher than the concentrations found in human plasma during propofol anesthesia (19) or sedation (20, 21), and the relevancy of these studies for patients exposed to propofol remains uncertain. Human data are scanty. Our group analyzed all 153 case reports of PRIS published between years 1990 and 2014 (22) and observed patterns in the relationship between time and dose of propofol infusion and reported signs of the syndrome; symptoms that could be caused by mitochondrial uncoupling (e.g., fever, heart failure) occurred relatively early and after high doses of propofol. On the other hand, signs, which would be consistent with accumulation of nonesterified fatty acids (NEFAs) (23–26), such as rhabdomyolysis or arrhythmias, occurred after protracted propofol infusions irrespective of doses. A cumulative dose of propofol was the main risk factor influencing the severity of PRIS and its mortality in our analysis, suggesting that rather than being an idiosyncratic reaction, PRIS might be an extreme manifestation, in susceptible individuals, of changes of cellular bioenergetics that normally occur after propofol administration, albeit in subtle form and remain asymptomatic in the vast majority of patients.

In light of this, we studied metabolic effects of 4 days exposure of human skeletal muscle cells to clinically relevant concentrations of propofol.

METHODS

Study Subjects

Vastus lateralis muscle biopsies were obtained by open technique from patients during hip replacement surgery ($n = 30$; age, 71.8 ± 7.1 ; body mass index, 28.5 ± 4.8) at the Department of Orthopaedic Surgery of Královské Vinohrady University Hospital in Prague. We excluded patients who had already received any dose of propofol or had known metabolic muscle disorder. Detailed characteristics of study subjects are in **Table S1** (Supplemental Digital Content 1, <http://links.lww.com/CCM/D63>). In addition, for [$1\text{-}^{14}\text{C}$]palmitate experiments (Experiment 7, see below), we obtained vastus lateralis samples under local anesthesia from five healthy volunteers by Bergstrom technique (27) in the Department of Pharmaceutical Biosciences at the University of Oslo. The study protocols were approved by respective research ethics boards in both institutions. All patients provided a prospective written informed consent.

Cell Culture Isolation

Skeletal muscle cells were isolated and cultured as previously described (28) (**Fig. S2A**, Supplemental Digital Content 1, <http://links.lww.com/CCM/D63>). Upon 80–90% confluence, myoblasts were passaged and seeded into: 1) gelatine-coated 24-well XF24 V7 cell culture microplates (Agilent Technologies Inc., Santa Clara, CA) for extracellular flux analyses, 2) gelatine-coated Petri dishes for later spectrophotometric analyses, 3) 96-well microplates for cell viability assay, and 4) 24-well plates for acid-soluble metabolites analysis. After 24-hour incubation, the medium was changed to differentiation medium (consisting of Dulbecco's Modified Eagle Medium with 2% of Horse Serum) to induce differentiation into myotubes

(**Fig. S2B**, Supplemental Digital Content 1, <http://links.lww.com/CCM/D63>). After 7 days, differentiated myotubes were exposed for 96 hours to a range of experimental conditions, which are schematically shown in **Fig. S1** (Supplemental Digital Content 1, <http://links.lww.com/CCM/D63>) and described below. All chemicals used in experiments were purchased from Sigma-Aldrich (St. Louis, MO) or Gibco-Life Technologies (Gaithersburg, MD).

Overview of Experiments on Myotubes Exposed to Propofol

First, we determined which concentrations of propofol in the media are survivable for the cells (Experiment 1) (**Fig. S1**, Supplemental Digital Content 1, <http://links.lww.com/CCM/D63>). Following this, we used extracellular flux analysis to determine global mitochondrial functional indices (Experiment 2) and fatty acid oxidation (Experiment 3) in intact cells. By extracellular flux analysis in permeabilized cells, we measured respiration linked to individual respiratory complexes I–IV (Experiment 4). In addition (Experiment 5), we homogenized cells and measured by spectrophotometry activities of selected enzymes, including respiratory complexes, acyl-CoA dehydrogenase (ACAD), and citrate synthase (CS). Then, we repeated the design of Experiment 2 in cells coexposed to propofol and fatty acids (Experiment 6). Last, while experiments 1–6 were performed on cells obtained from orthopedic patients ($n = 7$ for each experiment), in Experiment 7 we used cells isolated from healthy volunteers ($n = 5$) and applied [$1\text{-}^{14}\text{C}$]palmitate method to assess fatty acid oxidation. All experiments are briefly described below, whereas step-by-step protocols including detailed composition of culture media and other experimental solutions can be found in **supplementary appendix** (Supplemental Digital Content 1, <http://links.lww.com/CCM/D63>).

Experiment 1. Cell viability measurements were performed by a colorimetric MTS (3-(4,5-dimethylthiazol-2-yl)-5-(3-carboxymethoxyphenyl)-2-(4-sulfophenyl)-2H-tetrazolium) assay as previously described (29). We tested for propofol concentrations between 1 and 50 $\mu\text{g}/\text{mL}$. Given that concentrations greater than 10 $\mu\text{g}/\text{mL}$ impair cell survival (**Fig. S3**, Supplemental Digital Content 1, <http://links.lww.com/CCM/D63>), we used only lower concentrations for the bioenergetic experiments 2–7.

Experiment 2. Global mitochondrial functional indices were assessed by Seahorse XF Extracellular Flux Analyser (Agilent Technologies) (30). All the experiments were performed after calibration of the instrument with the temperature settled at 37°C and all the buffers were adjusted to pH 7.4 before measurement. In each experiment, there were six different experimental conditions tested in a 24-well microplate. Hence, each condition for each subject was measured in tri- or tetraplicates. We used a sequential addition of adenosine triphosphate (ATP) ase inhibitor, oligomycin, an uncoupler carbonyl cyanide-4-[trifluoromethoxy]phenylhydrazone (FCCP) and complex III inhibitor antimycin A (AA). Oxygen consumption rate (OCR) after addition of AA was considered nonmitochondrial. This enabled us to calculate OCR at baseline (basal OCR) (as OCR at baseline—nonmitochondrial), ATP consumption rate

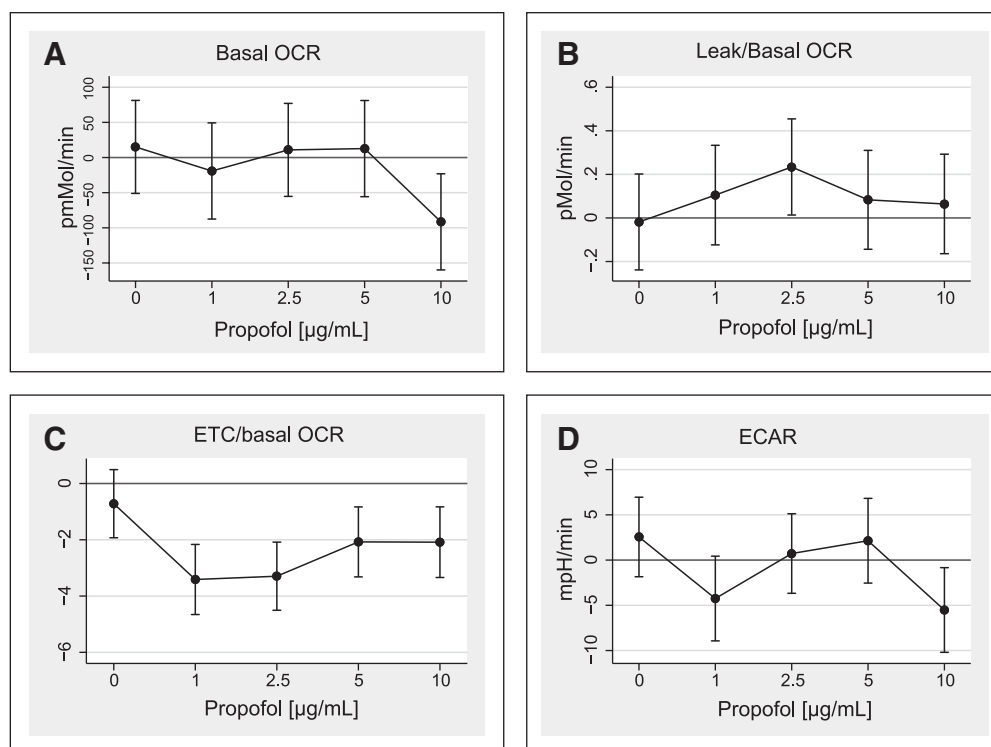


Figure 1. Differences in bioenergetic variables (y-axis) caused by a range of propofol concentrations (x-axis) diluted in 0.1% ethanol (propofol = 0 refers to ethanol alone) compared with reference cells cultured in fresh media (mean from $n = 6$; vertical bars represent 95% CIs). **A**, Basal oxygen consumption rate (OCR). **B**, Leak/basal OCR ratio. **C**, Electron transfer chain capacity (ETC)/basal OCR ratio. **D**, The extracellular acidification rate (ECAR) reflects the rate of anaerobic glycolysis.

(as a decrement of OCR after addition of oligomycin), OCR related to leak of protons through inner mitochondrial membrane (as basal OCR - ATP consumption), and the spare electron transfer chain capacity (ETC) capacity (calculated as OCR after the addition of FCCP—nonmitochondrial). Anaerobic glycolysis was measured in parallel using an embedded pH electrode, with extracellular acidification rate (ECAR) reflecting the production of lactate (30).

Experiment 3. Fatty acid oxidation was determined using extracellular flux analysis. Intact (nonpermeabilized) myotubes in a carnitine-rich media were first uncoupled by FCCP. Palmitate was then added to reach 200 μM , and fatty acid oxidation (FAO) was inhibited by etomoxir. The decrement of OCR with etomoxir is considered as the rate of FAO.

Experiment 4. Respiration linked to individual complexes of electron transport system was analyzed in saponin-permeabilized cells. In order to measure CI, II, and IV-linked respiration, we pretreated cells with adenosine diphosphate and malate + glutamate before using sequential addition of rotenone, succinate, AA, and N,N,N',N'-tetramethyl-p-phenylenediamine (TMPD) + ascorbate. Complex I respiration was calculated as the decrement after rotenone, complex II as the increment after the addition of succinate, and complex IV as the increment after addition of TMPD and ascorbate. Complex III-linked respiration was measured on a separate plate using freshly prepared duroquinone as the substrate.

Experiment 5. Spectrophotometric analysis of the activity of CS, individual respiratory complexes, and ACAD were

analyzed in cell homogenates disrupted by three freezing-thawing cycles as described previously (31-33). Protein content was determined using Bradford assay (34).

Experiment 6. Interaction of propofol with fatty acids. Propofol for infusions is diluted in 10% Intralipid, which is rapidly hydrolyzed into NEFAs (35, 36). In order to mimic this effect of propofol in vitro, we incubated cells also in fatty acid mixture resembling fatty acid composition of Intralipid (37), which is linoleate:oleate:palmitate equals to 6:3:1 in total concentration of 500 μM . In these experiments, cells were cultured in two different concentrations of propofol (2.5 and 10 $\mu\text{g/mL}$) with and without NEFA (groups P2.5, P10, and P2.5 + NEFA, P10 + NEFA). Control groups of

cells were cultured in fresh medium with and without fatty acid mixture (groups C, C+NEFA). After 96 hours of exposure, mitochondrial functional indices were determined by extracellular flux analysis in the setting identical with Experiment 2.

Experiment 7. Analysis of FAO by [^{14}C]palmitate method. After 96 hours of myotubes exposure, the medium was completely removed before addition of 0.5 $\mu\text{Ci/mL}$ [^{14}C]palmitic acid (PerkinElmer NEN, Boston, MA), given in DMEM-Glutamax (Dulbecco's modified Eagle's medium with Glutamax; Gibco, Life Technologies, Paisley, UK) with L-carnitine and bovine serum albumin (BSA). The cells were incubated at 37°C for 4 hours before the incubation media (100 μL) were collected, added to 30 μL BSA (6%) and 300 μL HClO_4 , and centrifuged at 10,000 rpm/4°C/10 min. Supernatant of about 200 μL was then counted by liquid scintillation (Packard Tri-Carb 1900 TR; PerkinElmer, Waltham, MA). Oxidation of [^{14}C] palmitic acid to acid-soluble metabolites, which consist mainly of tricarboxylic acid cycle metabolites, was used as the measure of the rate of FAO.

Statistics

For statistical analysis, we used software Stata 14.2 (Stata Corp., LLC, College Station, TX). In order to deal with hierarchical structure of the data, we used a four-level mixed effect model of linear regression. In the fixed part, the model consists of a dependent continuous variable (e.g., a bioenergetic variable) and an independent variable, which is a categorical variable describing

the experimental condition (e.g., the concentration of propofol). In the random part, the model reflects the following four levels: subjects, experimental condition, well, and repeated measures in each well. The data are presented as the difference (with a 95% CI and p value) between the mean value of the dependent variable of reference cells and the mean value of the dependent variable under the given experimental condition.

RESULTS

Cell Survival (Experiment 1) and Influence of Propofol on Mitochondrial and Protein Content

Four days of myotubes exposure to propofol up to 10 $\mu\text{g}/\text{mL}$ did not cause detectable changes in cell survival measured by MTS test, but higher concentrations (25 and 50 $\mu\text{g}/\text{mL}$) were toxic. Neither NEFA nor Intralipid alone affected cell survival. In all experiments, exposure to propofol caused a degree of dose-dependent reduction of both protein and mitochondrial contents (measured as Bradford assay or CS activity, respectively). These changes were mirrored in changes of basal OCR. See **Figures S3** and **S4** (Supplemental Digital Content 1, <http://links.lww.com/CCM/D63>). Hence, we normalized all functional mitochondrial indices derived from extracellular flux analysis to basal OCR.

Global Mitochondrial Functional Indices (Experiment 2)

Basal OCR was only affected by 10 $\mu\text{g}/\text{mL}$ (**Fig. 1A**). Leak through the inner mitochondrial membrane tended to be increased in a nonconcentration dependent manner (from 21% of basal OCR in controls to 24–40% in cells exposed to propofol), but this effect only reached statistical significance with 2.5 $\mu\text{g}/\text{mL}$ of propofol (**Fig. 1B**). Spare ETC capacity in control cells was 378% \pm 135% of basal OCR. This was significantly reduced across all concentrations of propofol (to 113% \pm 96%, 111% \pm 77%, 245% \pm 155%, 245% \pm 188% for 1.0, 2.5, 5.0, and 10 $\mu\text{g}/\text{mL}$ of propofol, respectively, $p < 0.01$ for all differences) (**Fig. 1C**). No effect was observed after incubation of cells in the Intralipid vehicle. Anaerobic glycolysis, as measured as the ECAR which reflects production of lactate (30), was highly variable and only reduced by 10 $\mu\text{g}/\text{mL}$ of propofol (**Fig. 1D**).

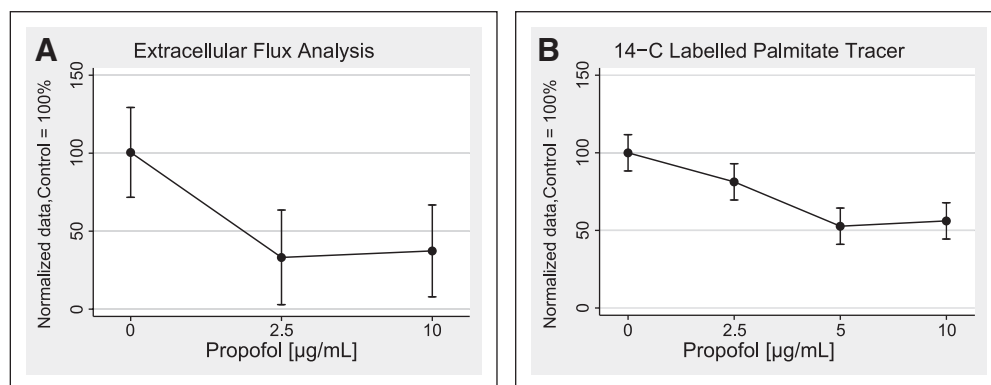


Figure 2. Changes in fatty acid oxidation rate caused by propofol measured by extracellular flux analysis (**A**) and by [^{14}C]palmitate (**B**). Data expressed as mean % of value in reference cells (i.e., cultured without propofol), which are arbitrarily set as 100%. Vertical bars are 95% CI.

Fatty Acid Oxidation (Experiments 3 and 7)

By extracellular flux analysis (Experiment 3), we found a profound inhibition of FAO which decreased to 36% and 33% of values in control cells with 2.5 or 10 $\mu\text{g}/\text{mL}$ of propofol, respectively ($p < 0.01$ for both) (**Fig. 2A**). In line (Experiment 7), we observed a significant decrease of FAO with 2.5, 5, and 10 $\mu\text{g}/\text{mL}$ of propofol (**Fig. 2B**) with [^{14}C]palmitate technique.

Influence of Propofol on the Capacity of Individual Respiratory Complexes (Experiments 4 and 5)

As determined in experiment 5 (i.e., when measured in isolation by spectrophotometry), we have not found any inhibition by propofol of the capacity of respiratory complexes II–IV nor ACAD. In intact mitochondria of saponin-permeabilized myotubes (Experiment 4), there was no effect of propofol 2.5 $\mu\text{g}/\text{mL}$ on ETC complexes either, but with 10 $\mu\text{g}/\text{mL}$, there was a reduction of the activity of the complexes III and IV (**Table 1**). There was no correlation between the activity of any of these complexes and ETC spare capacity (data not shown).

Interaction of Propofol With Nonesterified Fatty Acid Exposure in the Media (Experiment 6)

We exposed cells to 2.5 and 10 $\mu\text{g}/\text{mL}$ of propofol with and without NEFA. Addition of NEFA alone to the media did not affect cell survival or global mitochondrial functional indices, but it mitigated the inhibitory effects of propofol on basal OCR (**Fig. 3A**) and normalized spare ETC capacity (**Fig. 3B**) in cells coexposed to propofol.

DISCUSSION

In this study, we used an in vitro model of human skeletal muscle and studied the effects of propofol on major bioenergetics pathways. We exposed human myotubes to propofol concentrations in a range 1–10 $\mu\text{g}/\text{mL}$ for 96 hours in order to resemble levels achieved in patients during sedation in the ICU (1.2–4.5 $\mu\text{g}/\text{mL}$ [19, 20]) or during induction of general anesthesia (10.5 $\mu\text{g}/\text{mL}$ [19]). Although the highest propofol concentrations (10 $\mu\text{g}/\text{mL}$) affected mitochondrial content, and to some extent also activities of isolated respiratory complexes and cell survival, none of these effects were observed for

lower concentrations of propofol (2.5 $\mu\text{g}/\text{mL}$). Yet, even very low concentrations of propofol decreased spare ETC capacity, which reflects cellular ability to increase respiration when ATP demands are high. Because activities of individual respiratory complexes were unaffected by low propofol concentrations, we exploited propofol effects on upstream metabolic pathways, which feed electrons into ETC (**Fig. S1**, Supplemental Digital Content 1, <http://links.lww.com/>

TABLE 1. Mean activities (95% CIs) of Individual Mitochondrial Enzymes Expressed as % of Values in Control Cells Cultured in the Absence of Propofol

Mitochondrial Enzymes	Spectrophotometry (n = 6)		Extracellular Flux Analysis (n = 6)	
	Mean Enzyme Activity (Normalized to Citrate Synthase) Expressed as % of Controls (95% CI)		Mean Complex Capacity (Normalized to Basal Oxygen Consumption Rate) Expressed as % of Controls Without Propofol (95% CI)	
	Propofol Concentration: 2.5 µg/mL	Propofol Concentration: 10 µg/mL	Propofol Concentration: 2.5 µg/mL	Propofol Concentration: 10 µg/mL
Complex I	N/A	N/A	102 (93–112)	108 (98–117)
Complex II	102 (92–112)	124 ^a (114–134)	104 (97–110)	101 (94–109)
Complex III	123 (100–146)	109 (86–131)	82 (44–120)	41 ^a (10–92)
Complex IV	131 ^a (111–151)	104 (83–124)	85 (62–108)	73 ^a (46–99)
Acyl-CoA dehydrogenase	108 (85–130)	97 (74–119)	N/A	N/A

N/A = not applicable.

^ap < 0.05.

CCM/D63). We found a profound inhibition of fatty acid oxidation by extracellular flux analysis and confirmed this finding by the use of the [1-¹⁴C]palmitate tracer method. Furthermore, abundant NEFA in the media abolished the inhibitory effects of propofol on the spare ETC capacity. Taken together, these data suggest that propofol exposure limits spare ETC capacity by inhibiting FAO, rather than by inhibiting respiratory complexes or electron transfer within ETC.

Effects of propofol on bioenergetics have been extensively studied in animals, mostly by exposing isolated mitochondria from rat liver (11, 12, 14) or heart (13) to very high doses of propofol for a very short time (in order of minutes). In these studies, propofol inhibited complex I and, at high concentrations (> 35 µg/mL), also complex II (14). In the range 20–35 µg/mL, propofol caused mild uncoupling and dissipation of the transmembrane potential. Two hours of a propofol perfusion of isolated guinea pig hearts (9–37 µg/mL) slowed myoglobin desaturation during temporary ischemia, suggesting inhibitory effects of propofol on ETC (16). The only study of long-term (up to 18 hr) in vivo exposure to propofol is a landmark article of Vanlander et al (18), who, in rat tissue

homogenates, demonstrated an inhibition of complex II + III with 3.7 µg/mL of propofol, and of complex IV at 7.4 µg/mL, whereas activities of isolated complexes I, II, and III were unaffected. Ex vivo exposure required propofol concentrations of 10 times higher to cause a measurable inhibition of respiratory complexes (18). The authors explain the difference between in vivo and in vitro effects by different distribution of propofol within mitochondria. The inhibition of complex II + III by propofol was preventable with coincubation with coenzyme Q, which led the authors to the conclusion that in vivo inhibitory action of propofol on ETC can be explained by interference of propofol with coenzyme Q due to their structural similarity (18).

Ours is the first study looking at the long-term effects of propofol in an in vitro model of human tissue. We not only measured activities of individual ETC complexes but also studied effects of propofol on bioenergetics in a culture of intact or permeabilized cells by extracellular flux analysis, which we have previously adapted for the use in human myotubes (28). These are the main strengths of our study, particularly given our use of a prolonged exposure to concentrations found in

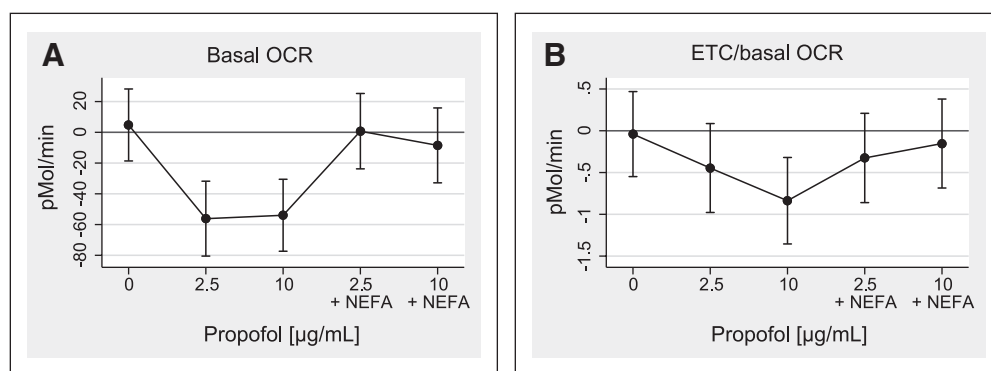


Figure 3. Interaction of propofol diluted in 0.1% ethanol with increased nonesterified fatty acids (NEFAs) in culture media (propofol = 0 are cells cultured in 0.1% ethanol). Reference cells were cultured in the fresh media. **A**, Changes in basal oxygen consumption rate (OCR). **B**, Changes in spare capacity of electron transfer chain ratio to basal OCR. ETC = electron transfer chain capacity.

to 2.5 µg/mL of propofol. Only the highest concentration (10 µg/mL) inhibited the activities of complexes III and IV, and only then if studied in permeabilized cells. Of note, we used the artificial substrates duroquinone and ascorbate/TMPD to measure activities of complexes III and IV, respectively. They donate electrons directly to respiratory complexes and bypass coenzyme Q, so their inhibition cannot be explained by the hypothesis by Kam and Cardone (38) and Vanlander et al (18) of propofol interference with coenzyme Q. Furthermore, spare ETC capacity and fatty acid oxidation were already limited by 2.5 µg/mL of propofol: a concentration, which did not cause any measurable inhibition of any of the respiratory complexes. Propofol-induced defect of fatty acid oxidation has long been hypothesized as the underlying mechanism of PRIS (8, 10). This is because PRIS shares some clinical signs with inborn defects of FAO, including rhabdomyolysis, skeletal myopathy, and arrhythmias. In FAO disorders, these abnormalities can be triggered by prolonged fasting or low-carbohydrate, ketogenic diet (39).

In one case, a child who was simultaneously receiving propofol sedation and ketogenic diet developed PRIS (40). Additionally, children with PRIS are often screened falsely positive for inborn defect of FAO as acyl-CoA derivatives are elevated in their blood (8, 10, 41) and these normalize in PRIS survivors after propofol withdrawal (8). Our data bring direct evidence of propofol inhibitory effect on FAO in human cells.

On the other hand, apart from measuring the activity of one of β -oxidation enzymes (ACAD) that was unaffected by propofol, we have not studied the mechanism of FAO inhibition any further. Propofol (or its intracellular metabolites) may inhibit carnitine-acyl transferases, β -oxidation complex, or electron transferring flavoprotein dehydrogenase. It is less likely that propofol-induced inhibition of FAO is secondary to an inhibition within ETC itself, as we have observed that any spare ETC capacity was unaffected if propofol-treated cells were cultured in fatty acid rich environment. However, it should be noted that although the range of total propofol concentration we exposed our cells to was in the range of that seen in propofol-sedated patients, free propofol concentrations might have been higher due to decreased protein binding in culture media as compared to plasma (42). In addition, added substances (BSA, palmitate) might have influenced propofol activity and confound the results. We chose skeletal muscle being a large body compartment comprising around 40% of total body mass and because it is directly affected in PRIS. It remains unclear how propofol affects bioenergetics in other human tissues and organs and whether any metabolic effects would be detectable at a whole-body level.

In conclusion, we have demonstrated that 96 hours of exposure of human skeletal muscle cells to concentrations of propofol found in plasma of propofol-sedated patients reduced the spare capacity of electron transfer chain and caused a profound inhibition of fatty acid oxidation. In the context of other studies in the field, our results generate the hypothesis that propofol affects fatty acid utilization at whole-body level.

Furthermore, in susceptible individuals (31), this may have adverse consequences, which, in extreme form, would result in the development of PRIS.

ACKNOWLEDGMENTS

We thank Zdeněk Drahota for valuable comments and support, Dr Jerome Cockings for proofreading, and all the volunteers who agreed to participate in this study.

REFERENCES

1. Notis fra Bivirkningsnaenet: Propofol (Diprivan) bivirkninger. [Adverse effects of propofol (Diprivan)]. *Ugeskr Laeger* 1990; 152:1176
2. Parke TJ, Stevens JE, Rice AS, et al: Metabolic acidosis and fatal myocardial failure after propofol infusion in children: Five case reports. *BMJ* 1992; 305:613–616
3. Bray RJ: Propofol infusion syndrome in children. *Paediatr Anaesth* 1998; 8:491–499
4. Marinella MA: Lactic acidosis associated with propofol. *Chest* 1996; 109:292
5. Stelow EB, Johari VP, Smith SA, et al: Propofol-associated rhabdomyolysis with cardiac involvement in adults: Chemical and anatomic findings. *Clin Chem* 2000; 46:577–581
6. Perrier ND, Baerga-Varela Y, Murray MJ: Death related to propofol use in an adult patient. *Crit Care Med* 2000; 28:3071–3074
7. Cremer OL, Moons KG, Bouman EA, et al: Long-term propofol infusion and cardiac failure in adult head-injured patients. *Lancet* 2001; 357:117–118
8. Wolf A, Weir P, Segar P, et al: Impaired fatty acid oxidation in propofol infusion syndrome. *Lancet* 2001; 357:606–607
9. Wolf AR, Potter F: Propofol infusion in children: When does an anesthetic tool become an intensive care liability? *Paediatr Anaesth* 2004; 14:435–438
10. Withington DE, Decell MK, Al Ayed T: A case of propofol toxicity: further evidence for a causal mechanism. *Paediatr Anaesth* 2004; 14:505–508
11. Branca D, Roberti MS, Lorenzin P, et al: Influence of the anesthetic 2,6-diisopropylphenol on the oxidative phosphorylation of isolated rat liver mitochondria. *Biochem Pharmacol* 1991; 42:87–90
12. Branca D, Roberti MS, Vincenti E, et al: Uncoupling effect of the general anesthetic 2,6-diisopropylphenol in isolated rat liver mitochondria. *Arch Biochem Biophys* 1991; 290:517–521
13. Branca D, Vincenti E, Scutari G: Influence of the anesthetic 2,6-diisopropylphenol (propofol) on isolated rat heart mitochondria. *Comp Biochem Physiol C Pharmacol Toxicol Endocrinol* 1995; 110:41–45
14. Rigoulet M, Devin A, Avéret N, et al: Mechanisms of inhibition and uncoupling of respiration in isolated rat liver mitochondria by the general anesthetic 2,6-diisopropylphenol. *Eur J Biochem* 1996; 241:280–285
15. Marian M, Bindoli A, Callegarin F, et al: Effect of 2,6-diisopropylphenol and halogenated anesthetics on tetraphenylphosphonium uptake by rat brain synaptosomes: Determination of membrane potential. *Neurochem Res* 1999; 24:875–881
16. Schenkman KA, Yan S: Propofol impairment of mitochondrial respiration in isolated perfused guinea pig hearts determined by reflectance spectroscopy. *Crit Care Med* 2000; 28:172–177
17. Bains R, Moe MC, Vinje ML, et al: Sevoflurane and propofol depolarize mitochondria in rat and human cerebrocortical synaptosomes by different mechanisms. *Acta Anaesthesiol Scand* 2009; 53:1354–1360
18. Vanlander AV, Okun JG, de Jaeger A, et al: Possible pathogenic mechanism of propofol infusion syndrome involves coenzyme Q. *Anesthesiology* 2015; 122:343–352
19. Herregods L, Rolly G, Versichelen L, et al: Propofol combined with nitrous oxide-oxygen for induction and maintenance of anaesthesia. *Anaesthesia* 1987; 42:360–365

20. Casati A, Fanelli G, Casaletti E, et al: Clinical assessment of target-controlled infusion of propofol during monitored anesthesia care. *Can J Anaesth* 1999; 46:235–239
21. Gong Y, Li E, Xu G, et al: Investigation of propofol concentrations in human breath by solid-phase microextraction gas chromatography-mass spectrometry. *J Int Med Res* 2009; 37:1465–1471
22. Krajčová A, Waldauf P, Anděl M, et al: Propofol infusion syndrome: A structured review of experimental studies and 153 published case reports. *Crit Care* 2015; 19:398
23. Bonnet D, Martin D, Pascale De Lonlay, et al: Arrhythmias and conduction defects as presenting symptoms of fatty acid oxidation disorders in children. *Circulation* 1999; 100:2248–2253
24. Choong K, Clarke JT, Cutz E, et al: Lethal cardiac tachyarrhythmia in a patient with neonatal carnitine-acylcarnitine translocase deficiency. *Pediatr Dev Pathol* 2001; 4:573–579
25. Iafolla AK, Thompson RJ Jr, Roe CR: Medium-chain acyl-coenzyme A dehydrogenase deficiency: Clinical course in 120 affected children. *J Pediatr* 1994; 124:409–415
26. Ruitenbeek W, Poels PJ, Turnbull DM, et al: Rhabdomyolysis and acute encephalopathy in late onset medium chain acyl-CoA dehydrogenase deficiency. *J Neurol Neurosurg Psychiatry* 1995; 58:209–214
27. Bergström J: Muscle-biopsy needles. *Lancet* 1979; 1:153
28. Krajcova A, Ziak J, Jiroutkova K, et al: Normalizing glutamine concentration causes mitochondrial uncoupling in an in vitro model of human skeletal muscle. *JPEN J Parenter Enteral Nutr* 2015; 39:180–189
29. Cory AH, Owen TC, Barltrop JA, et al: Use of an aqueous soluble tetrazolium/formazan assay for cell growth assays in culture. *Cancer Commun* 1991; 3:207–212
30. Ferrick DA, Neilson A, Beeson C: Advances in measuring cellular bioenergetics using extracellular flux. *Drug Discov Today* 2008; 13:268–274
31. Ijlst L, Wanders RJ: A simple spectrophotometric assay for long-chain acyl-CoA dehydrogenase activity measurements in human skin fibroblasts. *Ann Clin Biochem* 1993; 30 (Pt 3):293–297
32. Vanlander AV, Jorens PG, Smet J, et al: Inborn oxidative phosphorylation defect as risk factor for propofol infusion syndrome. *Acta Anaesthesiol Scand* 2012; 56:520–525
33. Sigma-Aldrich Company: Citrate Synthase Assay Kit. Available at: <http://www.sigmaaldrich.com/content/dam/sigmaaldrich/docs/Sigma/Bulletin/cs0720bul.pdf>. Accessed May 1, 2017
34. Bradford MM: A rapid and sensitive method for the quantitation of microgram quantities of protein utilizing the principle of protein-dye binding. *Anal Biochem* 1976; 72:248–254
35. Medsafe New Zealand Medicine and Medical Devices Safety Authority: Intralipid Production Information. 2016. Available at: <http://www.medsafe.govt.nz/profs/datasheet/i/Intralipidinf.pdf>. Accessed May 1, 2017
36. Edwards LM, Lawler NG, Nikolic SB, et al: Metabolomics reveals increased isoleukotoxin diol (12,13-DHOME) in human plasma after acute Intralipid infusion. *J Lipid Res* 2012; 53:1979–1986
37. Lou PH, Lucchinetti E, Zhang L, et al: The mechanism of Intralipid®-mediated cardioprotection complex IV inhibition by the active metabolite, palmitoylcarnitine, generates reactive oxygen species and activates reperfusion injury salvage kinases. *PLoS One* 2014; 9:e87205
38. Kam PC, Cardone D: Propofol infusion syndrome. *Anaesthesia* 2007; 62:690–701
39. Darras BT, Friedman NR: Metabolic myopathies: A clinical approach; part I. *Pediatr Neurol* 2000; 22:87–97
40. Baumeister FA, Oberhoffer R, Liebhaber GM, et al: Fatal propofol infusion syndrome in association with ketogenic diet. *Neuropediatrics* 2004; 35:250–252
41. Fodale V, La Monaca E: Propofol infusion syndrome: An overview of a perplexing disease. *Drug Saf* 2008; 31:293–303
42. Dawidowicz AL, Kalitynski R, Kobielski M, et al: Influence of propofol concentration in human plasma on free fraction of the drug. *Chem Biol Interact* 2006; 159:149–155

Příloha 4

Waldauf P, Gojda J, **Urban T**, Hrušková N, Blahutová B, Hejnová M, Jiroutková K, Fric M,
Jánský P, Kukulová J, Stephens F, Řasová K, Duška F.

Functional electrical stimulation-assisted cycle ergometry in the critically ill: protocol for a
randomized controlled trial.

Trials. 2019 Dec 16;20(1):724. doi: 10.1186/s13063-019-3745-1. PMID: 31842936; PMCID:
PMC6915865. IF 1.883

STUDY PROTOCOL

Open Access



Functional electrical stimulation-assisted cycle ergometry in the critically ill: protocol for a randomized controlled trial

Petr Waldauf¹, Jan Gojda², Tomáš Urban¹, Natália Hrušková³, Barbora Blahutová^{1,3}, Marie Hejnová^{1,3}, Kateřina Jiroutková¹, Michal Fric¹, Pavel Jánský¹, Jana Kukulová¹, Francis Stephens⁴, Kamila Řasová³ and František Duška^{1*} 

Abstract

Background: Intensive care unit (ICU)-acquired weakness is the most important cause of failed functional outcome in survivors of critical care. Most damage occurs during the first week when patients are not cooperative enough with conventional rehabilitation. Functional electrical stimulation-assisted cycle ergometry (FES-CE) applied within 48 h of ICU admission may improve muscle function and long-term outcome.

Methods: An assessor-blinded, pragmatic, single-centre randomized controlled trial will be performed. Adults ($n = 150$) mechanically ventilated for < 48 h from four ICUs who are estimated to need > 7 days of critical care will be randomized (1:1) to receive either standard of care or FES-CE-based intensified rehabilitation, which will continue until ICU discharge. Primary outcome: quality of life measured by 36-Item Short Form Health Survey score at 6 months. Secondary outcomes: functional performance at ICU discharge, muscle mass (vastus ultrasound, N-balance) and function (Medical Research Council score, insulin sensitivity). In a subgroup ($n = 30$) we will assess insulin sensitivity and perform skeletal muscle biopsies to look at mitochondrial function, fibre typing and regulatory protein expression.

Trial registration: ClinicalTrials.gov, [NCT02864745](https://clinicaltrials.gov/ct2/show/study/NCT02864745). Registered on 12 August 2016.

Keywords: Early rehabilitation, Critically ill, Intensive care unit, Functional electrical stimulation-assisted cycle ergometry, Mobility, Physical therapy

Background

Functional disability, a natural consequence of weakness, is a frequent and long-lasting complication in survivors of critical illness [1–3]. Over recent decades, mortality from acute critical illness has decreased with a consequent increasing number of ICU survivors. Understanding the post-ICU morbidity experienced by these survivors has become increasingly important. The greatest burdens that survivors of critical illness face are related to neuromuscular dysfunction and neuropsychological maladjustment [4]. In particular, neuromuscular abnormalities during critical illness are common, with a median prevalence of 57% [1]. In both patients with chronic critical illness and

survivors of severe critical illness, neuromuscular weakness may be substantial and persistent [5], resulting in important decrements in physical function and quality of life for years after discharge [1, 2].

In the past, routine features of general care provided in the ICU included liberal use of sedation and immobilization of the patient, which were thought to be necessary for facilitating interventions to normalize physiological function by artificial means. Over the last decade, there has been a paradigm shift away from this approach towards a more conservative treatment philosophy for patients in the ICU [4, 6, 7]. This paradigm shift is consistent with the observation that long-term physical problems in survivors of critical illness, particularly those with respiratory failure, may result from the protracted ICU stay and period of immobilization during which the patient is receiving organ support that is

* Correspondence: frantisek.duska@lf3.cuni.cz

¹Department of Anaesthesiology and Intensive Care Medicine, Charles University, 3rd Faculty of Medicine and KAR FNKV University Hospital, Fac Med 3, Srobarova 50, 10034 Prague, Czech Republic
Full list of author information is available at the end of the article



essential for survival [2, 4]. In line with this, a daily interruption of sedation policy has been widely adopted and proven to be beneficial [8] and early mobilization culture is spreading quickly across ICUs [9–13]. Indeed, these strategies, together with early physical therapy [9, 11, 12, 14–20], are the only safe [12, 20–22] and effective interventions in the prevention of long-term neuromuscular disability in survivors of intensive care. It should be stressed that in these studies early rehabilitation is defined as starting between days 2 and 5 of the ICU stay [9, 11, 12, 14–19] or as an activity beginning before ICU discharge [20].

Standard “early” rehabilitation cannot be started early enough, and FES-CE may be a solution to this dilemma. The first week in the ICU is critical as muscle mass and function is lost quickly. Immobility-associated muscle loss is evident as early as within 18–48 h of onset of acute critical illness or severe injury [23, 24] and is greatest during the first 2–3 weeks of critical illness [25, 26]. Up to 40% loss of muscle strength can occur within the first week of immobilization, with a daily rate of strength loss between 1.0 and 5.5% [27]. A 10–14% decrease in cross-sectional measurements of the rectus femoris muscle has been observed within the first week of the ICU stay [26]. Conventional rehabilitation during the first few days in the ICU is indeed limited in patients who are sedated and mechanically ventilated, and typically consists of passive limb movements, with or without the use of stretch reflex [16, 20]. Schweickert et al. [16] provided the earliest (within 48 h of intubation) and largest (26 ± 14 min a day for patients on mechanical ventilation) dose of rehabilitation and reported improvements of physical function at hospital discharge, but no measurements beyond. Active rehabilitation is delayed until the neurological condition of the patient improves enough to facilitate participation. In the sickest patients, who are at particular risk of developing ICU-acquired weakness (ICUAW), sedation and immobility may be prolonged well beyond the first week, when established damage to the muscle has already occurred.

There are several ways to deliver more effective physical exercise therapy to patients who are sedated and mechanically ventilated. For example, physical exercise can be delivered effectively and safely by passive supine cycling on a bicycle ergometer [15, 18, 28–30]. More recently, electrical neuromuscular stimulation (NMES) has been developed to mimic active exercise in patients who lack voluntary muscle activity [31–39]. During NMES, cutaneous electrodes placed over specific muscle groups electrically trigger muscle contractions. In order to achieve maximum efficacy, passive cycling and NMES can be delivered simultaneously and synchronized to produce a coordinated pattern of movements. The technique is called FES-CE (functional electrical stimulation-

assisted cycle ergometry). There is a large body of experience with these methods in the rehabilitation of patients with stroke and spinal cord injuries (reviewed in [40]). The method is effective in preventing the loss of muscle mass [41] and has been shown to improve anabolic resistance and insulin sensitivity in quadriplegic patients [42, 43].

The only study of FES-CE in critical illness is the pilot trial by Parry et al. [44], where the feasibility and safety of FES-CE was demonstrated in a small cohort of critically ill patients (eight patients received the FES-CE intervention, versus eight controls). Patients in the intervention group showed significant improvements in the Physical Function in Intensive Care Test and a faster recovery of functional milestones (e.g. time to stand from lying, walking on the spot). However, the mechanism by which this occurred is unknown. There are no data on the effect of FES-CE on long-term functional outcome in ICU survivors. In healthy volunteers [45] and patients with spinal cord injury [46], unloaded FES-CE can increase whole-body oxygen consumption. It is unknown whether these effects, including improving insulin sensitivity and protein metabolism [47], can also be achieved in critically ill patients.

Rationale

Mechanisms of muscle wasting and ICUAW

Pathophysiology of ICUAW is complex and multifactorial (reviewed in [4]), and there is a growing body of evidence suggesting the role of sarcopenia and metabolic derangement of skeletal muscle.

Firstly, *insulin resistance* is a well-known comorbidity in critical illness [48], contributing to and aggravating complications such as severe infections, organ dysfunction and death, and has also been implicated in the ICU-acquired weakness. Two main consequences of insulin resistance are hyperglycaemia and “anabolic resistance”. It has been observed that the provision of protein and energy to support the enhanced hypermetabolic demands of ICU patients is unable to prevent the rapid loss of muscle mass [49]. Indeed, skeletal muscle insulin resistance is the likely reason why nutritional support further exacerbates hyperglycaemia. Insulin therapy is often used in ICU patients to try and combat this, but it appears to be ineffective in ICU-acquired weakness and its safety in the ICU setting has been questioned [50]. Physical activity is an attractive alternative intervention target as it has profound effects on substrate metabolism in contracting skeletal muscle, with a single bout of muscle contraction known to increase muscle glucose uptake several fold and sensitize the muscle to insulin and the anabolic effects of amino acids for up to 24 h, including in individuals where insulin and anabolic resistance is evident [51]. It is not known whether

intensified rehabilitation can improve the insulin effect on glucose uptake and whether it influences the stimulatory effect of insulin and amino acids on muscle protein synthesis.

Secondly, *mitochondrial dysfunction* in skeletal muscle may play a role in the development of ICUAW. Mitochondrial depletion and dysfunction of mitochondrial respiratory complexes I and IV has been demonstrated in acute severe sepsis in association with multiorgan failure and death [52], and early activation of mitochondrial biogenesis predicted survival [53]. Our group has recently demonstrated in two pilot studies [54, 55] that, compared to healthy controls, there is a 50% reduction of mitochondrial functional capacity in skeletal muscle in the patients with protracted critical illness and ICUAW. This is accompanied by a significant relative increase in the abundance and functional capacity of respiratory complex II, which delivers electrons to the respiratory chain from fatty acid oxidation [54]. Weber-Carstens et al. [48] demonstrated that insulin fails to activate GLUT-4 translocation to cellular membranes in patients with ICUAW, causing skeletal muscle “intracellular glucose starvation” and a failure of AMP-activated protein kinase to respond to the impairment of ATP production. Most notably, in five subjects, these abnormalities were alleviated by NMES. In light of this, the relative increase of complex II capacity observed in our pilot study may represent a functional adaptation of muscle to the increased reliance on fatty acid oxidation. It is not known whether the severity of mitochondrial functional alteration reflects the degree of insulin resistance and the severity of muscle weakness, and whether the delivery of very early FES-CE has a potential to influence these changes.

In the light of this, we hypothesize the following:

H₁: As most of the damage to the structure and function of skeletal muscle occurs during the first week, intensified goal-directed rehabilitation, which includes FES-CE and starts within 48 h after ICU admission, improves the functional outcome of ICU survivors at 6 months when compared to the standard of care.

H₂: The intervention, as compared to standard of care, shall preserve muscle mass and improve muscle power at ICU discharge.

H₃: The intervention, as compared to standard of care, shall increase insulin-mediated whole-body oxidative glucose disposal and mitochondrial functional indices.

Objectives

1. To investigate, in a pragmatic, prospective, randomized, controlled, assessor-blinded trial, the effects of very early intensive rehabilitation using a

goal-directed protocol that includes FES-CE in mechanically ventilated ICU patients predicted to need a protracted ICU stay

2. To perform more detailed metabolic studies, including serial muscle biopsies and using euglycaemic hyperinsulinaemic clamps, in a nested subgroup. Insulin sensitivity in the whole study population will be compared by glucose control and consumption of intravenous insulin required to control blood glucose

Primary outcome

The primary outcome is the physical component of the SF-36 quality of life questionnaire measured in ICU survivors at 6 months. Based on the study by Kayambu et al. [12], where this measure was 60 ± 29 points in the control group, our study is powered to detect a change by 15 points or more, which is within the limits determined as clinically important for patients with COPD, asthma and myocardial infarction [56]. The SF-36 has been validated in the Czech Republic and endorsed by the Institution for Health Information and Statistics (<https://www.uzis.cz/en/node/8159>).

Secondary outcomes

- Four-item Physical Fitness in Intensive Care Test (time frame: at 28 days or discharge from the ICU, whichever occurs earlier) as the functional outcome at ICU D/C
- Muscle mass measured by rectus muscle cross-sectional area on B-mode ultrasound (time frame: at 7-day intervals up to day 28 or discharge from the ICU, whichever occurs earlier)
- Nitrogen balance measured in grams per metre-squared of body surface area (time frame: at 7-day intervals up to day 28 or discharge from the ICU, whichever occurs earlier) and the cumulative the difference between nitrogen intake and output
- Muscle power as per the Medical Research Council (MRC) score (time frame: at 7-day intervals up to day 28 or discharge from the ICU, whichever occurs earlier)
- Number of ventilator-free days (time frame: at 28 days); that is, number of days, out of 28 days after admission, that the patient has NOT been supported by mechanical ventilation
- Number of rehabilitation interruptions due to physiological deterioration (time frame: at 28 days or discharge from the ICU, whichever occurs earlier)
- Number of episodes of elevated intracranial pressure (time frame: at 28 days or discharge from the ICU, whichever occurs earlier)

- Number of dialysis interruptions (time frame: at 28 days or discharge from the ICU, whichever occurs earlier)
- Length of ICU stay in days (time frame: at 6 months)

Study population

One hundred and fifty participants meeting the eligibility criteria will be recruited in four ICUs at FNKV University Hospital.

Inclusion criteria: age ≥ 18 years; mechanical ventilation, or imminent need of it at presentation; predicted ICU length of stay ≥ 7 days.

Exclusion criteria: known primary neuromuscular disease or spinal cord lesion at admission; severe lower limb injury or amputation; bedridden pre-morbid state (Charleston Comorbidity Score > 4); approaching imminent death or withdrawal of medical treatment within 24 h; pregnancy; presence of external fixator or superficial metallic implants in lower limbs; open wounds or skin abrasions at electrode application points; presence of pacemaker, implanted defibrillator, or other implanted electronic medical device; predicted as unable to receive first rehabilitation session within 72 h of admission or transferred from another ICU after more than 24 h of mechanical ventilation; presence of other condition preventing the use of FES-CE or considered unsuitable for the study by a responsible medical team; prior participation in another functional outcome-based intervention research study.

With the exception that we do not limit the study population with sepsis, we have intentionally chosen similar criteria to the only study underway on FES-CE in ICU patients, which is primarily focused on muscle structure and function [57].

Interventions

The flow of participants throughout the trial is shown in Fig. 1 and the study procedures in Fig. 2. As soon as informed consent has been obtained, and prior to randomization, baseline testing including anthropometric examination will be performed. In addition, in patients with specific consent, a muscle biopsy will be obtained and hyperinsulinaemic clamp will be performed on the first morning (8.00–11.00 a.m.) and prior to the start of enteral nutrition.

Standard care group

Both groups will receive usual best medical and nursing care in the ICU, which includes daily sedation holds when applicable and delirium 12-hourly monitoring (by CAM-ICU scale [58]) and management as usual in the routine practice. Respiratory physiotherapy will also be delivered without alterations. The routine standard care

arm will undergo mobilization/rehabilitation delivered by personnel not involved in the study in a usual, routine way. Details of physiotherapy treatment will be recorded but not protocolled in the standard care arm.

Intervention group

In the intervention arm, early goal-directed rehabilitation is protocolled according to the patients' condition and degree of cooperation (Fig. 3), and there will be pre-defined safety criteria, which are in accordance with current recommendations for active rehabilitation of critically ill ventilated adults [13]. Whilst the safety criteria are binding for the study physiotherapist, the rehabilitation protocol is not and the delivery of physical exercise can be altered according to the actual patient's condition. However, any alteration and the reason for it will be recorded. The intervention will start as soon as possible and always within 72 h of ICU admission, continuing until ICU discharge. Supine cycling will be delivered as per protocol on a supine cycle ergometer attached to a neuromuscular stimulator. Surface electrodes will be applied to the gluteal, hamstring and quadriceps muscles on both legs. The intensity of muscle stimulation will be delivered at a level able to cause visible contractions (confirmed by palpation if uncertain) in all muscle groups without causing undue pain or discomfort to the participant, according to a regime specified by Parry et al. [44]. Once the patient is more alert, and able to participate, they will be provided with standardized encouragement to engage in therapy. To increase the intervention workload, resistance will be increased incrementally and cycling cadence. If a participant is readmitted to intensive care, the intervention will be re-initiated. The intervention continues until day 28 or ICU discharge, whichever occurs earlier.

Methods

Enrolment and randomization

All patients admitted to participating ICUs are screened daily by research nurses and all eligible patients or their representatives are approached by investigators as soon as possible, but always within 72 h of admission. Participants for whom informed consent was obtained will be randomly assigned (1:1) to receive either standard care or the intervention using offsite independent randomization protocols (www.randomization.com) embedded in the electronic case report form. Randomization will be stratified according to the presence or absence of sepsis and the availability of a biopsy at baseline. There is no restriction (blocking) during randomization.

Both the study team and clinical personnel will be made aware of subject treatment allocation. The outcome assessor is not involved in patient care and remains blinded to treatment allocations.

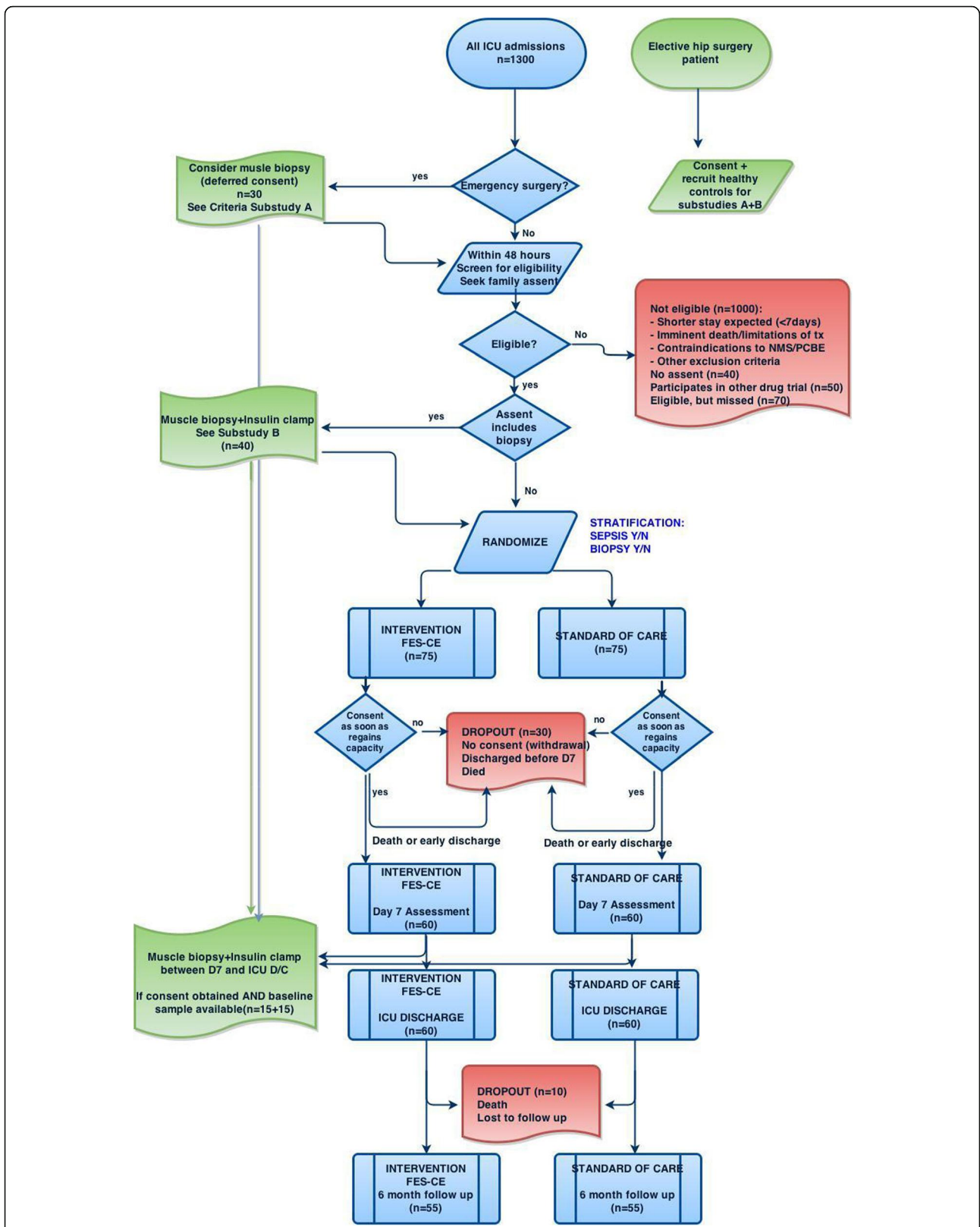


Fig. 1 Planned flowchart of patients enrolled into the trial. D7 day 7, D/C discharge, FES-CE functional electrical stimulation-assisted cycle ergometry, ICU intensive care unit, tx treatment, NMS neuromuscular stimulation, PCBE passive cycling-based exercise

TIMEPOINT**	STUDY PERIOD							
	Enrolment	Allocation	Post-allocation					Close out
	0-48h	0	D ₁₋₆	D ₇	D ₈₋₂₈	ICU D/C	Post ICU D/C	F-up D ₁₈₀
ENROLMENT:								
Eligibility screen	X							
Informed consent	X							
Sepsis Y/N, Biopsy Y/N	X							
Randomisation (stratified)		X						
INTERVENTIONS:								
Intervention (EGDR)			←————→					
Control (Standard RHB)			←————→					
Biopsy subgroup		Clamp + biopsy		Clamp + biopsy				Clamp + biopsy
ASSESSMENTS:								
Functional status	Before admission (CCS retrospect)	ROM		MRC		MRC PFIT		SF36 (primary outcome)
Adverse events		X	X	X	X	X	X	X
Vital functions		X	X	X	X	X		
SOFA, N-balance, Fluid balance			X	X	X	X		
Anthropometry		X		X				X
RHB Dose (min/day)	X	X	X	X	X	X		
MV, ICU, Hospital (Y/N)			X	X	X	X	X	X

Fig. 2 Standard Protocol Items: Recommendations for Interventional Trials (SPIRIT) figure. D day, D/C discharge, EGDR early goal-directed rehabilitation, F-up follow-up, ICU intensive care unit, MRC Medical Research Council, MV mechanical ventilation, RHB rehabilitation, SF-36 Short Form 36, SOFA Sequential Organ Failure Assessment, CCS Charlson comorbidity score, ROM range of motion, PFIT physical function test for use in the intensive care unit

Clinical data retrieval and handling

The ICUs are paperless and fully computerized, so vital functions and other physiological parameters are monitored and data are routinely stored in secure hospital data bases via a protected dedicated network (MetaVision; IMD Soft Inc.). This includes data about nutritional intake and urinary output. On top of this, research nurses will input data into an electronic, secure, customized online case report form database (eCRF; accessible at <https://195.113.79.251:9090/apex/f?p=103:101:14992036032980>). Data protection and encryption is in accordance with the EU’s General Data Protection Regulations as well as Czech data protection laws. The data will be audited by on a regular basis, but at least after each 10 patients are enrolled, by independent study

monitor. After the database is locked upon study completion, patients’ data will be de-identified and available in full in a public database.

Urine samples will be collected daily, surfaced with toluene and stored in a deep-freeze facility for later determination of nitrogen content and 3-methyl histidine levels (to calculate the muscle catabolism rate and nitrogen balance). In addition, all study patients will undergo assessment by a study physiotherapist, which includes a measurement of rectus muscle cross-sectional area on both legs and, whenever the patient regains consciousness, also muscle power by MRC score (standardized testing of muscle power (0–5) for 12 muscle groups on all four limbs, giving a score of 0–60 (60 suggesting normal muscle power)). Blood will be taken, and plasma

Stage	Condition	RASS score	Intervention	Frequency/da
0	Unstable (e.g. prone, FiO ₂ >0.6, high inotropes)	-5 to -4 ± muscle relaxants	Passive Range of Motion with stretch reflex to upper and lower limbs.	2x15 minutes (min)
			Electrical neuromuscular stimulation to major muscle groups on UL+LL	1x60 min
1	Sedated	-3 to -2	As Stage 0 + FES---assisted leg cycle ergometry (FES---CE)	1x30 min
2	Transition phase: needing inotropes, ventilation	-1 or 1 Borderline cooperation	AM (before sedation hold); FES---CE	1x60 min
			PM (after sedation hold) If cooperative:	2x10 min
			Active range of motion/lightly resisted UL+LL	2x5 min
			Sit up in bed/on edge	
			If delirious: Individualize approach	Aim to deliver >30 min
3	Weak	0 Cooperative	Active Range of Motion/Lightly resisted with upper and lower limbs	2x10 min
			Sit on the edge of bed	2x5 min
			Sit out with assistance FES---CE or active CE (low resistance)	2x60 min 2x15 min
4	Able to stand with assistance	0 Cooperative	Active Range of Motion/Lightly resisted with upper and lower limb	2x10 min
			Sit out (low to moderate resistance) Active CE	2x30 min 2x as tolerated
			Ambulation with assistive device and 1---2 therapists	2x30 min

Fig. 3 Protocol of intensified goal-directed rehabilitation. FES-CE functional electrical stimulation-assisted cycle ergometry, FIO₂ fraction of inspired oxygen, LL lower limb, RASS Richmond Agitation and Sedation Scale, UL upper limb

separated and frozen at - 80 °C for later analysis of cytokines and hormone levels. This assessment will be repeated at day 7 intervals and at ICU discharge. At ICU discharge, the patients and relatives will be asked to provide contact details for follow-up. After 6 months, the patient or family will be contacted for structured interview as required for the SF-36 questionnaire, and collected using the RAND methodology (www.rand.org). Whilst participants and the intervention physiotherapist cannot be blinded to group allocation, research staff assessing the outcome will be from a separate clinical department (JG, BB, MH) and thus will remain blinded to treatment allocation. Outcome assessors are familiar with the SF-36, which is in routine use for other trials, and received SF-36 re-training at induction to this trial. Strategies to improve adherence to intervention mainly include the 24/7 availability of one of the team of five research nurses as well as one full-time physiotherapist equivalent only reserved for study interventions, with extra budgeting to cover physiotherapy sessions in the intervention group during the weekend. The time of

physiotherapy sessions will be recorded by the physiotherapist and randomly checked by a hidden independent assessor (bedside ICU nurse receiving specific instructions). The primary outcome has been chosen also with respect to the fact that it can be collected over a structured telephone interview, thereby minimizing missing data.

Complementary studies: insulin resistance and mitochondrial function

These studies will be performed in addition to other study procedures in a nested subgroup of patients, who give specific consent. The first measurement will be performed at baseline prior to randomization, ideally the next morning after admission. Second measurement will be performed on day 7 of ICU stay, i.e. after at least 5 days of intervention.

Muscle biopsy

Muscle biopsy will be performed from the vastus lateralis muscle using the Bergstrom needle biopsy technique.

The sample will be separated into three parts (50–100 mg each). One part will be immediately frozen in liquid nitrogen for analysis of the protein/DNA ratio and for protein expression studies. The second part will be frozen in liquid nitrogen-cooled isopentane for muscle fibre typing and immunohistochemistry analysis. The third part put will be placed in BIOPS media on ice for the preparation of homogenates and measurement of citrate synthase activity, spectrophotometric analysis of the activity of respiratory complexes I–IV [52] and western blot analysis of respiratory complexes (as described in [55]). In the fresh muscle homogenates, we will use high-resolution respirometry (Oxygraph; Oroboros, Austria) to determine the function of individual respiratory complexes in the cytosolic context and measure basic functional metabolic indices by a method we have recently developed and calibrated against isolated mitochondria [59]. We will specifically look at the degree of mitochondrial uncoupling, the respiratory chain capacity and the function of individual complexes, including glycerol-3-phosphate shuttle. From the satellite cells we will prepare a culture of myotubes, which will serve as an in vitro model of skeletal muscle [60] and specifically measure the in vitro ability of myotubes to oxidize fatty acids by extracellular flux analysis (Seahorse Biosciences). Frozen muscle samples will be stored at -80°C for analysis of the DNA/protein ratio, mRNA and proteins involved in the regulation of proteolysis, substrate oxidation and anabolic pathways of skeletal muscle (MuRF, FOXO, atrogins) as well as immunohistochemistry and typing of muscle fibres. In order to determine which changes are caused by critical illness itself, we will also obtain control samples ($n = 15$) from age, sex and BMI-matched metabolically healthy volunteers undergoing elective hip surgery at the Department of Orthopaedic Surgery. In addition, we will look at the change of these indices after 7 days of critical illness and the influence of the intervention versus standard of care. We will look at correlation of these parameters with muscle power (i.e. compare the bioenergetics profile of skeletal muscle in those who develop ICUAW and in those who do not) and insulin resistance.

Insulin sensitivity and substrate oxidation will be measured after overnight fasting by hyperinsulinaemic euglycaemic clamp (as described in [61]). We will compare the effect of intervention on insulin-mediated glucose disposal.

Statistical analyses

Sample-size calculation

In studies of critical illness outcome at 6 months using SF-36 scores, the standard deviation varied between 10 and 30 points. In order to have 80% power to detect a 15-point difference in SF-36 scores between control and

intervention at the level of significance $p < 0.05$ in the population with a mean of 60 and SD of 30 [12], we would need 108 subjects (54 in each arm). In order to allow for deaths and dropouts, we plan to randomize 150 subjects.

Data analysis plan

The primary outcome and all secondary outcomes will be compared between the intervention and standard of care groups in an intention-to-treat population, with all tests two-sided and with the level of significance set at 5%, after the primary outcome has been collected in the last subject. There is no plan for any interim analysis. We will perform exploratory analyses in pre-specified subgroups of patients stratified according to APACHE II, and the length of intervention. We will also perform unadjusted analysis of odds ratio of being functionally independent (defined as ability to walk, use a telephone, self-care, use the toilet and groom) at 6 months after ICU admission in patients in the intervention and standard of care groups. We will perform adjustments on the disease severity (APACHE II score), admission diagnosis, baseline functional status and age. Missing data for primary outcome will be dealt by reporting both worst-case and per-protocol results; no imputation will be used.

Ethical considerations

This trial involves a two-tier consent process: first to the rehabilitation intervention and then additionally to the insulin clamp and muscle biopsies in a nested subgroup within the primary trial. All patients meeting the aforementioned criteria will be invited to participate and asked to provide written informed consent. It is expected that most screened patients will lack the capacity to provide informed consent. In this situation, the deferred consent policy will be applied: patient's next of kin (NOK) will be approached, and be given verbal and written information explaining the nature of the study given information leaflet and asked to provide assent. Discussion with the family will help inform the treating medical team regarding a best interest decision for assent to be recruited into the study. An option will be given to participate in the trial, but not to undergo insulin clamps and muscle biopsies. In a subgroup of patients when the family is unavailable within the first 48 h, an independent physician will be asked to review inclusion and exclusion criteria and weight benefits and risks of participation in the trial – all patients enrolled based on independent physician assent will proceed without insulin clamps and muscle biopsies. Participants themselves will be asked to provide ongoing consent as soon as they regain capacity. Again, they will be offered the option to continue participating in the trial without insulin clamps and/or muscle biopsies, if they so wish. Details of all

participants who refuse consent for muscle biopsy/insulin clams will be recorded. All serious adverse events that are suspected as being related to study interventions will be reported to the Research Ethics Board and regulatory authorities as per local legislation. Other adverse events deemed to be related or possibly related to treatment intervention will be discussed at regular monthly meetings of the study team with the decision on further action, as there is no formal steering committee for this trial. The final decision-making and reporting responsibility is with the principal investigator (FD). All adverse events will be recorded in the eCRF. All protocol amendments, should they be required, will be subjected to a priori approval by the REB. Once implemented, protocol amendments will be reported to the sponsor and registration body (www.clinicaltrials.gov).

Replication of key aspects of trial methods and conduct

The trial is designed to be fully reproducible in an ICU setting in larger, but not necessarily teaching or academic, hospitals, where the FES-CE equipment and trained physiotherapists are available 7 days a week.

The sponsor of the study is a state-governed grant agency that has not had nor will have any role in study design; collection, management, analysis and interpretation of data; writing of the report; or the decision to submit the report for publication.

Dissemination of results

We will submit the main results of the trial in an open-access peer-reviewed journal within 6 months after the 150th subject has completed the 6-month follow-up visit, which is expected to happen in Q2 of 2020. We will make fully de-identified record-level raw data available in a public database Additional file 2.

Trial status

This trial is recruiting (recruitment began November 2016, expected finish November 2019) (first patient recruited 4 October 2016, expected end of study 1 July 2020), protocol version 2.0 as of January 2018. For the full WHO Trial Registration Data Set, see Additional file 1.

Supplementary information

Supplementary information accompanies this paper at <https://doi.org/10.1186/s13063-019-3745-1>.

Additional file 1. WHO Trial Registration data set.

Additional file 2. SPIRIT 2013 Checklist: Recommended items to address in a clinical trial protocol and related documents.

Abbreviations

D/C: Discharge; FES-CE: Functional electrical stimulation-assisted cycle ergometry; ICU: Intensive care unit; MRC: Medical Research Council; SF-36: 36-Item Short Form Health Survey

Authors' contributions

FD is the author of the main idea and overlooks the conduct of the study. PW, KJ, MF and PJ are responsible for consenting and recruiting patients and performing clinical procedures. JK is the study monitor. PW is the data analyst and biostatistician. NH and KR are the study physiotherapists. MH and BB are blinded outcome assessors. TU, JG and FS are investigators of the metabolic sub-studies. All authors will have access to record-level data and will contribute to publication of the results. All authors read and approved the final manuscript.

Funding

This study was funded by the Grant Agency for Research in Healthcare AZV 16-28663A. For contact details, see <http://www.azvcr.cz/kontakt>.

Availability of data and materials

All cleaned de-identified raw data will be made available in an open online database (<https://data.mendeley.com/datasets>) within 6 months of publication of the main results of the trial.

Ethics approval and consent to participate

The trial design is in accordance with the Declaration of Helsinki and the protocol, care report form and informed consent formularies were reviewed and approved by FNKV University Hospital Research Ethics Board ("Ethical Committee") on 24 June 2015 (decision number EK-VP-27-0-2015). All patients or their legal representatives gave their prospective written informed consent to participate in the study.

Consent for publication

Not applicable.

Competing interests

The authors declare that they have no competing interests.

Author details

¹Department of Anaesthesiology and Intensive Care Medicine, Charles University, 3rd Faculty of Medicine and KAR FNKV University Hospital, Fac Med 3, Srobarova 50, 10034 Prague, Czech Republic. ²Department of Internal Medicine II, Charles University, 3rd Faculty of Medicine and FNKV University Hospital, Prague, Czech Republic. ³Department of Rehabilitation, Charles University, 3rd Faculty of Medicine and FNKV University Hospital, Prague, Czech Republic. ⁴College of Life and Environmental Sciences, Sport and Health Sciences, University of Exeter, Exeter, UK.

Received: 5 June 2019 Accepted: 23 September 2019

Published online: 16 December 2019

References

- Fan E, Dowdy DW, Colantuoni E, Mendez-Tellez PA, Sevransky JE, Shanholtz C, et al. Physical complications in acute lung injury survivors: a two-year longitudinal prospective study. *Crit Care Med*. 2014;42:849–59 United States.
- Herridge MS, Tansey CM, Matte A, Tomlinson G, Diaz-Granados N, Cooper A, et al. Functional disability 5 years after acute respiratory distress syndrome. *N Engl J Med*. 2011;364:1293–304 United States.
- Herridge MS, Moss M, Hough CL, Hopkins RO, Rice TW, Bienvenu OJ, et al. Recovery and outcomes after the acute respiratory distress syndrome (ARDS) in patients and their family caregivers. *Intensive Care Med*. 2016;42:725–38 United States.
- Kress JP, Hall JB. ICU-acquired weakness and recovery from critical illness. *N Engl J Med*. 2014;370:1626–35 United States.
- Sacarella E, Perez-Castejon JM, Nicolas JM, Masanes F, Navarro M, Castro P, et al. Functional status and quality of life 12 months after discharge from a medical ICU in healthy elderly patients: a prospective observational study. *Crit Care*. 2011;15:R105 England.
- Herridge MS. Mobile, awake and critically ill. *CMAJ*. 2008;178:725–6 Canada.
- Needham DM. Mobilizing patients in the intensive care unit: improving neuromuscular weakness and physical function. *JAMA*. 2008;300:1685–90 United States.
- Minhas MA, Velasquez AG, Kaul A, Salinas PD, Celi LA. Effect of protocolized sedation on clinical outcomes in mechanically ventilated intensive care unit patients: a systematic review and meta-analysis of randomized controlled trials. *Mayo Clin Proc*. 2015;90:613–23 England.

9. Saunders CB. Preventing secondary complications in trauma patients with implementation of a multidisciplinary mobilization team. *J Trauma Nurs.* 2015;22:170–4 United States.
10. Hanekom SD, Louw Q, Coetzee A. The way in which a physiotherapy service is structured can improve patient outcome from a surgical intensive care: A controlled clinical trial. *Crit Care.* 2012;16(6):R230.
11. Schaller SJ, Anstey M, Blobner M, Edrich T, Grabitz SD, Gradwohl-Matis I, et al. Early, goal-directed mobilisation in the surgical intensive care unit: a randomised controlled trial. *Lancet.* 2016;388:1377–88 Elsevier Ltd.
12. Kayambu G, Boots R, Paratz J. Early physical rehabilitation in intensive care patients with sepsis syndromes: a pilot randomised controlled trial. *Intensive Care Med.* 2015;41:865–74 Springer Berlin Heidelberg.
13. Sommers J, Engelbert RHH, Dettling-Ihnenfeldt D, Gosselink R, Spronk PE, Nollet F, et al. Physiotherapy in the intensive care unit: an evidence-based, expert driven, practical statement and rehabilitation recommendations. *Clin Rehabil.* 2015;29:1051–63 England.
14. Morris PE, Berry MJ, Files DC, Thompson JC, Hauser J, Flores L, et al. Standardized rehabilitation and hospital length of stay among patients with acute respiratory failure. *JAMA.* 2016;315:2694.
15. Burtin C, Clerckx B, Robbeets C, Ferdinande P, Langer D, Troosters T, et al. Early exercise in critically ill patients enhances short-term functional recovery. *Crit Care Med.* 2009;37:2499–505.
16. Schweickert WD, Pohlman MC, Pohlman AS, Nigos C, Pawlik AJ, Esbrook CL, et al. Early physical and occupational therapy in mechanically ventilated, critically ill patients: a randomised controlled trial. *Lancet.* 2009;373:1874–82 Elsevier Ltd.
17. Needham DM, Korupolu R, Zanni JM, Pradhan P, Colantuoni E, Palmer JB, et al. Early physical medicine and rehabilitation for patients with acute respiratory failure: a quality improvement project. *Arch Phys Med Rehabil.* 2010;91:536–42 United States.
18. Eggmann S, Verra ML, Luder G, Takala J, Jakob SM. Physiological effects and safety of an early, combined endurance and resistance training in mechanically ventilated, critically ill patients. *PLoS One.* 2018;101:e344–5.
19. Wright SE, Thomas K, Watson G, Baker C, Bryant A, Chadwick TJ, et al. Intensive versus standard physical rehabilitation therapy in the critically ill (EPICC): a multicentre, parallel-group, randomised controlled trial. *Thorax.* 2018;73:213–21.
20. Bailey P, Thomsen GE, Spuhler VJ, Blair R, Jewkes J, Bezdjian L, et al. Early activity is feasible and safe in respiratory failure patients. *Crit Care Med.* 2007;35:139–45 United States.
21. Denehy L, Skinner EH, Edbrooke L, Haines K, Warrillow S, Hawthorne G, et al. Exercise rehabilitation for patients with critical illness: a randomized controlled trial with 12 months of follow-up. *Crit Care.* 2013;17:R156.
22. Sricharoenchai T, Parker AM, Zanni JM, Nelliot A, Dinglas VD, Needham DM. Safety of physical therapy interventions in critically ill patients: a single-center prospective evaluation of 1110 intensive care unit admissions. *J Crit Care.* 2014;29:395–400 United States.
23. Levine S, Nguyen T, Taylor N, Friscia ME, Budak MT, Rothenberg P, et al. Rapid disuse atrophy of diaphragm fibers in mechanically ventilated humans. *N Engl J Med.* 2008;358:1327–35 United States.
24. Hermans G, De Jonghe B, Bruyninckx F, Van den Berghe G. Clinical review: Critical illness polyneuropathy and myopathy. *Crit Care.* 2008;12:238 England.
25. Gruther W, Benesch T, Zorn C, Paternostro-Sluga T, Quittan M, Fialka-Moser V, et al. Muscle wasting in intensive care patients: ultrasound observation of the M. quadriceps femoris muscle layer. *J Rehabil Med.* 2008;40:185–9 Sweden.
26. Puthuchery ZA, Rawal J, McPhail M, Connolly B, Ratnayake G, Chan P, et al. Acute skeletal muscle wasting in critical illness. *JAMA.* 2013;310:1591–600 United States.
27. Topp R, Dittmyer M, King K, Doherty K, Hornyak J 3rd. The effect of bed rest and potential of prehabilitation on patients in the intensive care unit. *AACN Clin Issues.* 2002;13:263–76 United States.
28. Machado ADS, Pires-Neto RC, Carvalho MTX, Soares JC, Cardoso DM, de Albuquerque IM. Effects that passive cycling exercise have on muscle strength, duration of mechanical ventilation, and length of hospital stay in critically ill patients: a randomized clinical trial. *J Bras Pneumol.* 2017;43:134–9.
29. Fossat G, Baudin F, Courtes L, Bobet S, Dupont A, Bretagnol A, et al. Effect of in-bed leg cycling and electrical stimulation of the quadriceps on global muscle strength in critically ill adults: a randomized clinical trial. *JAMA.* 2018; 320:368–78.
30. França E, Ribeiro L, Lamenha G, Magalhães I, Figueiredo T, Costa M, et al. Oxidative stress and immune system analysis after cycle ergometer use in critical patients. *Clinics.* 2017;72:143–9.
31. Zanotti E, Felicetti G, Maini M, Fracchia C. Peripheral muscle strength training in bed-bound patients with COPD receiving mechanical ventilation: effect of electrical stimulation. *Chest.* 2003;124:292–6 The American College of Chest Physicians.
32. Gerovasili V, Stefanidis K, Vitzilaios K, Karatzanos E, Politis P, Koroneos A, et al. Electrical muscle stimulation preserves the muscle mass of critically ill patients: a randomized study. *Crit Care.* 2009;13:R161.
33. Routsis C, Gerovasili V, Vasileiadis I, Karatzanos E, Pitsolis T, Tripodaki E, et al. Electrical muscle stimulation prevents critical illness polyneuromyopathy: a randomized parallel intervention trial. *Crit Care.* 2010;14(2):R74.
34. Abu-Khaber HA, Abouelela AMZ, Abdelkarim EM. Effect of electrical muscle stimulation on prevention of ICU acquired muscle weakness and facilitating weaning from mechanical ventilation. *Alexandria J Med.* 2013;49:309–15 Alexandria University Faculty of Medicine.
35. Kho ME, Truong AD, Zanni JM, Ciesla ND, Brower RG, Palmer JB, et al. Neuromuscular electrical stimulation in mechanically ventilated patients: a randomized, sham-controlled pilot trial with blinded outcome assessment. *J Crit Care.* 2014;30:32–9 Elsevier B.V.
36. Goll M, Wollersheim T, Haas K, Moergeli R, Malleike J, Nehls F, et al. Randomised controlled trial using daily electrical muscle stimulation (EMS) in critically ill patients to prevent intensive care unit (ICU) acquired weakness (ICUAW). *Intensive Care Med Exp.* 2015;3:1–2.
37. Fischer A, Spiegl M, Altmann K, Winkler A, Salamon A, Themessl-Huber M, et al. Muscle mass, strength and functional outcomes in critically ill patients after cardiothoracic surgery: does neuromuscular electrical stimulation help? The Catastim 2 randomized controlled trial. *Crit Care.* 2016;20:1–13 Critical Care.
38. Fontes Cerqueira TC, de Cerqueira Neto ML, de AP CL, Oliveira GU, da Silva Júnior WM, Carvalho VO, et al. Ambulation capacity and functional outcome in patients undergoing neuromuscular electrical stimulation after cardiac valve surgery: a randomised clinical trial. *Medicine (Baltimore).* 2018;97: e13012.
39. Koçan Kurtoğlu D, Taştekin N, Birtane M, Tabakoğlu E, Süt N. Effectiveness of neuromuscular electrical stimulation on auxiliary respiratory muscles in patients with chronic obstructive pulmonary disease treated in the intensive care unit. *Turk J Phys Med Rehab.* 2015;61:12–7.
40. Doucet BM, Lam A, Griffin L. Neuromuscular electrical stimulation for skeletal muscle function. *Yale J Biol Med.* 2012;85:201–15 United States.
41. Bauman WA, Spungen AM, Adkins RH, Kemp BJ. Metabolic and endocrine changes in persons aging with spinal cord injury. *Assist Technol.* 1999;11: 88–96 United States.
42. Kjaer M, Pollack SF, Mohr T, Weiss H, Gleim GW, Bach FW, et al. Regulation of glucose turnover and hormonal responses during electrical cycling in tetraplegic humans. *Am J Physiol.* 1996;271:R191–9 United States.
43. Gorgey AS, Dolbow DR, Dolbow JD, Khalil RK, Gater DR. The effects of electrical stimulation on body composition and metabolic profile after spinal cord injury—part II. *J Spinal Cord Med.* 2015;38:23–37 England.
44. Parry SM, Berney S, Warrillow S, El-Ansary D, Bryant AL, Hart N, et al. Functional electrical stimulation with cycling in the critically ill: a pilot case-matched control study. *J Crit Care.* 2014;29:695.e1–7 Elsevier Inc.
45. Gojda J, Waldauf P, Hruskova N, Blahutova B, Krájcova A, Urban T, et al. Lactate production without hypoxia in skeletal muscle during electrical cycling: crossover study of femoral venous–arterial differences in healthy volunteers. *PLoS One.* 2019;14:e0200228 United States.
46. Hettinga DM, Andrews BJ. Oxygen consumption during functional electrical stimulation-assisted exercise in persons with spinal cord injury: implications for fitness and health. *Sports Med.* 2008;38:825–38 New Zealand.
47. Farrell PA. Protein metabolism and age: influence of insulin and resistance exercise. *Int J Sport Nutr Exerc Metab.* 2001;11(Suppl):S150–63 United States.
48. Weber-Carstens S, Schneider J, Wollersheim T, Assmann A, Bierbrauer J, Marg A, et al. Critical illness myopathy and GLUT4: significance of insulin and muscle contraction. *Am J Respir Crit Care Med.* 2013;187: 387–96 United States.
49. Clifton GL, Robertson CS, Grossman RG, Hodge S, Foltz R, Garza C. The metabolic response to severe head injury. *J Neurosurg.* 1984;60:687–96 United States.
50. Finfer S, Chittock DR, Su SY-S, Blair D, Foster D, Dhingra V, et al. Intensive versus conventional glucose control in critically ill patients. *N Engl J Med.* 2009;360:1283–97 United States.

51. Dirks ML, Hansen D, Van Assche A, Dendale P, Van Loon LJC. Neuromuscular electrical stimulation prevents muscle wasting in critically ill comatose patients. *Clin Sci (Lond)*. 2015;128:357–65 England.
52. Brealey D, Brand M, Hargreaves I, Heales S, Land J, Smolenski R, et al. Association between mitochondrial dysfunction and severity and outcome of septic shock. *Lancet*. 2002;360:219–23 England.
53. Carre JE, Orban J-C, Re L, Felsmann K, Iffert W, Bauer M, et al. Survival in critical illness is associated with early activation of mitochondrial biogenesis. *Am J Respir Crit Care Med*. 2010;182:745–51 United States.
54. Jiroutkova K, Krajcova A, Ziak J, Fric M, Gojda J, Dzupa V, et al. Mitochondrial function in an in vitro model of skeletal muscle of patients with protracted critical illness and intensive care unit-acquired weakness. *JPEN J Parenter Enteral Nutr*. United States. 2017;41:1213–21.
55. Jiroutkova K, Krajcova A, Ziak J, Fric M, Waldauf P, Dzupa V, et al. Mitochondrial function in skeletal muscle of patients with protracted critical illness and ICU-acquired weakness. *Crit Care*. 2015;19:448 England.
56. Wyrwich KW, Tierney WM, Babu AN, Kroenke K, Wolinsky FD. A comparison of clinically important differences in health-related quality of life for patients with chronic lung disease, asthma, or heart disease. *Health Serv Res*. 2005; 40:577–91 United States.
57. Parry SM, Berney S, Koopman R, Bryant A, El-Ansary D, Puthuchery Z, et al. Early rehabilitation in critical care (eRICC): functional electrical stimulation with cycling protocol for a randomised controlled trial. *BMJ Open*. 2012;2(5) England.
58. Ely EW, Margolin R, Francis J, May L, Truman B, Dittus R, et al. Evaluation of delirium in critically ill patients: validation of the Confusion Assessment Method for the Intensive Care Unit (CAM-ICU). *Crit Care Med*. 2001;29:1370–9 United States.
59. Ziak J, Krajcova A, Jiroutkova K, Nemicova V, Dzupa V, Duska F. Assessing the function of mitochondria in cytosolic context in human skeletal muscle: adopting high-resolution respirometry to homogenate of needle biopsy tissue samples. *Mitochondrion*. 2015;21:106–12.
60. Krajcova A, Ziak J, Jiroutkova K, Patkova J, Elkalaf M, Dzupa V, et al. Normalizing glutamine concentration causes mitochondrial uncoupling in an in vitro model of human skeletal muscle. *J Parenter Enter Nutr*. 2015; 39(2):180–9.
61. Duška F, Fric M, Waldauf P, Páout J, Anděl M, Mokrejš P, et al. Frequent intravenous pulses of growth hormone together with glutamine supplementation in prolonged critical illness after multiple trauma: effects on nitrogen balance, insulin resistance, and substrate oxidation. *Crit Care Med*. 2008;36(6):1707–13.

Publisher's Note

Springer Nature remains neutral with regard to jurisdictional claims in published maps and institutional affiliations.

Ready to submit your research? Choose BMC and benefit from:

- fast, convenient online submission
- thorough peer review by experienced researchers in your field
- rapid publication on acceptance
- support for research data, including large and complex data types
- gold Open Access which fosters wider collaboration and increased citations
- maximum visibility for your research: over 100M website views per year

At BMC, research is always in progress.

Learn more biomedcentral.com/submissions



Příloha 5

Krajčová A, **Urban T**, Megvint D, Waldauf P, Balík M, Hlavička J, Budera P, Janoušek L,
Pokorná E, Duška F.

High resolution respirometry to assess function of mitochondria in native homogenates of
human heart muscle.

PLoS One. 2020 Jan 15;15(1):e0226142. doi: 10.1371/journal.pone.0226142. PMID:
31940313; PMCID: PMC6961865. IF 3.240

RESEARCH ARTICLE

High resolution respirometry to assess function of mitochondria in native homogenates of human heart muscle

Adéla Krajčová¹, Tomáš Urban¹, David Megvínét¹, Petr Waldauf¹, Martin Balík², Jan Hlavička³, Petr Budera³, Libor Janoušek⁴, Eva Pokorná⁵, František Duška^{1*}

1 OXYLAB – Laboratory of Mitochondrial Physiology, Department of Anaesthesia and Intensive Care, Third Faculty of Medicine, Charles University and FNKV University Hospital, Prague, Czech Republic, **2** Department of Anaesthesia and Intensive Care, 1st Medical Faculty, Charles University and General University Hospital, Prague, Czech Republic, **3** Department of Cardiac Surgery, Third Faculty of Medicine, Charles University and FNKV University Hospital, Prague, Czech Republic, **4** Transplantation Surgery Department, Institute for Clinical and Experimental Medicine, Prague, Czech Republic, **5** Department of Organ Recovery and Transplantation Databases, Institute for Clinical and Experimental Medicine, Prague, Czech Republic

* fduska@yahoo.com



OPEN ACCESS

Citation: Krajčová A, Urban T, Megvínét D, Waldauf P, Balík M, Hlavička J, et al. (2020) High resolution respirometry to assess function of mitochondria in native homogenates of human heart muscle. PLoS ONE 15(1): e0226142. <https://doi.org/10.1371/journal.pone.0226142>

Editor: Maria Moran, Instituto de Investigacion Hospital 12 de Octubre, SPAIN

Received: April 4, 2019

Accepted: November 20, 2019

Published: January 15, 2020

Copyright: © 2020 Krajčová et al. This is an open access article distributed under the terms of the [Creative Commons Attribution License](https://creativecommons.org/licenses/by/4.0/), which permits unrestricted use, distribution, and reproduction in any medium, provided the original author and source are credited.

Data Availability Statement: All relevant data are within the manuscript and its Supporting Information files.

Funding: The work has been supported solely from the grant of Czech Health Research Council, AZV No. NV18-06-00417 (PRASE). The electron microscopy was performed at the Microscopy Centre - Electron Microscopy CF, IMG AS CR supported by the Czech-Biolmaging large RI project (LM2015062 funded by MEYS CR) and by OP RDE (CZ.02.1.01/0.0/0.0/16_013/0001775).

Abstract

Impaired myocardial bioenergetics is a hallmark of many cardiac diseases. There is a need of a simple and reproducible method of assessment of mitochondrial function from small human myocardial tissue samples. In this study we adopted high-resolution respirometry to homogenates of fresh human cardiac muscle and compare it with isolated mitochondria. We used atria resected during cardiac surgery ($n = 18$) and atria and left ventricles from brain-dead organ donors ($n = 12$). The protocol we developed consisting of two-step homogenization and exposure of 2.5% homogenate in a respirometer to sequential addition of 2.5 mM malate, 15 mM glutamate, 2.5 mM ADP, 10 μ M cytochrome c, 10 mM succinate, 2.5 μ M oligomycin, 1.5 μ M FCCP, 3.5 μ M rotenone, 4 μ M antimycin and 1 mM KCN or 100 mM Sodium Azide. We found a linear dependency of oxygen consumption on oxygen concentration. This technique requires < 20 mg of myocardium and the preparation of the sample takes < 20 min. Mitochondria in the homogenate, as compared to subsarcolemmal and interfibrillar isolated mitochondria, have comparable or better preserved integrity of outer mitochondrial membrane (increase of respiration after addition of cytochrome c is up to $11.7 \pm 1.8\%$ vs. $15.7 \pm 3.1\%$, $p < 0.05$ and $11.7 \pm 3.5\%$, $p = 0.99$, resp.) and better efficiency of oxidative phosphorylation (Respiratory Control Ratio = 3.65 ± 0.5 vs. 3.04 ± 0.27 , $p < 0.01$ and 2.65 ± 0.17 , $p < 0.0001$, resp.). Results are reproducible with coefficient of variation between two duplicate measurements $\leq 8\%$ for all indices. We found that whereas atrial myocardium contains less mitochondria than the ventricle, atrial bioenergetic profiles are comparable to left ventricle. In conclusion, high resolution respirometry has been adapted to homogenates of human cardiac muscle and shown to be reliable and reproducible.

The funders had no role in study design, data collection and analysis, decision to publish, or preparation of the manuscript.

Competing interests: The authors have declared that no competing interests exist.

1. Introduction

Human heart muscle has very high and continuous energy demand, mostly due to its contractile work when propelling blood through the circulatory system [1–3]. Myocardium can generate and consume 15 times its own weight of ATP each day [3], and over 95% of ATP is generated in oxidative phosphorylation [4]. Intracellular stores of ATP and creatine phosphate can be exhausted within a few seconds [4] and any defect in mitochondrial metabolism leading to decreased ATP production results in rapid contractile dysfunction [4,5]. Thus, cardiac function depends on the continuous ability of myocardium to generate ATP at a high rate [3,4]. Cardiac cells contain around 5 000–10 000 mitochondria per cell [6], occupying about 30% of the cellular volume [3]. The major fuel for oxidative metabolism of a healthy human heart are fatty acids (70–90%) [4,7], the remainder being carbohydrates, lactate, ketone bodies and amino acids [4]. A range of congenital and acquired heart diseases are associated with altered mitochondrial metabolism and insufficient ATP production [8,9], as is cardiac aging [10]. In addition, there is growing interest in the research of cardiotoxicity of commonly used drugs which may cause severe damage to cardiac mitochondria leading to arrhythmias or heart failure [11]. Most data are obtained by studying cell lines or animal models [12], but their applicability to humans is questionable.

Assessing function of human cardiac mitochondria in a way that would reflect conditions *in vivo* and allow *in vitro* experimental manipulation remains a challenge. Human cardiac tissue can be obtained during cardiac surgery or by catheter endomyocardial biopsy, which limits the size of the sample to hundreds of milligrams at best. This amount of tissue allows for spectrophotometric measurement of the activity of isolated mitochondrial complexes or other enzymes, but this only poorly reflects the function of mitochondria and its alteration (e.g. an existing influence may not be seen on the enzymes measured, or, on the other hand, a severe inhibition of a functionally redundant enzyme may not affect the function of mitochondria as a whole). High-resolution respirometry offers the advantage of assessing mitochondrial function in the cytosolic context, but the intracellular contents leaks after membrane disruption and this method has also other limitations. When isolated mitochondria are evaluated, large amounts of tissue are needed [13–16]. The preparation of permeabilised muscle fibres is manually demanding and results can be operator-dependent [17,18].

The main purpose of this study was to develop a simple, reproducible technique for *ex vivo* bioenergetics profiling of the human myocardial tissue. We hypothesised that high resolution respirometry of tissue homogenates, as originally described by Pecinova et al. [19] and later modified for the use in human skeletal muscle [20], can be successfully adopted to human cardiac muscle. We set ourselves following objectives: (i) Perform optimization of experimental such as homogenate concentration, (ii) determine durability of muscle samples, (iii) determine dependence of oxygen consumption rate on oxygen concentration, (iv) compare the new technique with well-established respirometry in isolated mitochondria and, lastly, (v) determine, whether atrial myocardium has energetic profile representative of left ventricle myocardium.

2. Methods

2.1. Study subjects

The study protocol and consent form were approved by the Ethics Committee of the Institute for Clinical and Experimental Medicine and Thomayer Hospital and the Ethics Committee of Faculty Hospital Kralovske Vinohrady, Prague. All the patients at Department of Cardiac Surgery provided written informed consent. The informed consent of brain-dead donors were obtained from family members.

Myocardial tissue homogenates were prepared from biopsies of right atrial appendages (sample ~ 300 mg) obtained from patients undergoing coronary artery bypass grafting surgery or heart valve replacement at the Department of Cardiac Surgery of Královské Vinohrady University Hospital (n = 57, for all experiments). For studies comparing atrial and ventricular myocardium, we used samples obtained from brain-dead organ donors (n = 15) without cardiac disease, whose hearts were not suitable for transplantation due to donor age over 50 years (as per local protocol of Transplantation Centre of Institute of Clinical and Experimental Medicine) or logistic issues. Tissue samples from left ventricle myocardium and from left atrial appendage were obtained by the organ retrieval surgeon immediately after cardiac arrest artificially induced by ice-cold KCl-based cardioplegic solution (NaCl 110.0 mM, NaHCO₃ 10.0 mM, KCl 16.0 mM, MgCl₂ 16.0 mM, CaCl₂ 1.2 mM, pH 7.8). Patients with known heart disease (heart failure, severe arrhythmias incl. types II or III atrioventricular blocks, medical history of myocardial infarction, ejection fraction of left ventricle < 30%, re-operation and past or current inflammatory heart diseases and mitochondrial disorders) were a priori excluded. Detailed characteristics of study subjects are described in [Table 1](#).

2.2. Myocardial tissue homogenates preparation

After collection, samples were put on ice in biopsy preservation solution [BIOPS, 2.77 mM CaK₂EGTA, 7.23 mM K₂EGTA, 5.77 mM Na₂ATP, 6.56 mM MgCl₂ x 6 H₂O, 20 mM taurine, 15 mM Na₂Phosphocreatine, 20 mM imidazole, 0.5 mM dithiothreitol and 50 mM MES hydrate (pH 7.1)] [21], and transported to the lab within 5 or 30 min (for cardiac surgery patients or organ donors, respectively). According to modified protocol for human skeletal muscle homogenates [20], we removed connective and adipose tissue using pre-cold scissors and anatomic forceps under a microscope (See photographs in the **Supplementary Appendix** and the **Supplementary Video File**), so that only muscle tissue was homogenized. After gentle blotting by a piece of sterile gauze (~ less than 6 seconds), cardiac muscle tissue was placed on parafilm, weighted on an analytical scale and minced with scissors into fine fragments whilst placed on ice. Tissue fragments were then scraped into pre-chilled 1 mL Dounce Tissue Grinder (glass construction; Wheaton™, Millville, USA) (see [Fig 1](#)) on ice. Respiratory medium MiR05 [0.5 mM EGTA, 3 mM MgCl₂ x 6 H₂O, 60 mM lactobionic acid, 20 mM taurine, 10 mM KH₂PO₄, 20 mM HEPES, 110 mM sucrose and 1 g/l of BSA (pH 7.1)] [22] was subsequently added to the tissue to obtain a 10% tissue solution (~100 mg of tissue/per 1 mL of buffer).

Tissue fragments were then manually homogenized by 10–12 initial strokes up and down with a loose glass pestle (clearance = 0.114 ± 0.025 mm; Wheaton™, Millville, USA). The next step of homogenization in the Dounce grinder was performed with 5–6 slow strokes by a motor-driven pre-cold PTFE pestle of 2 mL Potter-Elvehjem homogenizer (rounded shape without notches; Wheaton™ 2mL Potter-Elvehjem Tissue Grinder; Wheaton™, Millville, USA; diameter shaft: 6.3 mm). The shaft of PTFE pestle was fixed in motor-driven homogenizer (HEi-Torque Value 100, Heidolph, Germany). Initially, the glass tube of 1 mL Dounce Tissue Grinder was inserted into plastic 50 mL Falcon tube filled with crushed ice. The PTFE pestle was immersed into the glass tube of 1 mL Dounce Tissue Grinder and motor-driven homogenizer was turned on. Whilst speed was increasing from 0 to 750 rpm, the pestle was slowly moved down to touch the bottom of the glass tube. When the speed reached 750 rpm, the pestle was manually moved up and down 5–6 times whilst it was still immersed in the homogenate in order to avoid bubble formation. After that, the speed was gradually slowed, and the pestle was pulled out of the glass grinder. The homogenate was then placed on ice and diluted in MiR05 buffer (from 1:1 to 1:9) to obtain the appropriate concentration for high-resolution

Table 1. Characteristics of study subjects. Note: CAD = coronary artery disease, CABG = coronary artery bypass grafting, COPD = chronic obstructive pulmonary disease, CPR = cardiopulmonary resuscitation, MI = myocardial infarction, T1DM/T2DM = Diabetes Mellitus, type 1 or 2, respectively.

Subject	Age	Sex	Surgery procedure	Cardiac disease/Cause of brain death	Other diseases, medication
Cardiac surgery 1	69	M	CABG	CAD, MI	CKD, T2DM, Hypothyreosis
Cardiac surgery 2	64	M	CABG	CAD, MI	Atrial fibrillation, Hypertension, T2DM
Cardiac surgery 3	71	M	CABG	CAD	Arterial hypertension, Hyperlipidaemia
Cardiac surgery 4	75	M	CABG	CAD	Hypertension, T2DM, COPD
Cardiac surgery 5	71	M	CABG	CAD	Hypertension, Hyperlipidaemia
Cardiac surgery 6	56	F	CABG	CAD, MI, mild congestive heart failure	Hypertension, T1DM, Hyperlipidaemia, Hypothyreosis
Cardiac surgery 7	69	M	Aortic valve replacement	Aortic valve stenosis	CAD, Hypercholesterolaemia, Glaucoma
Cardiac surgery 8	74	M	CABG	CAD, MI	Atrial fibrillation, Diabetes mellitus type 2
Cardiac surgery 9	71	M	CABG	CAD, MI	Atrial fibrillation, Hypertension
Cardiac surgery 10	65	M	CABG	CAD, MI	Hypertension, T2DM, Rectal cancer in the past
Cardiac surgery 11	76	M	CABG	CAD	Hypertension, Hyperlipidaemia
Cardiac surgery 12	60	M	CABG	CAD	Hypertension, T2DM, Hyperlipidaemia
Cardiac surgery 13	68	F	CABG	CAD	T1DM, Hyperlipidaemia
Cardiac surgery 14	72	M	CABG	CAD	Atrial fibrillation, Hypertension, Hyperlipidaemia
Cardiac surgery 15	68	M	CABG	CAD	Hypertension
Cardiac surgery 16	54	M	CABG	CAD, MI	Hypertension, Hyperlipidaemia, Asthma bronchiale
Cardiac surgery 17	64	M	CABG	CAD	Hypertension, Hyperlipidaemia, Urinary bladder cancer
Cardiac surgery 18	65	M	Aortic valve replacement	Aortic valve stenosis with acute cardiac failure	Pulmonary hypertension, Arterial hypertension
Organ donor 1	56	F	-	Hypoxic brain damage after road traffic accident	-
Organ donor 2	71	F	-	Spontaneous intracerebral haemorrhage	Hypertension, Asthma bronchiale
Organ donor 3	54	F	-	Subarachnoideal haemorrhage	Hypertension, Hypothyreosis
Organ donor 4	73	M	-	Spontaneous Intracerebral haemorrhage: hypertensive crisis	Arterial hypertension, T2DM
Organ donor 5	67	M	-	Traumatic brain injury	Hypertension
Organ donor 6	77	F	-	Subarachnoideal haemorrhage	COPD, Hypertension
Organ donor 7	40	F	-	Hypoxic brain injury after CPR	Eosinophilic pulmonary disease
Organ donor 8	63	M	-	Subarachnoideal haemorrhage	Arterial hypertension
Organ donor 9	42	F	-	Hypoxic brain injury after CPR	Pulmonary embolism
Organ donor 10	45	M	-	Aneurysmal intracerebral hemorrhage	-
Organ donor 11	84	F	-	Spontaneous intracerebral haemorrhage	Arterial hypertension, Hyperlipidaemia
Organ donor 12	55	F	-	Hypoxic brain injury after CPR	Bacterial meningitis
Organ donor 13	62	F	-	Aneurysmal intracerebral hemorrhage	Chronic kidney disease
Organ donor 14	75	F	-	Aneurysmal intracerebral hemorrhage	-
Organ 15	78	F	-	Spontaneous intracerebral haemorrhage	Atrial fibrillation, Arterial hypertension, T1DM

<https://doi.org/10.1371/journal.pone.0226142.t001>

respirometry and the homogenization was repeated by 3–4 additional strokes by motor-driven PTFE pestle. Raw homogenate was then filtered through a polyamide mesh (parameters: loop size 335 µm, fibre diameter 120 µm, open space 54%, material 100% polyamide; SILK & PROGRESS s.r.o., Czech Republic) in order to remove the remaining connective tissue,

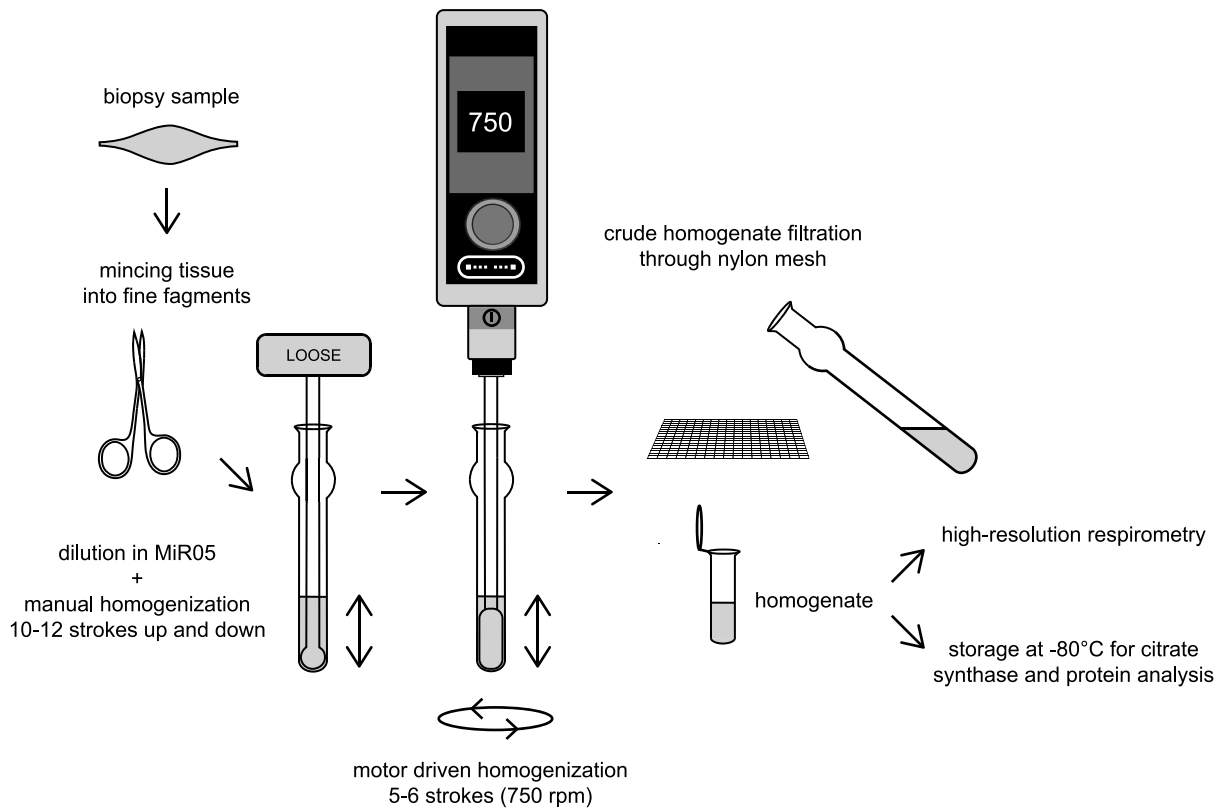


Fig 1. Step-by-step flowchart of cardiac muscle tissue homogenate preparation.

<https://doi.org/10.1371/journal.pone.0226142.g001>

transferred to a pre-cold Eppendorf tube and stored on ice until the measurement. Various homogenizer sets with different clearance between the grinder and the pestle made from different material (glass & PTFE) were tried as well as single- versus multi-step homogenization procedure (see **Supplementary Appendix** for more details). We included the filtration through polyamide mesh to increase the homogeneity of muscle homogenate by removing the rest of connective tissue. We kept all the samples on ice throughout preparation procedures. All tubes, scissors and glassware were properly rinsed with 70% ethanol and distilled water, dried and kept on ice to cool to 0°C before use. Similarly, glass and PTFE pestles were pre-cooled to 0°C before homogenization. The critical step was to perform functional studies within an hour after homogenization procedure (see *Durability of homogenates* in [Results](#)).

2.3. High resolution respirometry

Functional studies were performed using high-resolution respirometry Oxygraph-2k (O2k, Oroboros Instruments, Innsbruck, Austria) with a polarographic oxygen electrode and two 2 mL chambers allowing for parallel measurements [13,21]. In our experiments, we performed all initial steps including calibration according to the manufacturer's recommendations [21]. The oxygen solubility factor for MiR05 was set to 0.92 at 37°C [23]. The homogenate was then pipetted into both chambers, and these were carefully closed with stoppers avoiding the creation of bubbles in the medium. Oxygen concentration and flux were simultaneously recorded and analysed by Dat lab software (Datlab Version 7.0, Oroboros Instruments, Innsbruck,

Austria). Reagents were added through a small capillary tube in the chamber using Hamilton syringes (Oroboros Instruments, Innsbruck, Austria).

2.4. Optimization of homogenate concentration

Initially, we aimed to develop a simple protocol (up to 30-minutes of duration) with well detectable responses of mitochondria to injected substrates, but avoiding a rapid exhaustion of oxygen in the chamber. A range of concentrations of homogenate (1; 2.5; 5 and 10%) were tried at $n = 4$. Lower concentrations of homogenates were prepared by dilution of 10% homogenate in additional volume of respiration medium (MiR05).

2.5. Substrate—Inhibitor—Uncoupler titration (SUIT) protocol

With 2.5% homogenate we subsequently performed a series of experiments to identify the most effective concentrations of adenosine diphosphate (ADP), the uncoupler “Carbonyl cyanide-4(trifluoromethoxy) phenylhydrazone (FCCP)”, the ATPase inhibitor oligomycin and cytochrome *c* (cyt *c*). Each titration experiment was performed on $n = 7$ except of oligomycin experiments on FCCP-induced stimulated respiration, which was performed on $n = 3$. All reagents were obtained from Sigma-Aldrich (St. Louis, USA). Substrates were dissolved in distilled water and pH of each solution was adjusted to pH 7.0. Oligomycin, FCCP and antimycin A were dissolved in DMSO. Firstly, we made a number of measurements with increasing ADP concentration (0.5; 1; 1.5; 2.5 mM) to achieve a maximum increase of oxygen consumption rate. ADP was added after injection of substrates for complex I (malate + glutamate). After that, oligomycin was titrated at various concentrations (0.5; 1.0; 1.5; 2; 2.5 μM) to decrease oxygen flux until the curve achieved the plateau. A series of experiments has been performed with FCCP titration to find optimal concentration for maximal respiratory rate, i.e. full uncoupling without electron transfer system (ETS) inhibition. FCCP was injected in stepwise manner to achieve final concentrations of 0.25; 0.5; 0.75; 1; 1.25; 1.5 and 1.75 μM , and peak oxygen consumption rate was sought for. In addition, we tested a possible interaction between 2.5 and 0.5 μM oligomycin and FCCP as this problem has recently been discussed [24]. Finally, oxygen consumption was recorded at increasing concentrations of cytochrome *c* (10 and 20 μM).

2.6. Calculation of mitochondrial functional indices

Respiratory states and substrate concentrations used for final SUIT protocol are outlined in Fig 2. Mitochondrial parameters were derived as shown in Table 2.

2.7. Mitochondrial membrane integrity

Mitochondrial outer membrane integrity was tested by addition of 10 μM cytochrome *c*. Since an intact outer mitochondrial membrane provides a complete barrier against penetration of cytochrome *c*, an increase in respiration after addition of exogenous cytochrome *c* reflects disruption of outer mitochondrial membrane caused by homogenization and the isolation procedure [25]. Up to a 10–20% increase in respiration is considered acceptable as evidence of preserved integrity of mitochondrial membrane [26,27]. Damage to outer mitochondrial membrane was defined as percent of increase in oxygen consumption after addition of exogenous cytochrome *c*, when both ADP and mitochondrial substrates were present, and calculated as $100 \times (\text{cyt } c\text{-ADP})/\text{ADP}$. The *respiratory control ratio* (State 3/State 4), indicating mitochondrial coupling of respiration to phosphorylation, was used as an additional parameter testing functional integrity of mitochondria [26,28]. The morphology of mitochondria in the homogenate was assessed by electron microscopy using FEI Morgagni 268 transmission electron

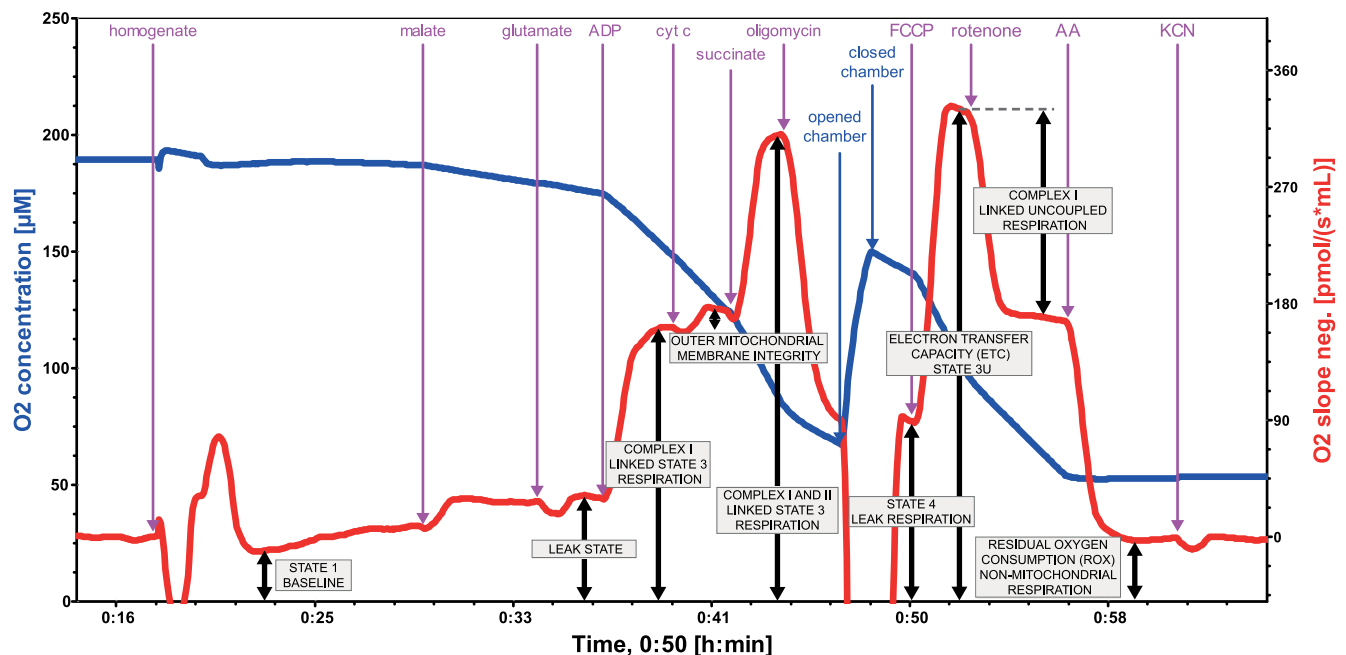


Fig 2. Mitochondrial functional indices measured by high-resolution respirometry on 2.5% homogenate of human cardiac muscle (left ventricle). Bioenergetic parameters were assessed at baseline (State 1) and by sequential addition of 2.5 mM malate and 15 mM glutamate (so-called pseudo-State 2 respiration representing LEAK state), 2.5 mM ADP (complex I linked State 3 respiration), 10 μ M cytochrome c (outer mitochondrial membrane integrity), 10 mM succinate (complex I+II linked State 3 respiration), 2.5 μ M oligomycin (State 4), 1.5 μ M FCCP (State 3u representing electron transfer capacity), 3.5 μ M rotenone (complex I linked uncoupled respiration), 4 μ M antimycin A (residual oxygen consumption representing non-mitochondrial respiration) and 1 mM KCN (to confirm that antimycin A provides an adequate non-mitochondrial background). Each concentration refers to final concentration of the agent in the chamber. Stepwise titration of the uncoupler is possible and recommended if time permits. We also verified that 2.5 μ M oligomycin does not inhibit uncoupled respiration as compared to 0.5 μ M oligomycin. Note: AA = antimycin A; ADP Mg = Adenosine diphosphate with Mg^{2+} ; Cyt c = cytochrome c; FCCP = uncoupler; oligo = oligomycin (F_1F_0 ATPase inhibitor); KCN = potassium cyanide.

<https://doi.org/10.1371/journal.pone.0226142.g002>

microscope (see Fig 3). The images were captured by Mega View III CCD camera (Olympus Soft Imaging Solutions). More details about preparation of mitochondria for electron microscopy and imaging are described in **Supplementary Appendix**.

2.8. Comparison of cardiac muscle homogenates with isolated mitochondria and reproducibility of the method

We compared the reproducibility and results of the new respirometry protocol using homogenates with isolated mitochondria, the gold standard to study mitochondrial function [29]. Muscle samples from the left ventricles of brain-dead organ donors ($n = 4$) were split and processed: one part used for preparation of a homogenate and the other for the preparation of mitochondria. Respirometry in homogenates and isolated mitochondria was done in parallel, using the same SUIIT protocol. The same process was repeated twice for each subject in order to test the reproducibility of the results. Isolation of both subsarcolemmal and interfibrillar mitochondria was performed in parallel with preparation of cardiac muscle tissue homogenates as previously described [19,28]. Briefly, minced cardiac tissue was homogenized in Isolation Medium containing 225 mM Mannitol, 75 mM Sucrose and 1 mM EGTA (pH 7.4) and subsequently centrifuged at low speed. Subsarcolemmal mitochondrial fraction was obtained from supernatant followed by centrifugation at high speed without the use of proteolytic enzymes. Interfibrillar mitochondria were isolated by multi-step centrifugation after the initial

Table 2. Mitochondrial functional indices.

Parameter (Abbreviation)	Name	Measured/Calculated	Note
STATE 1 [<i>pmol/(s*ml)</i>]	Basal respiration	Measured as OCR after addition of homogenate/mitochondria minus ROX	Represents basal respiration
% increase post addition of cyt c	-	Measured as 100 multiplied by (OCR after addition of substrates for complex I, ADP and cytochrome c minus OCR after addition of substrates for complex I, ADP)/divided by OCR after addition of substrates for complex I, ADP and cytochrome c	Represents damage of outer mitochondrial membrane
STATE 3 = OXPHOS CAPACITY (P') [<i>pmol/(s*ml)</i>]	Oxidative phosphorylation capacity	Measured as OCR after addition of substrates for CI, ADP, cyt c and substrate for CII minus ROX	Represents OXPHOS capacity
STATE 4 = leak respiration (L') [<i>pmol/(s*ml)</i>]	Leak respiration with adenylate	Measured as OCR after oligomycin addition minus ROX	Represents proton leak (in absolute values)
STATE 3u = ETS CAPACITY [<i>pmol/(s*ml)</i>]	Electron transfer system capacity	Measured as OCR after addition of substrates for CI and II, ADP, cyt c, oligomycin and FCCP minus ROX	Represents electron transfer system capacity
ROX [<i>pmol/(s*ml)</i>]	Residual oxygen consumption rate	Measured as OCR after addition of antimycin A	Represents non-mitochondrial respiration
Complex I [<i>pmol/(s*ml)</i>]	-	Measured as OCR after addition of malate+glutamate and ADP minus ROX	Represents complex I linked respiration
CI control ratio (CI/CI+II)	Complex I control ratio	Measured as OCR after addition of malate+glutamate and ADP/ divided by (this value + OCR value after subsequent succinate addition)	Represents control ratio for NADH electron transfer-pathway state
Complex II [<i>pmol/(s*ml)</i>]	-	Measured as OCR after addition of malate+glutamate, ADP, cyt c and succinate minus OCR after addition of malate+glutamate, ADP and cyt c	Represents complex II linked respiration
CII control ratio (CII/CI+II)	Complex II control ratio	Measured as OCR after addition of malate+glutamate, ADP, cyt c and succinate/ divided by (this value plus OCR after malate+glutamate and ADP addition)	Represents control ratio for succinate electron transfer-pathway state
Proton leak [%]	-	Measured as (100 multiplied by OCR after addition of substrates for CI and CII, ADP, cyt c and <i>oligomycin</i>)/ divided by OCR after addition of substrates for CI and CII, ADP and cyt c	Represents proton leak (%)
ATP production [%]	Adenosine triphosphate production	Measured as 100 minus value of proton leak (%)	Represents the rate of mitochondrial ATP production (%)
RCR	Respiratory control ratio	Calculated as the ratio of STATE 3/STATE 4	Represents OXPHOS coupling efficiency

Note: ADP = Adenosine diphosphate; ATP = Adenosine triphosphate; CI = complex I; CII = complex II; FCCP = Carbonyl cyanide-4-(trifluoromethoxy) phenylhydrazine; OCR = oxygen consumption rate; OXPHOS = oxidative phosphorylation; RCR = respiratory control ratio; ROX = residual oxygen consumption.

<https://doi.org/10.1371/journal.pone.0226142.t002>

pellet had been treated with nagarse (see **Supplementary Appendix** for more details). Mitochondrial yield was calculated as the % of citrate synthase activity in isolated mitochondria compared to whole homogenate[13] and was $13 \pm 4\%$ of total activity in the homogenate. To test the reproducibility of both methods, from duplicate measurements we calculated coefficient of variability (CV). To assess the reproducibility of the technique on atrial homogenates, we performed duplicate parallel measurements of homogenates. Each pair of homogenates was prepared from the same biopsy obtained from the patients undergoing cardiac surgery (n = 9) and also calculated CV.

2.9. Atrial vs. ventricular samples

Samples from brain-dead organ donors (n = 9) were obtained from the left appendage and ventricle of the same heart, processed in parallel by the same protocol and measured simultaneously in the two respirometry chambers. Abundant tissue obtained from organ donors allowed us to perform these measurements in duplicates or triplicates. Whilst doing so, we

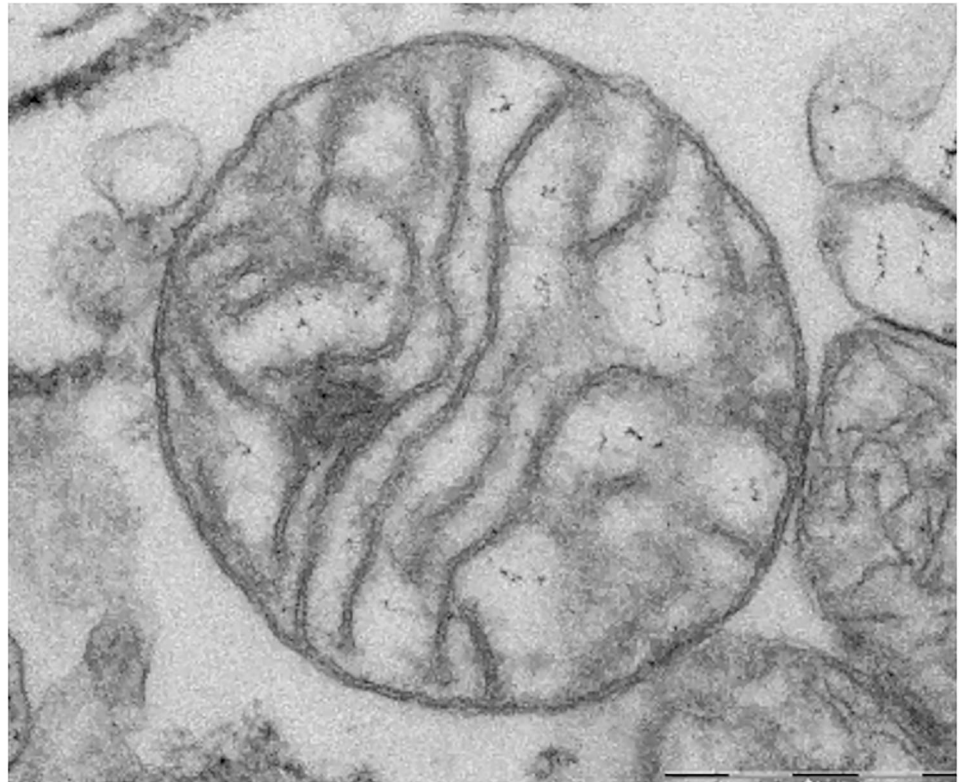


Fig 3. Detail of intact mitochondria in human heart muscle homogenate (from left ventricle) on electron microscopy. Scale bar: 0.5 μm .

<https://doi.org/10.1371/journal.pone.0226142.g003>

stored the intact heart muscle sample on ice and repeated the process of homogenisation immediately prior to the measurements.

2.10. Citrate synthase activity

Data were normalized to citrate synthase activity which is routinely used as a marker of mitochondrial density in the sample[30]. Immediately after the filtration step, the homogenized sample was divided into the two equal parts containing the same amount of homogenate: one part was subsequently used for high resolution respirometry and the second part was taken and stored at -80°C until the citrate synthase analysis. Citrate synthase assay was then performed as previously described[30].

2.11. Durability tests and cryopreservation experiments

Durability of muscle samples. The atrial samples from brain-dead donors ($n = 3$) were divided into 5 parts and stored on melting ice in a fridge ($0-2^{\circ}\text{C}$). After 0, 12, 24, 48 and 72 hours one randomly selected part of the sample was homogenised and the respirometry protocol performed immediately afterwards.

Durability of tissue homogenates. In analogy, we prepared homogenates from fresh heart samples of brain-dead donors ($n = 4$), divided into aliquots, measured at baseline, and then 2, 4, 6, 12 and 24 hours after homogenate storage on ice. Results in time were compared to determine the influence of storage time on mitochondrial functional indices, particularly coupled and uncoupled ETS capacity, and leak through inner mitochondrial membrane.

Cryopreservation of homogenates and cardiac muscle samples. Homogenate was prepared in MiR05 and frozen at -80°C ($n = 3$; each sample was prepared from the individual cardiac muscle biopsy). Analogously, cardiac muscle samples ($n = 3$) in BIOPS with 30% DMSO and 10 mg/ml BSA were frozen and stored in liquid nitrogen as previously described[31]. Later the muscle was thawed, washed and homogenized in MiR05. In both experiments, high resolution respirometry (SUIT protocol) was performed at baseline (before freezing) and immediately after thawing.

2.12. Sensitivity of detection of complex I inhibition

During preliminary experiments ($n = 3$; each sample was prepared from the individual cardiac muscle biopsy), we first found that a concentration $0.003\ \mu\text{M}$ of rotenone decreases complex I linked respiration by $39\pm 5\%$. In order to assess whether our SUIT protocol is able to detect such a degree of complex I inhibition, in parallel chambers we tested the effect of addition of $0.003\ \mu\text{M}$ of rotenone to Complex I substrate (malate+glutamate) and ADP in the presence or absence of complex II substrates (succinate).

2.13. Dependence of oxygen consumption rate on oxygen concentration

Human atrial homogenates ($n = 7$; each sample was prepared from the individual cardiac muscle biopsy) were observed after injection of substrates (2.5 mM malate, 15 mM glutamate, 10 mM succinate and $10\ \mu\text{M}$ cytochrome c) and uncoupler ($1.5\ \mu\text{M}$ FCCP) until the oxygen concentration was completely exhausted. Afterwards, the chamber was opened and oxygen consumption measured again to ensure that energy substrates were not depleted during the experiment and oxygen concentration was the only factor influencing oxygen consumption rate.

2.14. Statistics

Continuous data are presented as means \pm SD. Coefficient of Variation [CV] was calculated as $\text{CV} [\%] = 100 * \text{SD}/\text{mean}$, where SD is standard deviation. Raw respirometry parameter data were modelled using linear mixed effect model (LMEM). In the fixed part, the model consists of a dependent continuous parameter (e.g. oxygen consumption rate) and a categorical independent parameter (e.g. substrates, inhibitors or time intervals [in durability analysis]). In the random part, there was a random intercept (ID of a patient) and correlation matrix of residuals, if statistically significant (as assessed by likelihood ratio test). LMEM also was used for fitting linear part of relationship between normalized O_2 consumption and O_2 concentration. Here we use random intercept (ID of a patient) and random coefficient (O_2 concentration). Models were fit by maximum likelihood method. P value < 0.05 was considered significant. For all statistical analyses we used software Stata 15.1 (Stata Corp., LLC, U.S.A.).

3. Results

Final protocol

Preparation of homogenates. Homogenization is the crucial step, as too thorough homogenisation disrupts mitochondrial membranes and too gentle procedure leads to an inhomogeneous sample. More detailed results and discussion on homogenization are in **Supplementary appendix**. The best results were obtained by a two-step homogenization process. First, minced tissue fragments were diluted in MiR05 buffer to obtain a 10% homogenate and manually homogenized by 10–12 strokes up and down using a Dounce tissue grinder set with a clearance 0.114 ± 0.025 mm. Second, 5–6 slow strokes were delivered at 750 rpm by motor-

driven PTFE pestle (2 mL Potter-Elvehjem homogenizer) placed in the same glass tube. The sample was filtered through a polyamide mesh before measurements (See **Supplementary Video File** showing homogenization procedure).

Final SUIT protocol. Titration experiments (See **Supplementary Appendix**) resulted in the final protocol: Initially, 1900 µl MiR05 was pipetted to the chamber. After calibration, 200 µl of 2.5% homogenate from either atrial or ventricular myocardium (~5 mg myocardial tissue wet weight homogenized in 200 µL of MiR05) was added into each chamber and the lid was closed. Bioenergetic parameters were assessed by standard sequence of substrates, inhibitors and the uncoupler (See **Fig 2**).

Comparison of homogenates with isolated mitochondria prepared from ventricular myocardium

Mitochondrial structure in homogenates seemed intact under electron microscopy (see **Fig 3**). Mitochondrial membranes tend to be better preserved in homogenates as compared to isolated mitochondria. The increase of oxygen consumption after addition of cytochrome c (an index of mitochondrial outer membrane damage) was 11.7±1.8% in homogenates vs. 15.7±3.1% (p<0.05) and 11.7±3.5% (p = 0.99) in subsarcolemmal and interfibrillar isolated mitochondria, respectively. Respiratory control ratio (an index of efficiency of OXPHOS) was 3.65±0.5 in homogenates vs. 3.04±0.27 (p<0.01) and 2.65±0.17 (p<0.0001) in subsarcolemmal and interfibrillar isolated mitochondria, respectively. OXPHOS and ETS capacity normalized to CS activity were not significantly changed in homogenates compared to isolated mitochondria (OXPHOS/CS 8239±5374 vs. 7985±2504, p = 0.88; ETS/CS 7535±4545 vs. 6777±2174, resp., p = 0.60). Duplicate measurements of all dimensionless mitochondrial parameters had lower coefficient of variability in homogenates as compared to isolated mitochondria (CV ≤ 4% vs. 20%; see S1 Table in **S1 Appendix** for more detailed information).

Similar coefficients of variation were obtained for mitochondrial functional indices obtained by duplicate measurements of homogenates prepared from identical samples of right atrial appendage. See **Table 3**.

Table 3. Raw data from 6 duplicate measurements (homogenate A vs homogenate B) from right atrial appendages. Mitochondrial functional parameters. Note: ETS = Electron Transfer System, OXPHOS = oxidative phosphorylation, RCR = Respiratory Control Ratio, CI = Complex I, CII = Complex II, ROX = Residual Oxygen Consumption, ET = Electron Transfer.

Biopsy	Sample 1		Sample 2		Sample 3		Sample 4		Sample 5		Sample 6		Mean ± SD	Mean CV[%] ± SD
	A	B	A	B	A	B	A	B	A	B	A	B		
Homogenate														
STATE 1 [pmol/(s*ml)]	7	7	9	9	8	8	9	8	5	5	7	6	7±2	5.4±3.9
% increase post addition of cyt c	16	15	16	16	17	18	15	16	15	17	11	13	15±2	5.4±3.3
STATE 3 = OXPHOS CAPACITY (P') [pmol/(s*ml)]	181	195	223	249	234	209	216	212	216	186	167	145	203±29	7.2±3.4
STATE 4 = leak respiration (L') [pmol/(s*ml)]	51	59	82	81	77	72	74	76	74	67	52	51	68±12	4.2±3.7
ROX [pmol/(s*ml)]	1	0	-3	-4	-3	-2	-3	-2	-1	1	1	3	N/A	
Complex I [pmol/(s*ml)]	89	92	108	115	105	89	100	97	97	82	85	68	94±13	8±6
CI control ratio (CI/CII+II)	0.55	0.51	0.52	0.50	0.49	0.46	0.49	0.49	0.48	0.49	0.55	0.52	0.5±0.03	2.8±2.1
Complex II (CII) [pmol/(s*ml)]	72	87	98	116	111	103	102	100	104	86	70	64	93±17	8.7±4.8
CII control ratio (CII/CI+II)	0.45	0.49	0.48	0.50	0.51	0.54	0.51	0.51	0.52	0.51	0.45	0.48	0.5±0.03	3.0±2.4
Proton leak [%]	28	30	37	33	33	34	34	36	34	36	31	35	33±2.54	5.0±4.5
ATP production [%]	72	70	63	67	67	66	66	64	66	64	69	65	66.5±2.64	5.0±2.7
STATE 3u = ET capacity (E') [pmol/(s*ml)]	196	206	227	260	248	217	210	197	210	180	157	133	203.4±35.39	2.5±1.4
RCR	3.84	3.51	2.74	3.15	3.18	2.99	2.79	2.57	2.81	2.71	3.04	2.69	3.00±0.37	6.3±2.7

<https://doi.org/10.1371/journal.pone.0226142.t003>

Durability and cryopreservation experiments

Serial measurements of atrial myocardium samples stored in transport media at 0–4°C demonstrated preserved mitochondrial functional parameters (unchanged uncoupling and ETS >92% of baseline) for up to 12 hours. Afterwards we observed a steady decline of respiratory capacity and increased uncoupling. After 24, 48 and 72 hours, uncoupled respiration dropped to $87\% \pm 18\%$, $81\% \pm 20\%$ and $60 \pm 44\%$, respectively. In contrast, respiration attributable to leak of protons through inner mitochondrial membrane increased steadily from 33% to 90% after 72 hours. If homogenate was prepared first and then stored on ice, the signs of decay occurred earlier, within 2–4 hours. ETS gradually declined over time, and dropped to $89 \pm 7\%$, $93 \pm 1\%$, $63 \pm 29\%$, $52 \pm 27\%$ after 2, 4, 6, and 12 hours. Proton leak increased steadily to almost double in 12 and 24 hours after homogenization. Cryopreservation of both homogenates or intact muscle resulted in damage and uncoupling of both mitochondrial membranes and 80% resp. 44% decrease in Complex I-linked respiration. (See **Supplementary Appendix**).

Representativeness of atrial appendage samples—Comparison with ventricular myocardium

When samples of atrial appendage were compared with myocardium from the apex of left ventricle of the same subject ($n = 16$ pairs from 9 hearts) and processed through the same protocol, no significant differences were found in any of the derived dimensionless mitochondrial functional indices (proton leak $35 \pm 9\%$ vs. $34 \pm 6\%$, $p = 0.794$; RCR 3.2 ± 1.3 vs. 3.1 ± 0.5 , $p = 0.258$; CI control ratio 0.58 ± 0.07 vs. 0.57 ± 0.06 , $p = 0.493$; CII control ratio 0.42 ± 0.07 vs. 0.43 ± 0.06 , $p = 0.503$ in atrial appendages and ventricles respectively; see [Fig 4A](#)). The absolute mitochondrial indices in ventricular samples were ~ 2 fold higher ($n = 5$ pairs from 5 hearts; see [Fig 4B](#)). The values are still ~ 1.2 fold higher when normalized to citrate synthase activity (see [Fig 4C](#)), but the differences disappear completely when oxygen consumption rate is corrected to baseline value (see [Fig 4D](#)). Most importantly, as demonstrated in the dot plots in [Fig 5A](#), when respirometry measurements are performed in the homogenates of atrial and ventricular samples, the physiological variability among patients is higher than the variability between atrial vs. ventricular samples or the variability between duplicate measurements. In addition, Bland Altman plot (see [Fig 5B](#)), demonstrates the absence of any pattern of the differences between ETS in atria and ventricles.

Sensitivity of detection of complex I inhibition

We found a decrease by 87 ± 14 pmol/(s*ml) vs. 71 ± 17 pmol/(s*ml) [82%] in the chamber with substrates for complex I only vs. chamber with full SUIT protocol (i.e. substrates for both complexes I and II). Thus, <40% decrease in Complex I linked respiration is still detectable even in the presence of abundant substrate of complex II.

Influence of oxygen concentration on uncoupled respiration

In fully uncoupled mitochondria, we observed a quasi-hyperbolic relationship between oxygen concentration and consumption (See **Supplementary Appendix**). Firstly, there is a linear portion of the curve with mean slope 0.205 (CI95 0.138–0.272). Then, below ~20 μM of oxygen there was a very steep decline of respiration.

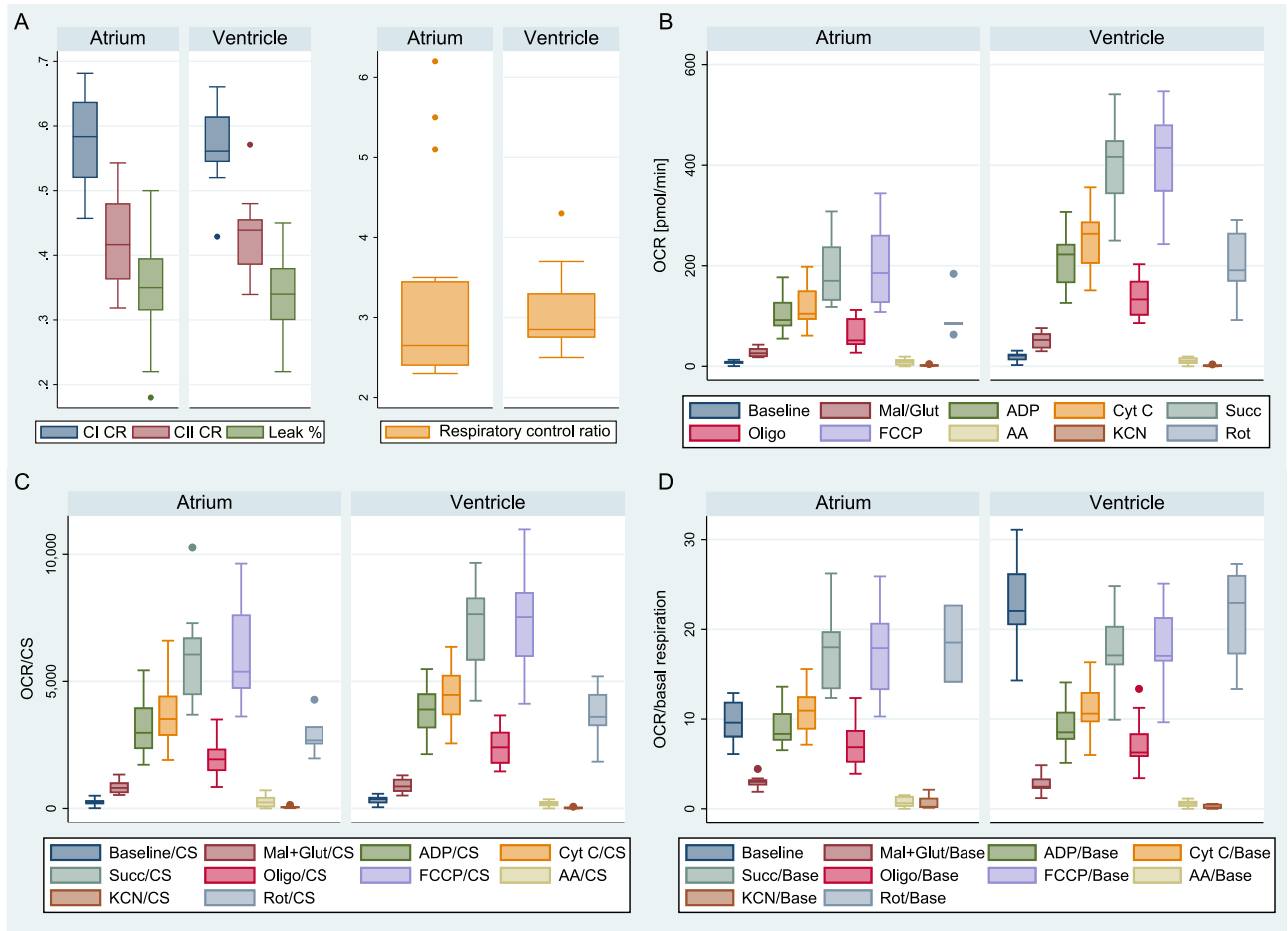


Fig 4. Comparison of atrial and ventricular mitochondrial functional indices (left atrium; left ventricle). A) Dimensionless functional indices. B) Raw data (absolute values). C) Values corrected to citrate synthase activity. D) Values corrected to baseline respiration.

<https://doi.org/10.1371/journal.pone.0226142.g004>

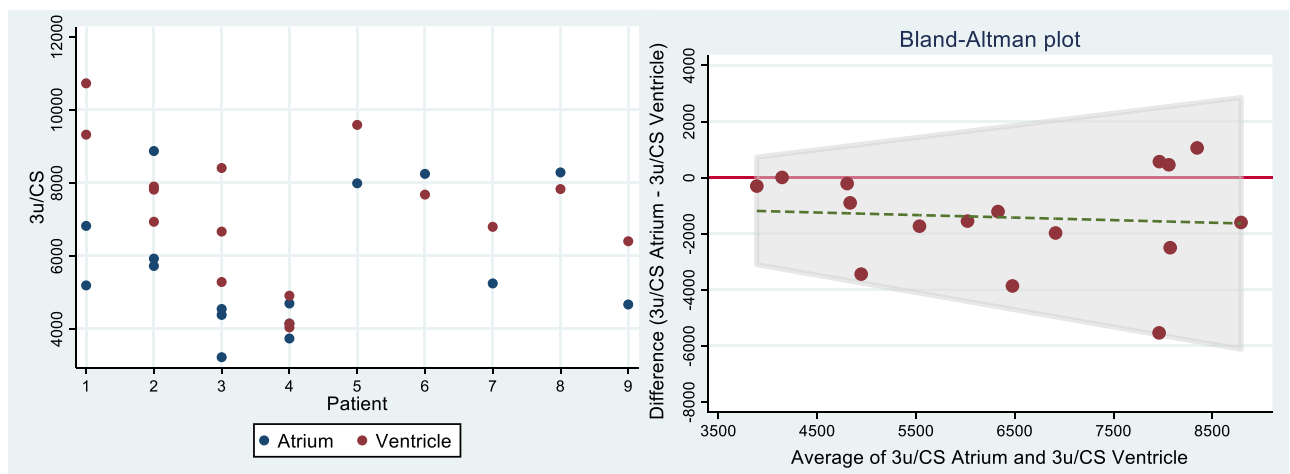


Fig 5. A-left: Dot-plot of interclass variability of electron transfer capacity normalised to citrate synthase activity (Denoted as state 3u = uncoupled). B-right: Bland-Altman plot showing the individual differences in the same parameter between atria and ventricles. Ventricles have generally a bit higher 3u/CS than atria, but there is no dependency on absolute value.

<https://doi.org/10.1371/journal.pone.0226142.g005>

Possible extension of basic respirometry protocol—Measuring respiratory fluxes through individual ETS complexes and fatty acid oxidation

By modifying the protocol so that specific inhibitors are added in the presence of abundant substrate and ADP, the technique enables the measurement of the complex II-linked uncoupled respiration (by addition of inhibitor = malonate 5 mM in uncoupled state instead of rotenone) or complex IV (by addition of substrate = ascorbate/TMPD 10/0.2 mM and inhibitor = 100 mM Sodium Azide), or fatty acid oxidation (by addition of substrate = palmitoyl-carnitine 20 μ M and FAO inhibitor = etomoxir 40 μ M). For more details See **Supplementary Appendix**.

4. Discussion

In this study, we adopted high resolution respirometry to homogenates of human atrial myocardium to enable measurement of mitochondrial function from a sample of less than 20 mg of fresh muscle. We demonstrated that this simple technique (transport media-to-respirometer time <20 min) has better variability and the same or better preservation of outer membrane integrity and OXPHOS coupling efficiency than the established techniques of respirometry in isolated mitochondria [11,13,24,42]. The method has been shown to be sensitive enough to detect <40% inhibition of Complex I-linked respiration. We also have shown that bioenergetic parameters of atrial myocardium are representative of left ventricle of the same heart provided that the adjustment to mitochondrial content is made. Crucial to the reliability of the technique is avoiding hypoxia and when parallel measurements are made (e.g. experimental vs. control), both measurements should be performed at similar oxygen concentration. Notably, 10% decrease in oxygen concentration causes ~2% decrease of oxygen consumption rate—this phenomenon is also observed with permeabilised fibers (See Pesta et al. 2012[21]). Thus, when oxygen concentrations in the two chambers start to be different, we recommend opening both chambers and allow equilibration with ambient air. Although respiratory function declines slowly, it is possible to store the muscle sample on ice up to 12 hours prior to homogenization and measurement. Once homogenized, the respirometry must be performed immediately as small, but significant decreases occur as early as 2 hours after homogenization. We have not found any successful cryopreservation technique, and it is necessary to process samples with 12 hours of sampling.

Mitochondrial function in the human heart has conventionally been assessed by polarographic measurement performed on isolated mitochondria[32–35], using a classical Clark electrode[36]. For this technique a minimum of ~0.5 g is required [35]. Such an amount of tissue can only be obtained from brain dead donor hearts unsuitable for donation (similar to what we did in this study), or explanted failing hearts, which are known to be dysfunctional [8,34,37]. Moreover, the isolation procedure itself can lead to artificial damage of mitochondria during centrifugation[38], which only yields 20–40% of mitochondria in the sample[13–16,39], potentially inducing a selection bias[40]. Because isolation of mitochondria disrupts native environment of mitochondrial network and intracellular communication with other organelles[41], the generalizability of the results to *in vivo* environment have been questioned [29,42]. In 1987, Veksler et al.[43] described the technique of permeabilisation of cardiac muscle fibers by saponin, which interacts with cholesterol and creates pores in plasma membrane which becomes permeable for small molecules (such as for ADP, or other substrates and inhibitors needed in SUIT respirometry protocol), so that cytosol is washed out from otherwise intact cells[17,44]. This *in situ* technique is therefore more representative of *in vivo* mitochondrial arrangement than isolated mitochondria and allows determination of mitochondrial functional parameters in small endomyocardial biopsy samples[43,45,46] stored for up to 24

hours[17]. Major disadvantage of permeabilisation is that the process is manually demanding and takes at least ~2 hours[17]. Due to the challenges of assessing citrate synthase activity from permeabilised fibers recovered from the respirometry chamber [17,18], mitochondrial functional indices were normalized to wet weight of manually isolated fibers blotted on a filter paper to remove excess of fluid[17,18]. A recent study showed a relatively large variability (CV of 15.2%) between the measurements of two bundles of skeletal muscle fibers from the same subject[18], roughly the same variability as we have seen in isolated mitochondria in our study, and twice the variability we have seen by using homogenates in this study.

Another factor, which has to be considered when comparing experimental approaches to the assessment of mitochondrial bioenergetics is the degree of damage mitochondria during the pre-analytical phase. The increase of ADP-driven respiration after the addition of cytochrome c was $15\pm 2\%$ with our technique, suggesting acceptable integrity of outer mitochondrial membrane. The leak of cytochrome c through damaged outer mitochondrial leads to an increase of respiration over 20%[26,27]. The damage of inner mitochondrial membrane causes uncoupling of oxidative phosphorylation from ETS. With our technique, respiratory control ratio (see Table 3) was 3.0 ± 0.4 a bit lower than in human permeabilised fibres of myocardium (5.0 ± 0.4)[47] and skeletal muscle[48]. It remains unclear, what is causing the artificial uncoupling, but it should be noted that it was not seen in fresh homogenates of human skeletal muscle, where RCR was 7.8[20] nor it was observed in saponin-permeabilised cardiac fibres harvested by very similar methods[47]. Myosin-ATPases are known to increase the apparent KM for ADP[49]. Of note, oxygen flux after addition of oligomycin is leak + non-mitochondrial oxygen consumption. Although non-mitochondrial oxygen consumption was close to 0 in our experiments (see Table 3), we recommend routine addition of ultimate ETS inhibitor, that allows determination of non-mitochondrial oxygen consumption. In case it is elevated, leak respiration should be determined by subtracting it from oxygen flux after oligomycin.

In practice, using high resolution respirometry on cardiac muscle homogenates enables *ex vivo* interventional studies (e.g. manipulations with substrate environment or exposure to drugs such as antiarrhythmics propafenone or amiodaron, which was the original purpose, why we aimed to develop this method), using e.g. atrial appendages resected during the insertion of extracorporeal circuit cannula during cardiac surgery. This is a risk-free source of heart muscle for research, in contrast to endomyocardial biopsy[45], and the simplicity of the technique together with durability of the sample 12 hrs allows for repeated measurements from the same atrium. In line with the finding of Lemieux et al.[47], we found that bioenergetics profile of atrial myocardium reflects that of ventricular myocardium, when adjusted to increased mitochondrial content. Indeed, the ability to study specific activities of individual ETS complexes is yet another advantage of this method, e.g. for further research in the field of mitochondrial myopathies.

The major weakness of our study is relatively limited number of brain-dead organ donors in which we were able to compare variability between atria and ventricles ($n = 12$). Based on post-hoc power analysis (data not shown), this number of subjects would only allow to detect differences in the main mitochondrial parameters in the range >20 to $>30\%$ and did not allow us to look at various subgroups of patients with a range of cardiac diseases, nor allowed a robust multiple regression analysis looking at factors influencing the bioenergetic differences between atrial and ventricular myocardium. Indeed, there are no operations on healthy hearts and underlying diseases leading to cardiac surgery may have affected mitochondrial function [45]. The technique itself has the main limitation in the degree of artificial uncoupling of the inner mitochondrial membrane.

In conclusion, we have (i) adapted homogenization procedure and high resolution respirometry technique for small samples of human myocardium, (ii) determined that whilst tissue

samples can be stored for up to 12 hours, homogenates are to be processed within 2 hours. We have shown (iii), that there is an oxygen limitation requiring oxygen fluxes be adjusted to oxygen concentration or experiments in parallel chambers be conducted at identical O₂ concentration. When compared with respirometry in isolated mitochondria (iv) the new technique requires ~10 times smaller sample, is less time consuming, more reproducible, but leads to some degree of artificial uncoupling. Lastly (v), we have determined, that atrial myocardium has energetic profile representative of left ventricle myocardium.

Supporting information

S1 Video.

(AVI)

S1 Appendix.

(DOCX)

S1 Data.

(ZIP)

Acknowledgments

Our thanks belong to all cardiac surgery patients who voluntarily donated their atrial tissue to enable this project, but in particular we thank to all deceased organ donors for their gift of life, and grieved families who consented to it. The electron microscopy was performed at the Microscopy Centre—Electron Microscopy CF, IMG AS CR supported by the Czech-BioImaging large RI project (LM2015062 funded by MEYS CR) and by OP RDE (CZ.02.1.01/0.0/0.0/16_013/0001775 “Modernization and support of research activities of the national infrastructure for biological and medical imaging Czech-BioImaging”). We also thank Dr. Zdenek Drahotka for valuable comments and support and prof. Charles Hoppel for proofreading.

Author Contributions

Conceptualization: Adéla Krajčová.

Data curation: Petr Waldauf.

Formal analysis: Petr Waldauf, František Duška.

Funding acquisition: Martin Balík, František Duška.

Investigation: Adéla Krajčová, Tomáš Urban, David Megvinet.

Methodology: Adéla Krajčová, Tomáš Urban, David Megvinet.

Resources: Martin Balík, Jan Hlavička, Petr Budera, Libor Janoušek, Eva Pokorná.

Supervision: Martin Balík, František Duška.

Validation: Petr Waldauf, František Duška.

Writing – original draft: Adéla Krajčová.

Writing – review & editing: Martin Balík, František Duška.

References

1. Gibbs CL. Cardiac energetics. *Physiol Rev.* 1978; 58: 174–254. <https://doi.org/10.1152/physrev.1978.58.1.174> PMID: 146205

2. Suga H. Ventricular energetics. *Physiol Rev.* 1990; 70: 247–77. <https://doi.org/10.1152/physrev.1990.70.2.247> PMID: 2181496
3. Lopaschuk G, Naranjan S. *Cardiac Energy Metabolism in Health and Disease.* Springer. <https://doi.org/10.1007/978-1-4939-1227-8> 2014.
4. Doenst T, Nguyen T, Abel E. Cardiac Metabolism in Heart Failure—Implications beyond ATP production. *Circ Res.* 2013; 113: 709–724. <https://doi.org/10.1161/CIRCRESAHA.113.300376> PMID: 23989714
5. Neubauer S. The Failing Heart—An Engine Out of Fuel. *N Engl J Med.* 2007; 356: 1140–51. <https://doi.org/10.1056/NEJMra063052> PMID: 17360992
6. Varikmaa M, Guzun R, Grichine A, Gonzalez-Granillo M, Usson Y, Boucher F, et al. Matters of the heart in bioenergetics: Mitochondrial fusion into continuous reticulum is not needed for maximal respiratory activity. *J Bioenerg Biomembr.* 2013; 45: 319–331. <https://doi.org/10.1007/s10863-012-9494-4> PMID: 23271420
7. Lionetti V, Stanley WC, Recchia FA. Modulating fatty acid oxidation in heart failure. *Cardiovasc Res.* 2011; 90: 202–209. <https://doi.org/10.1093/cvr/cvr038> PMID: 21289012
8. Quigley A, Kapsa R, Esmore D, Hale G, Byrne E. Mitochondrial respiratory chain activity in idiopathic dilated cardiomyopathy. *J Card Fail.* 2000; 6: 47–55. [https://doi.org/10.1016/s1071-9164\(00\)00011-7](https://doi.org/10.1016/s1071-9164(00)00011-7) PMID: 10746819
9. Jarreta D, Orús J, Barrientos A, Miró O, Roig E, Heras M, et al. Mitochondrial function in heart muscle from patients with idiopathic dilated cardiomyopathy. *Cardiovasc Res.* 2000; 45: 860–865. [https://doi.org/10.1016/s0008-6363\(99\)00388-0](https://doi.org/10.1016/s0008-6363(99)00388-0) PMID: 10728411
10. Tocchi A, Quarles EK, Basisty N, Gitari L, Rabinovitch PS. Mitochondrial dysfunction in cardiac aging. *Biochim Biophys Acta.* Elsevier B.V.; 2015; 1847: 1424–1433. <https://doi.org/10.1016/j.bbabi.2015.07.009> PMID: 26191650
11. Varga ZV, Ferdinandy P, Liaudet L, Pacher P. Drug-induced mitochondrial dysfunction and cardiotoxicity. *Am J Physiol Hear Circ Physiol.* 2015; 309: 1453–1467. <https://doi.org/10.1152/ajpheart.00554.2015> PMID: 26386112
12. Lemieux H, Hoppel C. Mitochondria in the human heart. *J Bioenerg Biomembr.* 2009; 41: 99–106. <https://doi.org/10.1007/s10863-009-9211-0> PMID: 19353253
13. Lanza IR, Nair KS. Functional Assessment of Isolated Mitochondria In Vitro. *Methods Enzym.* 2009; 457: 349–372. [https://doi.org/10.1016/s0076-6879\(09\)05020-4](https://doi.org/10.1016/s0076-6879(09)05020-4) PMID: 19426878
14. Figueiredo P, Ferreira R, Appell H, Duarte J. Age-induced morphological, biochemical, and functional alterations in isolated mitochondria from murine skeletal muscle. *J Gerontol A Biol Sci Med Sci.* 2008; 63: 350–359. <https://doi.org/10.1093/gerona/63.4.350> PMID: 18426958
15. Rasmussen U, Krstrup P, Kjaer M, Rasmussen H. Experimental evidence against the mitochondrial theory of aging. A study of isolated human skeletal muscle mitochondria. *Exp Gerontol.* 2003; 38: 877–886. [https://doi.org/10.1016/s0531-5565\(03\)00092-5](https://doi.org/10.1016/s0531-5565(03)00092-5) PMID: 12915209
16. Saks V, Veksler V, Kuznetsov A, Kay L, Sikk P, Tiivel T, et al. Permeabilized cell and skinned fiber techniques in studies of mitochondrial function in vivo. *Mol Cell Biochem.* 1998; 184: 81–100. https://doi.org/10.1007/978-1-4615-5653-4_7 PMID: 9746314
17. Kuznetsov AV., Veksler V, Gellerich FN, Saks V, Margreiter R, Kunz WS. Analysis of mitochondrial function in situ in permeabilized muscle fibers, tissues and cells. *Nat Protoc.* 2008; 3: 965–976. <https://doi.org/10.1038/nprot.2008.61> PMID: 18536644
18. Cardinale DA, Gejl KD, Ørtenblad N, Ekblom B, Blomstrand E, Larsen FJ. Reliability of maximal mitochondrial oxidative phosphorylation in permeabilized fibers from the vastus lateralis employing high-resolution respirometry. *Physiol Rep.* 2018; 6: e13611. <https://doi.org/10.14814/phy2.13611> PMID: 29464938
19. Pecinová A, Drahotka Z, Nůsková H, Pecina P, Houštěk J. Evaluation of basic mitochondrial functions using rat tissue homogenates. *Mitochondrion.* 2011; 11: 722–8. <https://doi.org/10.1016/j.mito.2011.05.006> PMID: 21664301
20. Ziak J, Krajcova A, Jiroutkova K, Nemcova V, Dzupa V, Duska F. Assessing the function of mitochondria in cytosolic context in human skeletal muscle: Adopting high-resolution respirometry to homogenate of needle biopsy tissue samples. *Mitochondrion.* Elsevier; 2015; 21: 106–112. <https://doi.org/10.1016/j.mito.2015.02.002> PMID: 25701243
21. Pesta D, Gnaiger E. High-resolution respirometry: OXPHOS protocols for human cells and permeabilized fibers from small biopsies of human muscle. *Methods Mol Biol.* 2012; 810: 25–58. https://doi.org/10.1007/978-1-61779-382-0_3 PMID: 22057559
22. Gnaiger E, Kuznetsov A V, Schneeberger S, Seiler R, Brandacher G, Steurer W, et al. Mitochondria in the Cold. In: Heldmaier G, Klingenspor M (eds) *Life in the Cold*, 1st edn. Springer, Berlin, Heidelberg. 2000. s. 431–442. https://doi.org/10.1007/978-3-662-04162-8_45

23. Gnaiger E. Polarographic Oxygen Sensors, the Oxygraph, and High-Resolution Respirometry to Assess Mitochondrial Function. In: Dykens JA, Will Y (eds) *Drug-Induced Mitochondrial Dysfunction*, 1st edn. John Wiley & Sons, Inc. 2008. s. 325–352. <https://doi.org/10.1002/9780470372531.ch12>
24. Ruas JS, Siqueira-Santos ES, Amigo I, Rodrigues-Silva E, Kowaltowski AJ, Castilho RF. Underestimation of the maximal capacity of the mitochondrial electron transport system in oligomycin-treated cells. *PLoS One*. 2016; 11: 1–20. <https://doi.org/10.1371/journal.pone.0150967> PMID: 26950698
25. Wikström M, Casey R. The oxidation of exogenous cytochrome c by mitochondria. Resolution of a long-standing controversy. *FEBS Lett*. 1985; 183: 293–298. [https://doi.org/10.1016/0014-5793\(85\)80796-1](https://doi.org/10.1016/0014-5793(85)80796-1) PMID: 2985431
26. Perry CGR, Kane DA, Lanza IR, Neuffer PD. Methods for assessing mitochondrial function in diabetes. *Diabetes*. 2013; 62: 1041–1053. <https://doi.org/10.2337/db12-1219> PMID: 23520284
27. Larsen S, Kraunsøe R, Gram M, Gnaiger E, Helge J, Dela F. The best approach: homogenization or manual permeabilization of human skeletal muscle fibers for respirometry? *Anal Biochem*. 2014; 1: 64–8. <https://doi.org/10.1016/j.ab.2013.10.023> PMID: 24161612
28. Palmer J, Tandler B, Hoppel C. Biochemical properties of subsarcolemmal and interfibrillar mitochondria isolated from rat cardiac muscle. *J Biol Chem*. 1977; 252: 8731–9. PMID: 925018
29. Picard M, Taivassalo T, Gouspillou G, Hepple RT. Mitochondria: isolation, structure and function. *J Physiol*. 2011; 589: 4413–4421. <https://doi.org/10.1113/jphysiol.2011.212712> PMID: 21708903
30. Srere PA. Citrate Synthase. *Methods Enzymol*. 1969; 13: 3–11. [https://doi.org/10.1016/0076-6879\(69\)13005-0](https://doi.org/10.1016/0076-6879(69)13005-0)
31. Kuznetsov AV, Kunz WS, Saks V, Usson Y. Cryopreservation of mitochondria and mitochondrial function in cardiac and skeletal muscle fibers. *Anal Biochem*. 2003; 2697. [https://doi.org/10.1016/S0003-2697\(03\)00326-9](https://doi.org/10.1016/S0003-2697(03)00326-9)
32. Toleikis A, Dzeja P, Praskevicius A, Jasaitis A. Mitochondrial functions in ischemic myocardium. I. Proton electrochemical gradient, inner membrane permeability, calcium transport and oxidative phosphorylation in isolated mitochondria. *J Mol Cell Cardiol*. 1979; 11: 57–76. [https://doi.org/10.1016/0022-2828\(79\)90452-8](https://doi.org/10.1016/0022-2828(79)90452-8) PMID: 423257
33. Chance B, Hagihara B. Activation and inhibition of succinate oxidation following adenosine diphosphate supplements to pigeon heart mitochondria. *J Biol Chem*. 1962; 237: 3540–3545. [https://doi.org/10.1016/0006-291x\(60\)90091-7](https://doi.org/10.1016/0006-291x(60)90091-7) PMID: 14019996
34. Chidsey CA, Weinbach EC, Pool PE, Morrow AG. Biochemical studies of energy production in the failing human heart. *J Clin Invest*. 1966; 45: 40–50. <https://doi.org/10.1172/JCI105322> PMID: 5901178
35. Mela L, Seitz S. Isolation of Mitochondria with Emphasis on Heart Mitochondria from Small Amounts of Tissue. *Methods Enzymol*. 1979; 55: 39–46. [https://doi.org/10.1016/0076-6879\(79\)55006-x](https://doi.org/10.1016/0076-6879(79)55006-x)
36. Chappell JB. The Oxidation of Citrate, Isocitrate and cis-Aconitate by Isolated Mitochondria. *Biochem J*. 1964; 90: 225–237. <https://doi.org/10.1042/bj0900225> PMID: 4378636
37. Scheubel RJ, Tostlebe M, Simm A, Rohrbach S, Prondzinsky R, Gellerich FN, et al. Dysfunction of mitochondrial respiratory chain complex I in human failing myocardium is not due to disturbed mitochondrial gene expression. *J Am Coll Cardiol*. Elsevier Masson SAS; 2002; 40: 2174–2181. [https://doi.org/10.1016/S0735-1097\(02\)02600-1](https://doi.org/10.1016/S0735-1097(02)02600-1)
38. Wilson M, Cascarano J, Wooten W, Pickett C. Quantitative isolation of liver mitochondria by zonal centrifugation. *Anal Biochem*. 1978; 85: 255–64. [https://doi.org/10.1016/0003-2697\(78\)90297-x](https://doi.org/10.1016/0003-2697(78)90297-x) PMID: 629384
39. Tonkonogi M, Fernström M, Walsh B, Ji L, Rooyackers O, Hammarqvist F, Wernerman J, Sahlin K. Reduced oxidative power but unchanged antioxidative capacity in skeletal muscle from aged humans. *Pflugers Arch*. 2003; 446: 261–9. <https://doi.org/10.1007/s00424-003-1044-9> PMID: 12684796
40. Krieger D, Tate C, McMillin-Wood J, Booth F. Populations of rat skeletal muscle mitochondria after exercise and immobilization. *J Appl Physiol*. 1980; 48: 23–8. <https://doi.org/10.1152/jappl.1980.48.1.23> PMID: 6444398
41. Picard M, Taivassalo T, Ritchie D, Wright KJ, Thomas MM, Romestaing C, et al. Mitochondrial structure and function are disrupted by standard Isolation methods. *PLoS One*. 2011; 6: 1–12. <https://doi.org/10.1371/journal.pone.0018317> PMID: 21512578
42. Saks V, Guzun R, Timohhina N, Tepp K, Varikmaa M, Monge C, et al. Structure-function relationships in feedback regulation of energy fluxes in vivo in health and disease: Mitochondrial Interactosome. *Biochim Biophys Acta*. Elsevier B.V.; 2010; 1797: 678–697. <https://doi.org/10.1016/j.bbabi.2010.01.011> PMID: 20096261
43. Veksler V, Kuznetsov A, Sharov V, Kapelko V, Saks V. Mitochondrial respiratory parameters in cardiac tissue: a novel method of assessment by using saponin-skinned fibers. *Biochim Biophys Acta*. 1987; 892: 191–6. [https://doi.org/10.1016/0005-2728\(87\)90174-5](https://doi.org/10.1016/0005-2728(87)90174-5) PMID: 3593705

44. Mathers KE, Staples JF. Saponin-permeabilization is not a viable alternative to isolated mitochondria for assessing oxidative metabolism in hibernation. *Biol Open*. 2015; 4: 858–864. <https://doi.org/10.1242/bio.011544> PMID: 25979709
45. From AM, Maleszewski JJ, Rihal CS. Current status of endomyocardial biopsy. *Mayo Clin Proc*. 2011; 86: 1095–1102. <https://doi.org/10.4065/mcp.2011.0296> PMID: 22033254
46. Murphy J, Frantz R, Cooper L. Endomyocardial biopsy. In: Murphy J, Lloyd M (eds). *Mayo Clinic Cardiology: Concise Textbook*, 3rd edn. Mayo Clinic Scientific Press, pp 1481–1487.
47. Lemieux H, Semsroth S, Antretter H, Höfer D, Gnaiger E. Mitochondrial respiratory control and early defects of oxidative phosphorylation in the failing human heart. *Int J Biochem Cell Biol*. 2011; 43: 1729–38. <https://doi.org/10.1016/j.biocel.2011.08.008> PMID: 21871578
48. Boushel R, Gnaiger E, Schjerling P, Skovbro M, Kraunsøe R, Dela F. Patients with type 2 diabetes have normal mitochondrial function in skeletal muscle. *Diabetologia*. 2007; 50: 790–796. <https://doi.org/10.1007/s00125-007-0594-3> PMID: 17334651
49. Perry CGR, Kane DA, Lin C, Kozy R, Brook L, Lark DS, et al. Inhibiting Myosin-ATPase Reveals Dynamic Range of Mitochondrial Respiratory Control in Skeletal Muscle. *Biochem J*. 2013; 437. <https://doi.org/10.1042/BJ20110366> PMID: 21554250

Příloha 6

Waldauf P, Hrušková N, Blahutova B, Gojda J, **Urban T**, Krajčová A, Fric M, Jiroutková K,
Řasová K, Duška F.

Functional electrical stimulation-assisted cycle ergometry-based progressive mobility programme for mechanically ventilated patients: randomised controlled trial with 6 months follow-up.

Thorax. 2021 Jul;76(7):664-671. doi: 10.1136/thoraxjnl-2020-215755. Epub 2021 Apr 30.

PMID: 33931570; PMCID: PMC8223653. IF 9.203



OPEN ACCESS

Original research

Functional electrical stimulation-assisted cycle ergometry-based progressive mobility programme for mechanically ventilated patients: randomised controlled trial with 6 months follow-up

Petr Waldauf,¹ Natália Hrušková,² Barbora Blahutova ,¹ Jan Gojda,³ Tomáš Urban,¹ Adéla Krajčová,¹ Michal Fric,¹ Kateřina Jiroutková,¹ Kamila Řasová,² František Duška ¹

► Additional supplemental material is published online only. To view, please visit the journal online (<http://dx.doi.org/10.1136/thoraxjnl-2020-215755>).

¹Department of Anaesthesiology and Intensive Care Medicine, 3rd Faculty of Medicine and FNKV University Hospital, Charles University, Prague, Czech Republic

²Department of Rehabilitation, 3rd Faculty of Medicine and FNKV University Hospital, Charles University, Prague, Czech Republic

³Department of Internal Medicine, 3rd Faculty of Medicine and FNKV University Hospital, Charles University, Prague, Czech Republic

Correspondence to

Dr František Duška, Fac Med 3, Charles University, PRAGUE, Czech Republic, Czech Republic; frantisek.duska@lf3.cuni.cz

Received 7 July 2020
Revised 15 March 2021
Accepted 6 April 2021



► <http://dx.doi.org/10.1136/thoraxjnl-2020-215093>



© Author(s) (or their employer(s)) 2021. Re-use permitted under CC BY-NC. No commercial re-use. See rights and permissions. Published by BMJ.

To cite: Waldauf P, Hrušková N, Blahutova B, et al. *Thorax* Epub ahead of print: [please include Day Month Year]. doi:10.1136/thoraxjnl-2020-215755

ABSTRACT

Purpose Functional electrical stimulation-assisted cycle ergometry (FESCE) enables in-bed leg exercise independently of patients' volition. We hypothesised that early use of FESCE-based progressive mobility programme improves physical function in survivors of critical care after 6 months.

Methods We enrolled mechanically ventilated adults estimated to need >7 days of intensive care unit (ICU) stay into an assessor-blinded single centre randomised controlled trial to receive either FESCE-based protocolised or standard rehabilitation that continued up to day 28 or ICU discharge.

Results We randomised in 1:1 ratio 150 patients (age 61±15 years, Acute Physiology and Chronic Health Evaluation II 21±7) at a median of 21 (IQR 19–43) hours after admission to ICU. Mean rehabilitation duration of rehabilitation delivered to intervention versus control group was 82 (IQR 66–97) versus 53 (IQR 50–57) min per treatment day, $p<0.001$. At 6 months 42 (56%) and 46 (61%) patients in interventional and control groups, respectively, were alive and available to follow-up (81.5% of prespecified sample size). Their Physical Component Summary of SF-36 (primary outcome) was not different at 6 months (50 (IQR 21–69) vs 49 (IQR 26–77); $p=0.26$). At ICU discharge, there were no differences in the ICU length of stay, functional performance, rectus femoris cross-sectional diameter or muscle power despite the daily nitrogen balance was being 0.6 (95% CI 0.2 to 1.0; $p=0.004$) gN/m² less negative in the intervention group.

Conclusion Early delivery of FESCE-based protocolised rehabilitation to ICU patients does not improve physical functioning at 6 months in survivors.

Trial registration number NCT02864745.

INTRODUCTION

Preserving independent functioning and acceptable quality of life is as important as survival for most patients in intensive care. Unfortunately, functional disability, a natural consequence of weakness, is a frequent and long-lasting complication in survivors of critical illness.^{1,2} Minimising sedation and a culture of early mobility has potential to reduce long-term sequelae of critical illness.^{3–5}

Key messages

What is the key question?

► Functional-electrical stimulation cycle ergometry allows delivery of exercise to patients who are sedated and unconscious and can enhance progressive mobility programme, but its effects on patients-centred outcomes are unknown.

What is the bottom line?

► Application of very early intensive cycling-based progressive mobility programmes to intensive care unit (ICU)-long stayers did not improve muscle mass and power in ICU or physical function at 6 months.

Why read on?

► This is the first large randomised controlled trial on the use of early cycling-based protocolised rehabilitation in the critically ill.

Protocolised physical therapy has been shown to reduce the duration of mechanical ventilation and intensive care unit (ICU) length of stay,⁶ but these benefits are not consistently translated into improved long-term functional outcomes.^{7–10} The delivery of protocolised physical therapy requires the concomitant presence of a cooperative patient and a trained physiotherapist, often a precious resource in the ICU. In turn, implementation of early mobility strategies may fail in randomised controlled trials and in clinical practice. Only six randomised controlled trials out of 43 published to date in the field reported data of protocol implementation.⁶ Moreover, during acute critical illness no active exercise can be delivered.^{11,12} Yet, immobility-associated muscle loss is evident as early as within 18–48 hours of onset of acute critical illness^{13,14} and during the first week patients lose 10%–20% of rectus femoris muscle cross-sectional diameter¹⁵ and up to 40% of muscle strength.¹⁶

Neuromuscular electrical stimulation (NMES) may mimic active exercise in patients, who lack voluntary muscle activity.^{17–25} During NMES, cutaneous electrodes placed over specific muscle

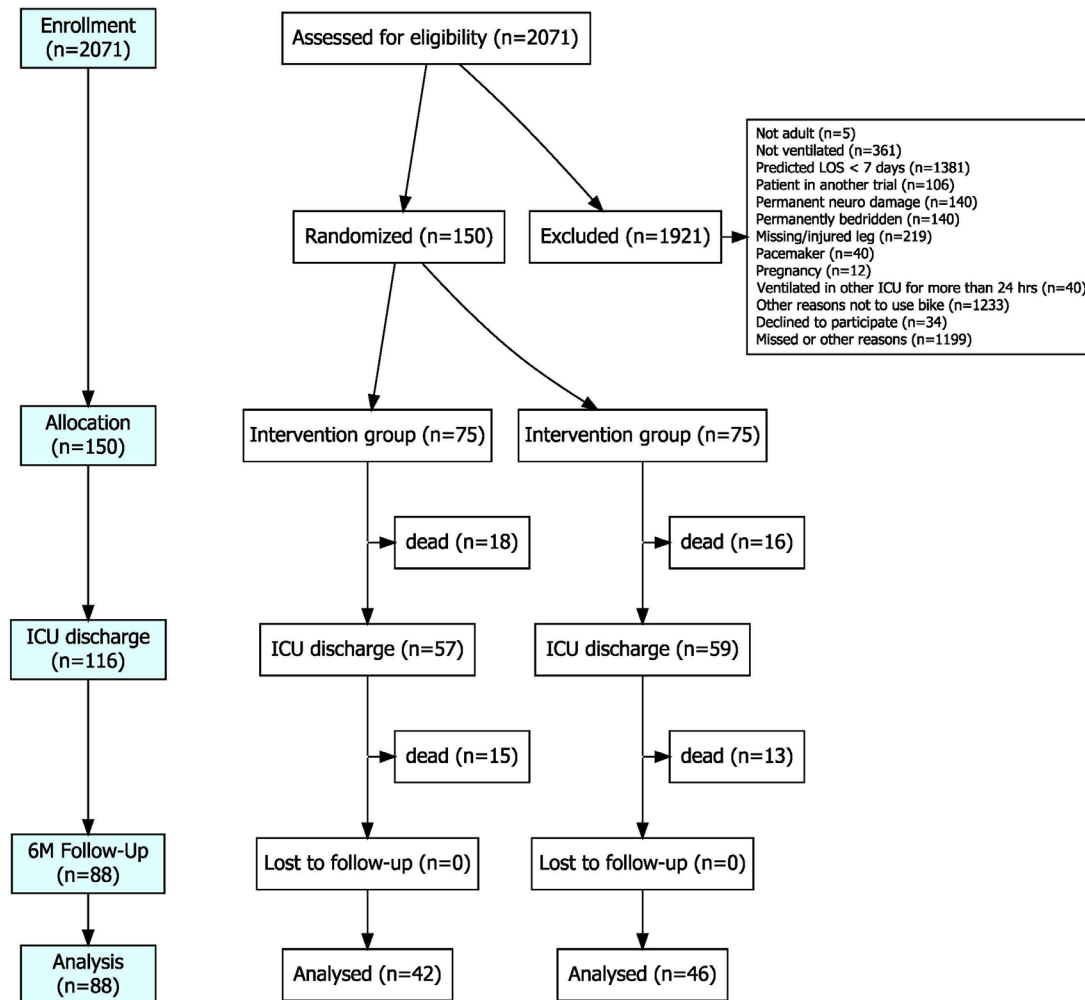


Figure 1 Flowchart of patients enrolled into the trial. Each patient could have one or more reasons not to be included and therefore the sum of reasons exceed the number of patients excluded. Other reasons included missed patients due to logistical reasons or patients who were deemed unlikely to survive; all patients who had been enrolled based on legal representative assent and regained capacity, gave written informed consent by the end of the follow-up period. ICU, intensive care unit; LOS, length of stay

groups electrically trigger muscle contractions. Passive cycling and NMES can be delivered simultaneously and synchronised to produce a coordinated pattern of movements (see online supplemental video 1) and increase whole-body energy expenditure.²⁶ The technique is called functional electrical stimulation-assisted cycle ergometry (FESCE). FESCE is beneficial to patients with stroke and spinal cord injuries (reviewed in Doucet *et al*²⁷) as it prevents the loss of muscle mass²⁸ and improved anabolic resistance and insulin sensitivity in quadriplegic patients.^{29 30} In a pilot study, FESCE seems to be safe and feasible in the critically ill.³¹

In the light of this we aimed to test early FESCE-based protocolised rehabilitation in a randomised controlled trial powered to test treatment effects on patient-centred outcomes. We hypothesised that protocolised progressive mobility programme, which includes FESCE and starts within 72 hours after ICU admission, would improve functional outcomes of ICU survivors at 6 months when compared with the standard of care.

METHODS

This was a single centre, prospective, randomised controlled parallel group trial with a blinded outcome assessor, which had been registered prior to enrolling the first patient at www.clinicaltrials.gov

and the full protocol has been published.³² We used a deferred consent procedure, where patients without capacity were enrolled based on assent gained from legal representatives and asked to provide consent as soon as they regained capacity.

Participants

Participants were recruited in two multidisciplinary ICUs of 11 and 10 level three beds, respectively, at tertiary FNKV University Hospital in Prague, Czech Republic. We included adult (≥ 18 years) patients who received mechanical ventilation for less than 72 hours but were predicted to need ICU for a week or more. We excluded patients bedridden before ICU admission, with missing or injured lower limbs, irreversible paralysis or those with pacemakers (see online supplemental appendix 1 for full list of eligibility criteria).

Standard care group

Both groups received usual best medical and nursing care in the ICU, which included daily sedation holds when applicable, respiratory physiotherapy and management as usual in the routine practice. Both groups received standard physiotherapy delivered

Table 1 Study subject characteristics

Baseline characteristics		Intervention (n=75)	Control (n=75)	P value
Demographic	Sex male/female (% male)	53/22 (71%)	57/18 (76%)	0.46
	Age (years)	59.9±15.1	62.3±15.4	0.34
	Body mass index (kg/m ²)	29.3±6.3	30.7±8.3	0.24
Pre-admission health and function	Charlson Comorbidity Score	2.8±2.3	3.4±2.4	0.15
	Physical activity (RAPA score)	1 (IQR 1–3)	2 (IQR 1–5)	0.17
	Level of independence (IAPA score)	8 (IQR 7–8)	8 (IQR 7–8)	0.52
Current disease severity	Sepsis on admission (n, %)	19 (25.3%)	18 (24.0%)	0.85
	APACHE II	22.1±5.2	22.2±7.7	0.91
	SOFA score at enrolment	8.8±2.6	8.8±3.2	0.89
Primary reason for admission	Respiratory failure (COPD, pneumonia)	20 (27%)	17 (23%)	0.7
	Isolated TBI	16 (21%)	10 (13%)	0.28
	Multiple trauma with TBI	12 (16%)	9 (12%)	0.64
	Multiple trauma without TBI	2 (3%)	5 (7%)	0.44
	Septic shock (non-respiratory)	8 (11%)	10 (13%)	0.8
	Out-of-hospital cardiac arrest	5 (7%)	6 (8%)	1
	Haemorrhagic stroke (operated)	2 (3%)	6 (8%)	0.28
	Congestive heart failure	2 (3%)	4 (5%)	0.68
	Haemorrhagic shock, non-traumatic	1 (1%)	3 (4%)	0.62
	Meningitis, encephalitis	2 (3%)	2 (3%)	1
	Other diagnoses	5 (7%)	3 (4%)	0.72
	Time from admission to enrolment (hours)*		31.5±19.0	30.8±17.4

CCS³¹; IAPA ranges 0–8 with higher number meaning higher functional independence³²; RAPA score ranges from 1 'I almost never do any physical activities' to 5 'I do 30 min or more per day of moderate physical activity 5 or more days per week'³³.

*Intervention began next calendar day after enrolment.

APACHE, Acute Physiology and Chronic Health Evaluation; CCS, Charlson Comorbidity Score; IAPA, Instrumental Activities Of Daily Living Scale; RAPA, Rapid Assessment of Physical Activity; SOFA, Sequential Organ Failure Assessment; TBI, traumatic brain injury.

two times a day 6 days in a week in a routine way by physiotherapists not involved in the study and adhering to the published safety criteria.³³ Most importantly, a fraction of inspired oxygen less than 0.6 with a percutaneous oxygen saturation more than 90% and a respiratory rate less than 30 breaths/min and normal and stable intracranial pressure (ICP) were required for in-bed and out-of-bed mobilisation. In the control group the therapy was initiated on request of the treating physician and was documented, but not protocolised. It included passive and active range of motion, application of stretch reflex to upper and lower extremities and activation of global motor response according to Vojta reflex locomotion, positioning in bed, sitting, mobility activities progressing from activity in-bed to out-of-bed activities such as up to chair or ambulation, multi-component intervention (eg, combination with respiratory physiotherapy) and education.

Intervention group

The intervention began the calendar day after randomisation and consisted of a progressive mobility programme tailored to patients' condition and supplemented by the use of FESCE (online supplemental table 1). The goal was to deliver a total of 90 min of active exercise a day until ICU discharge or day 28 whichever occurred earlier. Early in the course of the disease the intervention included FESCE (RT300 System, Restorative Therapies 2005-2016. LB100108 V.37).³¹ See online supplemental appendix 1—online supplemental table 1 for details. In brief, after warm-up phase (5 min of passive cycling), patients received therapy consisting of functional electrical stimulation or active cycling with duration adjusted per protocol and patient's

tolerance) followed by relaxation phase (5 min of passive cycling). FES impulses had pulse width 250 μ s, pulse frequency 40 Hz and the lowest output per channel (in a range 0–60 mA) that allowed locomotive movement of lower extremities. Once the patient was more alert and able to participate, they were encouraged to engage in therapy. To increase the intervention workload, both resistance (3–10 Nm) and cycling cadence were increased incrementally. Face-to-face individual therapy was delivered two times a day by a certified physical therapist (MSc) specially trained in FESCE application in ICU.

Measures to ensure protocol implementation

Study physiotherapists (NH, KR) were appointed as 1.8 full working time equivalent specifically for this study and delivered the intervention 7 days/week. Throughout the study, 20 randomly selected exercise sessions were monitored by a hidden observer to ensure reliability and consistency of protocol implementation data reported by physiotherapists. Rehabilitation after discharge from ICU was not altered nor monitored in either group. Data on safety outcomes (ICP elevation, dialysis interruptions) were collected from clinical information system Metavision V.5, iMDsoft, Israel. A multi-step approach was used to minimise number of patients lost to follow-up (see online supplemental appendix 1 for more details).

Outcomes

The primary outcome of this trial was the Physical Component Summary (PCS) score of the SF-36 quality of life questionnaire

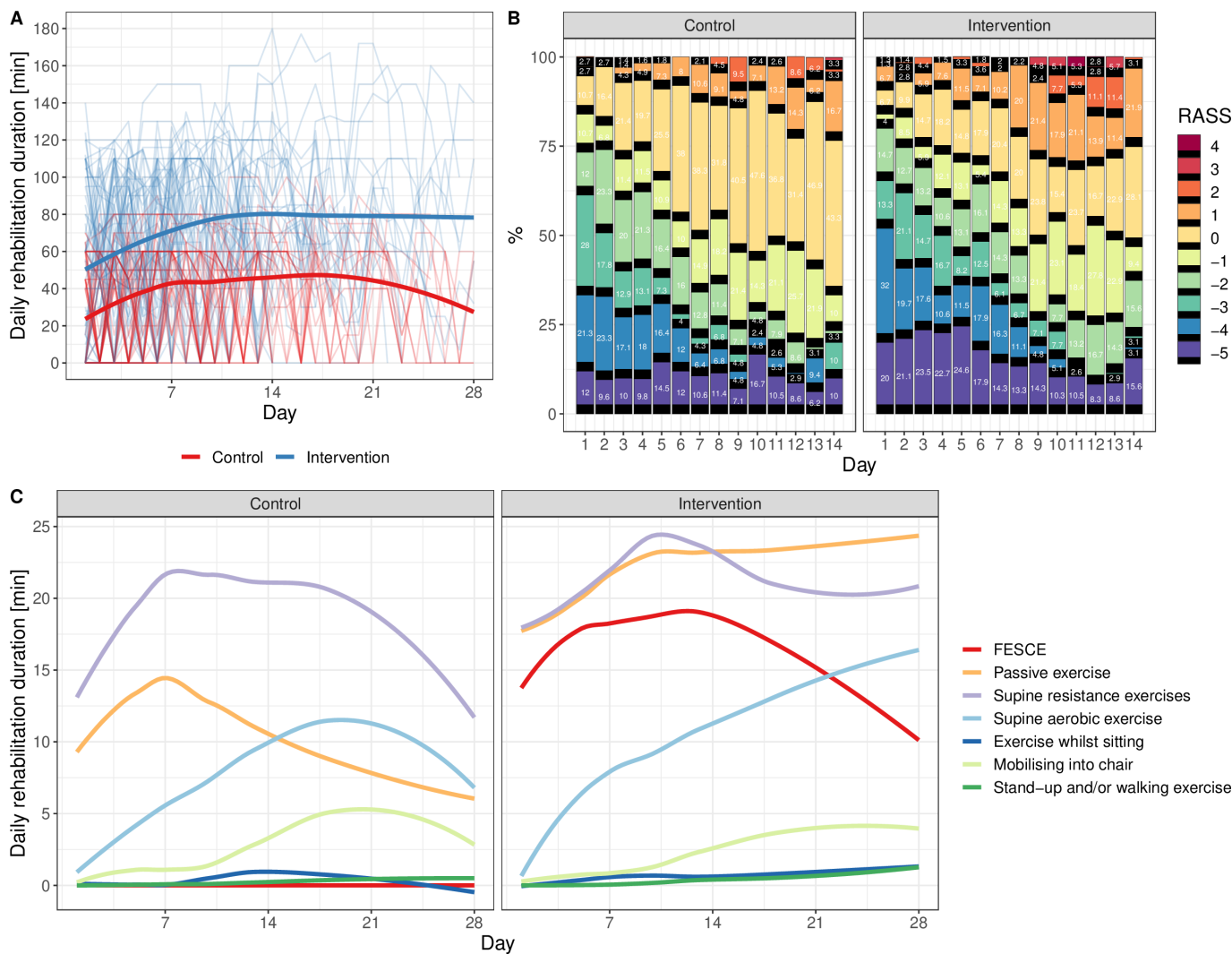


Figure 2 Protocol implementation indices. (A) Average duration of rehabilitation in intervention (blue line) and control (red line) groups in all days of all patients (ie, including days without rehabilitation). Thin lines are individual patients (one outlier received up to 180 min of rehabilitation a day due to protocol violation). (B) Sedation level heatmap. (C) Average types of exercise delivered daily. FESCE, functional electrical stimulation-assisted cycle ergometry; RASS, Richmond Agitation-Sedation Scale, where 0 (alert and calm) or -1 (drowsy) were target levels of sedation management.

measured in ICU survivors at 6 months and calculated as per RAND methodology, V.1.³⁴ Because there was no study in similar population reporting on PCS, we calculated the power of the study based on an important determinant of PCS, which is physical function. Based on the study by Kayambu *et al*,³⁵ where physical function score was 60.0 ± 29.4 points in the control group, 108 patients are required in order to have 80% chance to detect a difference (at $p < 0.05$) a change by 15.8 points or more, which is within the limits determined as clinically important for patients with COPD, asthma and myocardial infarction.³⁶ To compensate for 28% mortality, we aimed to randomise 150 patients. More details on power analysis are in online supplemental appendix 1.

Secondary outcomes were Four-item Physical Fitness in Intensive Care Test (PFIT-s),³⁷ rectus muscle cross-sectional diameter on B-mode ultrasound, mean daily nitrogen balance, muscle power as per the Medical Research Council score, number of ventilator-free days and ICU length of stay, all measured at discharge from ICU or day 28, whichever occurred earlier. Prespecified secondary safety outcomes were the number of episodes of elevated ICP and dialysis interruptions. Detailed

description of secondary outcome assessment is in online supplemental appendix 1.

Randomisation

Eligible patients were randomly assigned (1:1) to receive either standard care or the intervention using offsite independent randomisation protocol embedded in the electronic case report form. Randomisation was stratified according to the presence or absence of sepsis and whether a specific consent was given to be involved in a nested metabolic substudy that included serial muscle biopsies.^{32 38} There were permuted blocks of four in each stratum. Both the study team and clinical personnel were aware of subject treatment allocation. The outcome assessors (JG, BB) were not involved in patient care and remained blinded to treatment allocations.

Statistical methods

The primary outcome and all secondary outcomes were reported as medians (IQR) in an intention-to-treat population and compared between the intervention and standard of care

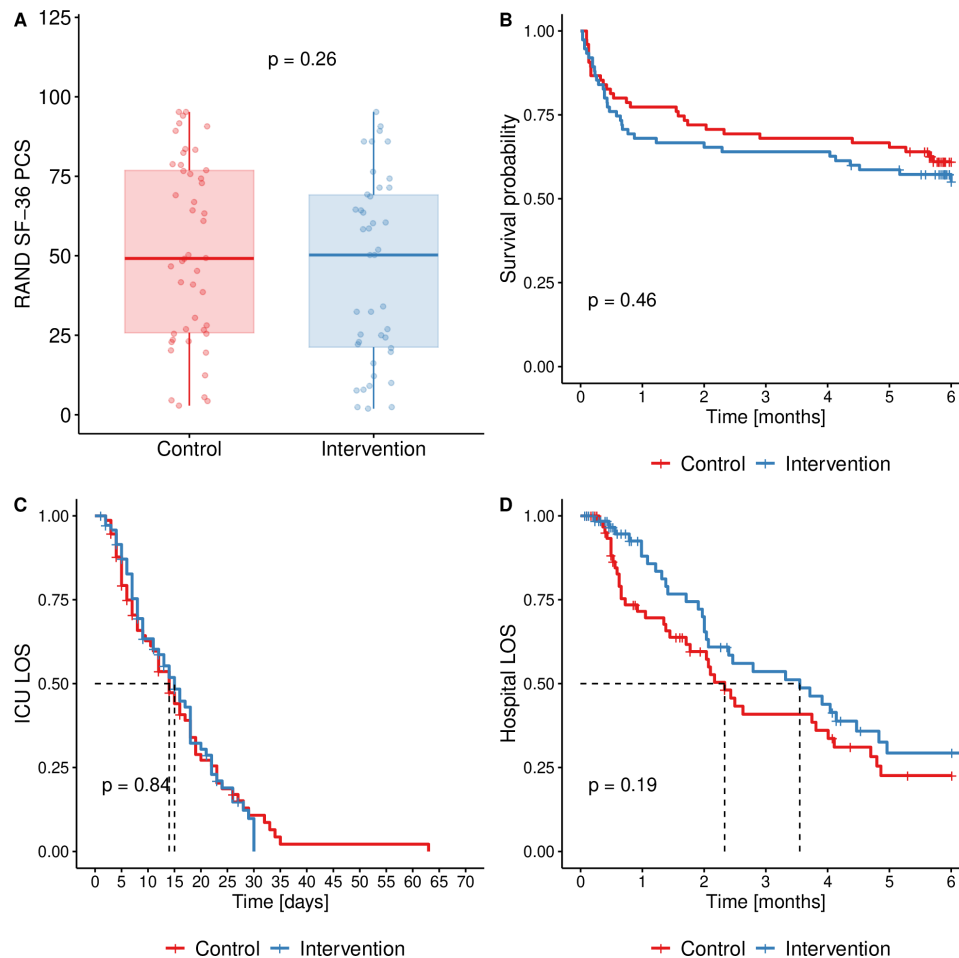


Figure 3 (A) Physical component summary of SF-36 score (primary outcome); (B) Kaplan-Meier curve of survival in the study; (C) Kaplan-Meier curve of patients in the ICU (censored for non-survivors); (D) Kaplan-Meier curve of patients at hospital (censored for non-survivors). P values are from Wilcoxon in (A) and log-rank test in (B), (C) and (D). ICU, intensive care unit; LOS, length of stay; PCS, Physical Component Summary.

groups, with all tests two-sided using the level of significance set at $p < 0.05$. Normality of data distribution was tested by Shapiro-Wilks' test and data are reported as means \pm SD or median (IQR), as appropriate. We used log-rank test for time-to-event analyses, t-test or Wilcoxon test for continuous variables (depending on normality of distribution), and χ^2 for frequency of event comparisons. No imputation of missing data was used. All calculations were performed in R, V.4.0.3 (updated on 10 October 2020) and ggplot2 package was used to create figures.

RESULTS

Between October 2016 and November 2019 (see online supplemental figure 3), 2071 patients were screened in order to enrol the prespecified number of 150 (7.2%) participants into the trial. Participant flow is shown in figure 1 and baseline characteristics of randomised patients in table 1.

Protocol implementation

Patients in intervention and control arms stayed for a median of 12 (IQR 7–21) and 12 (IQR 6–19) days in ICU ($p = 0.76$ log-rank test). Six and eleven patients randomised to intervention and control group, respectively, received no rehabilitation. At least one physiotherapy session was delivered in 817 out of 932 (88%) versus 615 out of 895 (69%) ICU days ($p < 0.001$, χ^2 test) and the first rehabilitation occurred 63 (IQR 45–84) versus 68 (48–95) hours after ICU admission ($p = 0.14$ Wilcoxon) in the

intervention versus control groups, respectively. During the days where rehabilitation was delivered, the median daily duration of it was 82.2 (IQR 65.6–96.6) versus 53.3 (IQR 50.1–57.1) min in the intervention and control group, respectively (median difference 29 min, $p < 0.001$, Wilcoxon test). This included in the intervention group 33 (IQR 22–39) min per treatment day of FESCE (figure 2). Further details on rehabilitation in both groups can be found in online supplemental appendix 1 (online supplemental tables 2A, 2B and 3).

Outcomes

Forty-two (56%) and forty-six (61%) patients were alive and all available to follow-up at 6 months in intervention and control groups, respectively ($p = 0.51$, χ^2 test). This represents 81.5% (88/108) of prespecified sample size. Median physical component score of SF-36 in survivors (primary outcome) was 50 (IQR 21–69) in the intervention group and 49 (IQR 26–77) in controls ($p = 0.261$, Wilcoxon test, see also online supplemental figures 4–6 and Table S5 in online supplemental data file). Patients' in the intervention group had by 0.6 (95% CI 0.2 to 1.0) g/m^2 of body surface area less negative mean daily nitrogen balance ($p = 0.004$, t-test) as compared with control group, in the small subgroup with ICP monitoring in place ($n = 4$ vs 3) more ICP elevations in the interventional (23 elevations/15 ICP days vs 0/15; $p = 0.018$, Wilcoxon test), none of which occur during or immediately after FESCE exercise (see online supplemental

Table 2 Secondary outcomes

Secondary outcomes	Intervention	Standard of care	P value
PFIT-s at ICU discharge	9.4 (8.0 to 10.8) n=37	9.6 (8.3 to 10.9) n=42	0.77*
Rectus muscle diameter at ICU discharge (mean difference from baseline (cm))	-11 (-17 to -6) % n=57	-13 (-19 to -7) % n=54	0.64
MRC score at ICU discharge	42.4 (39.2 to 45.6)	39.4 (36.5 to 42.4)	0.13
Nitrogen balance (gN/m ² /day)	-2.7 (-3.1 to -2.4) n=852 days of 75 patients	-3.4 (-3.7 to -3.0) n (days)=759 days of 75 patients	0.004
Ventilator-free days at D28	9.3 (6.5 to 12.0) n=75	11.0 (8.2 to 13.8) n=75	0.33
Number of untoward dialysis interruptions/days of rehabilitation during dialysis	0/17	0/41	N/A
Numbers of ICP elevations/days with ICP measured	1.5 (0.2 to 2.9) (n=4 patients, 15 ICP days)	0 (n=3 patients, 15 ICP days)	0.018*

Unless stated otherwise, data presented as means (95% CIs) and p values are from t-test.

PFIT-s ranging from 0 to 12 points with lower scores meaning higher degree of disability, see also online supplemental figure 1 and online supplemental table 4 in online supplemental appendix 1.

MRC score ranging from 0 to 60 points with higher scores meaning increasing muscle power.

Bold values indicate statistical significance.

*Wilcoxon test.

ICP, intracranial pressure; ICU, intensive care unit; MRC, Medical Research Council; PFIT-s, Four-item Physical Fitness in Intensive Care Test.

appendix 1). There were no significant differences in any of seven other prespecified secondary outcomes (see [figure 3](#) and [table 2](#)).

Ancillary analyses

Of note, although not a prespecified outcome, in the intervention group there was worse mental component summary score of SF-36 at 6 months 54.8 (IQR 37.1–69.6) versus 70.2 (IQR 51.5–81.3), $p=0.009$, Wilcoxon test (see online supplemental figures 5 and 7 in online supplemental appendix 1). Despite neither number of ICU days on pharmacological treatment for delirium (36% vs 37%, $p=0.86$, χ^2 test) nor doses of sedatives (see online supplemental figure 8 in online supplemental appendix 1) were different, patients in the intervention group spent more time in the ICU either agitated or deeply sedated as seen on the heatmap in online supplemental figure 2B and online supplemental table 10 in online supplemental appendix 1.

DISCUSSION

The main finding of this study is that in mechanically ventilated patients with anticipated long ICU length of stay, progressive mobility programme started very early and containing FESCE did not improve physical disability 6 months after surviving critical illness. The intervention led to 0.6 gN/m²/day improvement in nitrogen balance, which during a median of 11 days equals to sparing of approximately 380 g of lean body mass. This did not translate into measurable preservation into leg muscle mass, muscle power, physical fitness at ICU discharge or shortening of mechanical ventilation or ICU stay.

There are only limited number of other randomised controlled trials looking at long term effects on functional outcomes of a rehabilitation intervention delivered in ICU. Randomised controlled trials investigating in-bed cycling only^{39 40} and most studies on progressive mobility programmes^{7–10 41 42} demonstrated no difference in physical health after 6 months. The lack of effect in these trials could have been caused by problems with protocol implementation⁶ as in the only study reporting on duration of rehabilitation that was delivered,⁷ it was only 24% of prescribed duration (22 min vs 90 min per protocol). Largest

trial so far by Morris *et al*⁹ randomised 300 ICU patients very similar to ours to receive up to three sessions of resistance exercise delivered 7 days/week or a standard rehabilitation. There was no effect on the duration of hospital stay (primary outcome) and physical function was identical at hospital discharge; interestingly, patients in the intervention group improved faster after discharge and reached significantly better physical function scores after 6 months.⁹ Kayambu *et al*³⁵ also demonstrated better physical function at 6 months in ICU patients with sepsis exposed to protocolled rehabilitation, but this study is criticised due to small sample size and 40% loss of follow-up. Therefore, when designing our trial, we put emphasis on achieving protocol implementation and minimising loss of follow-up. Indeed, rigorously monitored delivery of exercise and successful protocol implementation is the main strength of this trial. Intervention group received exercise on 88% ICU days (as compared with 66% in the control group, see also online supplemental figure 9) with median duration per treatment day of 82 min with clear and significant separation of the rehabilitation duration from the control group. Despite successful implementation, we failed to demonstrate short-term or long-term effects, with the exception of the slight improvement of nitrogen economy. Preservation of lean body mass could be clinically meaningful, but in our study, it occurred unaccompanied by any signal of improvement of muscle function and its significance is therefore questionable. Indeed, the difference could have also occurred by chance due to multiple testing.

The lack of effect of the intervention could have been caused by multiple factors. First, median rehabilitation duration in our control group of 53 min per treatment day was far longer than expected and rare among rehabilitation trials.⁴³ Our patients were discharged from ICU in better functional status (higher PFIT-s scores) than in other trials,^{44 45} which could mean that our discharge policy is conservative or reflect the fact that the rehabilitation in the control group was effective and FESCE-based intervention added no further benefit. On the same note, if rehabilitation delivered to the control group was close to the tolerable maximum, the intervention could have overstretched physiological reserves of some patients and offset potential

benefits. In a study on healthy volunteers²⁶ we have found that unloaded FESCE as used in our study can lead to aerobic lactate production and increase whole-body energy to $138\pm 29\%$ and leg blood flow to $160\pm 30\%$ of baseline, analogously to 25 W aerobic exercise. In contrast, physical therapy in the critically ill is known to cause very little increase in energy expenditure only analogous to 6 W exercise.⁴⁶ Second, as shown in figure 2, in the intervention group there were more patients who were either agitated or unresponsive, possibly due to unequal distribution of patients with traumatic brain injury at baseline (37% vs 25%, in the intervention vs control groups, respectively $p=0.11$). Therefore, the increment in the duration of rehabilitation in the interventional group mostly consisted of passive elements of therapy (for details see online supplemental appendix 1) while out of bed mobilisation therapy duration was very similar to control group.

With regards of safety of the intervention, during 1000 FESCE sessions delivered to ICU patients, we have not observed any immediate impairment of cardiorespiratory function nor dialysis malfunction. We aimed to specifically look at safety of FESCE in patients with neurological injuries and allowed the intervention in patients with ICP monitoring in place, provided that ICP was normal and stable and the patient had not been receiving any second-tier therapy. The subgroup of enrolled patients with ICP monitoring in place was small ($n=7$) and we have not observed any immediate effect of FESCE or control rehabilitation on ICP. In line, none of the sessions had to be interrupted due to ICP elevation. Nonetheless, delayed ICP elevations only occurred in the intervention group and after 6 months mental health as well as emotional and social functions were worse in interventional compared with control group. The use of sedatives and antipsychotics was not different between groups offering no explanation for these phenomena. It should be stressed that mental function after 6 months was measured as a part of SF-36 score, but on its own it was not a prespecified secondary outcome and the difference may have occurred by chance. Nonetheless, we cannot rule out that the use of FESCE itself was responsible for the impairment of central nervous system function, as progressive mobility programme alone was safe in neuro patients⁴⁷ or led to improvement of mental functions in unselected ICU patients.³⁹ In the most recent multicentre RCT of Berney *et al*³⁴ randomised 162 patients with sepsis or systemic inflammation to receive 60 min/day of FESCE in addition to usual rehabilitation or usual rehabilitation alone (median of 15 min of active exercise per day). FESCE was delivered for a median of 53 min per day for a median of 5 days in the intervention group, there was no difference in muscle strength at hospital discharge and no major adverse events. Patients with neurological injuries at baseline had been excluded from Berney *et al*'s study. Although underpowered, this trial also did not demonstrate any influence of the intervention on the incidence of cognitive impairment at 6 months, in keeping with our results.

Indeed, although our study adds important knowledge to the field, its limitations are to be recognised, too. Due to higher-than-expected mortality (in fact, 41% of enrolled patients were not alive after 6 months) the study only achieved 81.5% of the prespecified sample size evaluated for primary outcome (88 out of 108) and it is therefore underpowered. In addition, our sample size was based on surrogate physical function in the control group of 16 patients in the study of Kayambu.³⁵ Based on data in our study ($PCS=51.7\pm 28.8$ in the control group), 133 patients would be needed to demonstrate 15 points difference in PCS at $\alpha=0.8$ and $p<0.05$. The generalisability of our results is limited by single-centre design and relatively very intensive exercise in the control group. It is possible and likely

that in different clinical environment with less intense rehabilitation in the control group, results would be different. In addition, we have not controlled nor monitored patient recovery pathway between ICU discharge and collection of the primary outcome.

Future outcome-based trials should certainly put emphasis on delivering progressive mobility element in the interventional group, enrol more homogeneous and specific patients' populations.³⁷ So far, the safety of FESCE-based is uncertain in patients with neurological injuries and needs investigation. There is also a burning need for studies focused on understanding physiology of FES-triggered contraction of healthy muscle versus muscle altered by underlying critical illness.³ In the meantime, protocolised physical therapy delivered by appropriately trained personnel remains the only evidence-based intervention to shorten duration of ICU stay and possibly improve long-term outcomes.

In conclusion, early FESCE-based protocolised physiotherapy delivered to mechanically ventilated patients does not change PCS score 6 months after discharge, nor duration of mechanical ventilation or any parameters of skeletal muscle mass, power and function at ICU discharge, apart from borderline improvement of nitrogen balance. These results must be interpreted in the context of very high dose and early start of rehabilitation in the control group, and relatively good physical functional status achieved by patients in the control group compared with other studies of long-stay ICU patients.

Twitter František Duška @FrantaDuska

Acknowledgements We thank the team of physiotherapists and research nurses, namely Marie Hejnová, Irena Kozáková, Jana Kukulová, Šárka Gregorová, Šárka Vosalová and Kateřina Topková. The study was funded exclusively from Agentura pro zdravotnický výzkum (grant agency of Czech Ministry of Health) AZV number 16-28663A.

Contributors PW and FD are the authors of the main idea and overlooked the conduct of the study. PW, KJ and MF were responsible for consenting and recruiting patients and performing clinical procedures. PW is data analyst and biostatistician. NH and KR are the study physiotherapists. JG and BB were blinded outcome assessors. All authors have access to record-level data and have seen and approved the final version of the manuscript.

Funding Grant Agency for Research in Healthcare AZV 16-28663A, email info@azvcr.cz ISDS: f7eike4, Phone: +420 271 019 257 For updated contact details, see <http://www.azvcr.cz/kontakt>.

Competing interests None declared.

Patient consent for publication Not required.

Ethics approval The trial design is in accordance with Declaration of Helsinki and the protocol, care report form and informed consent formularies were reviewed and approved by FNKV University Hospital Research Ethics Board ('Ethical Committee') on 24 June 2015 (decision number EK-VP-27-0-2015). All patients or their legal representatives gave their prospective written informed consent to participate in the study.

Provenance and peer review Not commissioned; externally peer reviewed.

Data availability statement All data relevant to the study are included in the article or uploaded as supplementary information. We will sent de-identified patient-level data upon reasonable request to the corresponding author.

Author note FD, KAR FNKV, Charles University, Fac Med 3, Srobarova 50, 10034 Prague, Czech Republic. Phone: +420267162451, Email: frantisek.duska@lf3.cuni.cz.

Open access This is an open access article distributed in accordance with the Creative Commons Attribution Non Commercial (CC BY-NC 4.0) license, which permits others to distribute, remix, adapt, build upon this work non-commercially, and license their derivative works on different terms, provided the original work is properly cited, appropriate credit is given, any changes made indicated, and the use is non-commercial. See: <http://creativecommons.org/licenses/by-nc/4.0/>.

ORCID iDs

Barbora Blahutova <http://orcid.org/0000-0003-1617-0656>
František Duška <http://orcid.org/0000-0003-1559-4078>

REFERENCES

- 1 Herridge MS, Tansey CM, Matté A, *et al.* Functional disability 5 years after acute respiratory distress syndrome. *N Engl J Med* 2011;364:1293–304.
- 2 Herridge MS, Moss M, Hough CL, *et al.* Recovery and outcomes after the acute respiratory distress syndrome (ARDS) in patients and their family caregivers. *Intensive Care Med* 2016;42:725–38.
- 3 Herridge MS, Mobile HMS. Mobile, awake and critically ill. *CMAJ* 2008;178:725–6.
- 4 Needham DM. Mobilizing patients in the intensive care unit: improving neuromuscular weakness and physical function. *JAMA* 2008;300:1685–90.
- 5 Kress JP, Hall JB. ICU-acquired weakness and recovery from critical illness. *N Engl J Med* 2014;370:1626–35.
- 6 Waldauf P, Jiroutková A, Krajčová A, *et al.* Effects of rehabilitation interventions on clinical outcomes in critically ill patients: systematic review and meta-analysis of randomized controlled trials. *Crit Care Med* 2020;48:1055–65.
- 7 Wright SE, Thomas K, Watson G, *et al.* Intensive versus standard physical rehabilitation therapy in the critically ill (EPICC): a multicentre, parallel-group, randomised controlled trial. *Thorax* 2018;73:213–21.
- 8 Hodgson CL, Bailey M, Bellomo R, *et al.* A binational multicenter pilot feasibility randomized controlled trial of early goal-directed mobilization in the ICU. *Crit Care Med* 2016;44:1145–52.
- 9 Morris PE, Berry MJ, Files DC, *et al.* Standardized rehabilitation and hospital length of stay among patients with acute respiratory failure: a randomized clinical trial. *JAMA* 2016;315:2694.
- 10 Moss M, Nordon-Craft A, Malone D, *et al.* A randomized trial of an intensive physical therapy program for patients with acute respiratory failure. *Am J Respir Crit Care Med* 2016;193:1101–10.
- 11 Bailey P, Thomsen GE, Spuhler VJ, *et al.* Early activity is feasible and safe in respiratory failure patients. *Crit Care Med* 2007;35:139–45.
- 12 Schweickert WD, Pohlman MC, Pohlman AS, *et al.* Early physical and occupational therapy in mechanically ventilated, critically ill patients: a randomised controlled trial. *Lancet* 2009;373:1874–82.
- 13 Levine S, Nguyen T, Taylor N, *et al.* Rapid disuse atrophy of diaphragm fibers in mechanically ventilated humans. *N Engl J Med* 2008;358:1327–35.
- 14 Hermans G, De Jonghe B, Bruyninckx F, *et al.* Clinical review: critical illness polyneuropathy and myopathy. *Crit Care* 2008;12:238.
- 15 Puthuchery ZA, Rawal J, McPhail M, *et al.* Acute skeletal muscle wasting in critical illness. *JAMA* 2013;310:1591–600.
- 16 Topp R, Ditmyer M, King K, *et al.* The effect of bed rest and potential of prehabilitation on patients in the intensive care unit. *AACN Clin Issues* 2002;13:263–76.
- 17 Zanotti E, Felicetti G, Maini M, *et al.* Peripheral muscle strength training in bed-bound patients with COPD receiving mechanical ventilation: effect of electrical stimulation. *Chest* 2003;124:292–6.
- 18 Gerovasili V, Stefanidis K, Vitzilaios K, *et al.* Electrical muscle stimulation preserves the muscle mass of critically ill patients: a randomized study. *Crit Care* 2009;13:R161.
- 19 Routsis C, Gerovasili V, Vasileiadis I, *et al.* Electrical muscle stimulation prevents critical illness polyneuropathy: a randomized parallel intervention trial. *Crit Care* 2010;14:R74.
- 20 Abu-Khabeir HA, Abouelela AMZ, Abdelkarim EM. Effect of electrical muscle stimulation on prevention of ICU acquired muscle weakness and facilitating weaning from mechanical ventilation. *Alexandria J Med* 2013;49:309–15.
- 21 Kho ME, Truong AD, Zanni JM, *et al.* Neuromuscular electrical stimulation in mechanically ventilated patients: a randomized, sham-controlled pilot trial with blinded outcome assessment. *J Crit Care* 2015;30:32–9.
- 22 Goll M, Wollersheim T, Haas K, *et al.* Randomised controlled trial using daily electrical muscle stimulation (EMS) in critically ill patients to prevent intensive care unit (ICU) acquired weakness (ICUAW). *Intensive Care Med Exp* 2015;3:1–2.
- 23 Fischer A, Spiegl M, Altmann K, *et al.* Muscle mass, strength and functional outcomes in critically ill patients after cardiothoracic surgery: does neuromuscular electrical stimulation help? the Catastim 2 randomized controlled trial. *Crit Care* 2016;20:1–13.
- 24 Fontes Cerqueira TC, Cerqueira Neto MLde, Cacao LdeAP, *et al.* Ambulation capacity and functional outcome in patients undergoing neuromuscular electrical stimulation after cardiac valve surgery: a randomised clinical trial. *Medicine* 2018;97:e13012.
- 25 Koçan Kurtoglu D, Tastekin N, Birtane M, *et al.* Effectiveness of neuromuscular electrical stimulation on auxiliary respiratory muscles in patients with chronic obstructive pulmonary disease treated in the intensive care unit. *Turk J Phys Med Rehab* 2015;61:12–17.
- 26 Gojda J, Waldauf P, Hrušková N, *et al.* Lactate production without hypoxia in skeletal muscle during electrical cycling: crossover study of femoral venous-arterial differences in healthy volunteers. *PLoS One* 2019;14:e0200228.
- 27 Doucet BM, Lam A, Griffin L. Neuromuscular electrical stimulation for skeletal muscle function. *Yale J Biol Med* 2012;85:201–15.
- 28 Bauman WA, Spungen AM, Adkins RH, *et al.* Metabolic and endocrine changes in persons aging with spinal cord injury. *Assist Technol* 1999;11:88–96.
- 29 Kjaer M, Pollack SF, Mohr T, *et al.* Regulation of glucose turnover and hormonal responses during electrical cycling in tetraplegic humans. *Am J Physiol* 1996;271:R191–9.
- 30 Gorgey AS, Dolbow DR, Dolbow JD, *et al.* The effects of electrical stimulation on body composition and metabolic profile after spinal cord injury—Part II. *J Spinal Cord Med* 2015;38:23–37.
- 31 Parry SM, Berney S, Warrillow S, *et al.* Functional electrical stimulation with cycling in the critically ill: a pilot case-matched control study. *J Crit Care* 2014;29:695.e1–695.e7.
- 32 Waldauf P, Gojda J, Urban T, *et al.* Functional electrical stimulation-assisted cycle ergometry in the critically ill: protocol for a randomized controlled trial. *Trials* 2019;20:724.
- 33 Sommers J, Engelbert RHH, Dettling-Ihnenfeldt D, *et al.* Physiotherapy in the intensive care unit: an evidence-based, expert driven, practical statement and rehabilitation recommendations. *Clin Rehabil* 2015;29:1051–63.
- 34 Berney S, Hopkins RO, Rose JW, *et al.* Functional electrical stimulation in-bed cycle ergometry in mechanically ventilated patients: a multicentre randomised controlled trial. *Thorax* 2020. doi:10.1136/thoraxjnl-2020-215093. [Epub ahead of print: 15 Dec 2020].
- 35 Kayambu G, Boots R, Paratz J. Early physical rehabilitation in intensive care patients with sepsis syndromes: a pilot randomised controlled trial. *Intensive Care Med* 2015;41:865–74.
- 36 Wyrwich KW, Tierney WM, Babu AN, *et al.* A comparison of clinically important differences in health-related quality of life for patients with chronic lung disease, asthma, or heart disease. *Health Serv Res* 2005;40:577–92.
- 37 Denehy L, de Morton NA, Skinner EH, *et al.* A physical function test for use in the intensive care unit: validity, responsiveness, and predictive utility of the physical function ICU test (scored). *Phys Ther* 2013;93:1636–45.
- 38 Ziak J, Krajcova A, Jiroutkova K, *et al.* Assessing the function of mitochondria in cytosolic context in human skeletal muscle: adopting high-resolution respirometry to homogenate of needle biopsy tissue samples. *Mitochondrion* 2015;21:106–12.
- 39 Fossat G, Baudin F, Courtes L, *et al.* Effect of in-bed leg cycling and electrical stimulation of the quadriceps on global muscle strength in critically ill adults: a randomized clinical trial. *JAMA* 2018;320:368–78.
- 40 Eggmann S, Verra ML, Luder G. Physiological effects and safety of an early, combined endurance and resistance training in mechanically ventilated, critically ill patients. *PLoS One* 2018;101:e344–5.
- 41 Amundadóttir OR, Jónasdóttir RJ, Sigvaldason K. Effects of intensive upright mobilisation on outcomes of mechanically ventilated patients in the intensive care unit: a randomised controlled trial with 12-months follow-up. *Eur J Physiother* 2019;0:1–11.
- 42 Denehy L, Skinner EH, Edbrooke L, *et al.* Exercise rehabilitation for patients with critical illness: a randomized controlled trial with 12 months of follow-up. *Crit Care* 2013;17:R156.
- 43 Dall'Acqua AM, Sachetti A, Santos LJ, *et al.* Use of neuromuscular electrical stimulation to preserve the thickness of abdominal and chest muscles of critically ill patients: a randomized clinical trial. *J Rehabil Med* 2017;49:40–8.
- 44 Nordon-Craft A, Schenkman M, Edbrooke L, *et al.* The physical function intensive care test: implementation in survivors of critical illness. *Phys Ther* 2014;94:1499–507.
- 45 Parry SM, Denehy L, Beach LJ, *et al.* Functional outcomes in ICU – what should we be using? – an observational study. *Crit Care* 2015;19:127.
- 46 Hickmann CE, Roeseler J, Castanares-Zapatero D, *et al.* Energy expenditure in the critically ill performing early physical therapy. *Intensive Care Med* 2014;40:548–55.
- 47 Bahouth MN, Power MC, Zink EK, *et al.* Safety and feasibility of a neuroscience critical care program to mobilize patients with primary intracerebral hemorrhage. *Arch Phys Med Rehabil* 2018;99:1220–5.

Příloha 7

Krajčová A, Skagen C, Džupa V, **Urban T**, Rustan AC, Jiroutková K, Bakalář B, Thoresen GH, Duška F.

Can functional electrical stimulation-assisted cycle ergometry replace insulin infusion in patients? A nested substudy in a randomized controlled trial with 6 months' follow-up.

JPEN J Parenter Enteral Nutr. 2022 Jan;46(1):249-253. doi: 10.1002/jpen.2213. Epub 2021 Jul 29. PMID: 34165818. IF 3.896

BRIEF COMMUNICATION

Can functional electrical stimulation–assisted cycle ergometry replace insulin infusion in patients? A nested substudy in a randomized controlled trial with 6 months' follow-up

Petr Waldauf MD¹ | Tomáš Urban MSc¹ | Adéla Krajčová MD, PhD¹ |
 Kateřina Jiroutková MD, PhD¹ | Barbora Blahutová MD¹  | Bob Bakalář MD¹ |
 Kamila Řasová PhD²  | Marcela Grünerová-Lippertová MD, PhD² | Jan Gojda MD, PhD³
 | František Duška MD, PhD¹ 

¹ Department of Anaesthesia and Intensive Care Medicine, Charles University, The Third Faculty of Medicine and FNKV University Hospital, Prague, Czech Republic

² Department of Rehabilitation, Charles University, The Third Faculty of Medicine and FNKV University Hospital, Prague, Czech Republic

³ Department of Medicine, Charles University, The Third Faculty of Medicine and FNKV University Hospital, Prague, Czech Republic

Correspondence

František Duška, Department of Anaesthesia and Intensive Care Medicine, Srobarova 50, 10034 Prague, Czech Republic.
 Email: frantisek.duska@lf3.cuni.cz

Petr Waldauf and Tomáš Urban contributed equally to this work and are joint first authors.

Abstract

Background: Functional electrical stimulation–assisted cycle ergometry (FESCE) can deliver active exercise to critically ill patients, including those who are sedated. Aerobic exercise is known to stimulate skeletal muscle glucose uptake. We asked whether FESCE can reduce intravenous insulin requirements and improve insulin sensitivity in intensive care unit (ICU) patients.

Method: We performed an a priori–planned secondary analysis of data from an outcome-based randomized controlled trial (NCT 02864745) of FESCE-based early-mobility program vs standard of care in mechanically ventilated patients. We analyzed glucose profile, glucose intake, and insulin requirements during ICU stay in all enrolled patients. In a nested subgroup, we performed hyperinsulinemic (120 mIU/min/m²) euglycemic clamps at days 0, 7, and 180 (n = 30, 23, and 11, respectively).

Results: We randomized 150 patients 1:1 to receive intervention or standard of care. Seventeen (23%) patients in each study arm had a history of diabetes. During ICU stay, patients received 137 ± 65 and 137 ± 88 g/day carbohydrate (P = .97), and 31 vs 35 (P = .62) of them required insulin infusion to maintain blood glucose 8.61 ± 2.82 vs 8.73 ± 2.67 mM (P = .75, n = 11,254). In those treated with insulin, median daily dose was 53 IU (interquartile range [IQR], 25–95) vs 62 IU (IQR, 26–96) in the intervention and control arm, respectively (P = .44). In the subgroup of patients undergoing hyperglycemic clamps, insulin sensitivities improved similarly and significantly from acute and protracted critical illness to 6 months after discharge.

Conclusion: The FESCE-based early-mobility program does not significantly reduce insulin requirements in critically ill patients on mechanical ventilation.

KEYWORDS

critically ill, glucose control, hyperinsulinemic clamp, insulin resistance

CLINICAL RELEVANCY STATEMENT

Treatment of hyperglycemia in critical illness with continuous intravenous insulin infusion is not without risks. In this paper, we show how the delivery of an early-mobility program, which includes electrical exercise, influences insulin sensitivity and glucose control in enterally fed general intensive care unit (ICU) patients. In addition, this study is the first one to show the natural evolution of critical illness-induced insulin resistance measured by serial hyperinsulinemic clamps in the ICU and 6 months afterward.

INTRODUCTION

Insulin resistance is a well-recognized phenomenon in critically ill patients.¹ Acute injury, inflammation, and catecholamine surge induce a catabolic response in which glycogen, fat, and protein are degraded to provide substrates for immune cells and wound healing. Bed rest, insulin-counteracting drugs such as steroids or vasopressors, and carbohydrate delivery in the form of artificial nutrition may further exacerbate hyperglycemia, which has repeatedly been associated with intensive care unit (ICU) morbidity and mortality, even after adjustments to disease severity.² Insulin infusion is effective in controlling blood glucose levels, but it may increase the risk of hypoglycemia and mortality.^{3,4} In healthy individuals, skeletal muscle is the main organ responsible for insulin-mediated glucose disposal, and even a short bout of aerobic exercise increases glucose uptake up to fivefold.⁵ Animal studies suggest that mechano-signaling pathways exist in skeletal muscle and can circumvent molecular pathways affected by insulin resistance.⁶ Technology advances, such as functional electrical stimulation-assisted cycle ergometry (FESCE), allow the delivery of active exercise even before the patient regains consciousness,^{7,8} and it is tempting to hypothesize that compared with standard of care, an FESCE-based early-mobility program delivered to mechanically ventilated patients would reduce intravenous insulin requirements and increase insulin-mediated glucose disposal during hyperinsulinemic clamp. In this study, we also aimed to investigate the dynamics of insulin sensitivity during and 6 months after critical illness.

MATERIALS AND METHODS

We performed an a priori planned secondary analysis of an outcome-based, prospective, randomized controlled trial, Electric Mobility and Insulin Resistance (EMIR; ClinicalTrials.gov, NCT02864745), performed in the ICU of FNKV University Hospital in Prague, Czech Republic. Clinical outcomes are reported elsewhere [Waldau, Thorax 2021], the full protocol of the study has been published,⁷ and details can also be found in the supplementary materials.

In brief, mechanically ventilated adult critically ill patients who were expected to need a protracted (>7 days) ICU stay were recruited within 72 h of hospital admission. Exclusion criteria include bedrid-

den, premonitory status and contraindications to FESCE, such as limb fractures or pacemaker. The standard care arm underwent standard rehabilitation delivered by personnel not involved in the study. In the intervention arm, the rehabilitation followed a protocol according to the patient's condition and degree of cooperation, with a dedicated full-time study physiotherapist aiming to deliver 90 min of exercise a day, 7 days a week. Before patients regained the ability to engage in the mobilization program, they received two sessions of FESCE (RT-300; Restorative Therapies, Baltimore, MD, USA) per day. This technique involved synchronized transcutaneous electrical stimulations of the gluteal, hamstrings, and quadriceps muscles on both legs to produce a coordinated pattern of movements on a supine bicycle. The exercise intervention continued until day 28 or ICU discharge, whichever occurred earlier. All other aspects of intensive care (including nutrition and insulin treatment) were driven by the clinical team, who were not directly involved in the study but for whom patients' treatment allocations were not anonymized. Nutrition was delivered preferably enterally (Supportan; Fresenius Kabi, Bad Homburg, Germany) as tolerated, with the aim to deliver 1.5 g/kg/day protein. Insulin was started when blood glucose level reached 11 mM, and the sliding-scale insulin infusion rate was then adjusted by a bedside nurse, aiming for blood glucose levels of 6–8 mM. Arterial blood glucose levels were checked in all patients at 5 AM, 5 PM, and 10 PM by blood gas analyzer ABL-90 (Radiometer, Denmark) and ad hoc as per bedside nurse discretion by a portable glucometer. Patients' vital functions; all laboratory data, including blood glucose levels; and data from syringe drivers are automatically and in real time uploaded into the clinical information system (MetaVision, version 5; IMD-Soft, Israel). We have extracted data on blood glucose levels, glucose intake, and insulin dose from these (see the supplementary materials and Figure S1 for details).

Metabolic studies

In a subgroup of patients whose representatives specifically consented to it (see the flowchart in Figure S1), we performed hyperglycemic euglycemic clamps at fasting state in the morning of day 1 (baseline). These studies were repeated in the ICU after 7 days ($n = 23$) and in outpatients after 180 days (range, 171–186; $n = 11$). At baseline, an arterial blood sample for measurement of fasting blood glucose, insulin, and C-peptide was taken. After a 10-min priming infusion at a double rate, insulin infusion (1 unit/ml in 0.9% saline) was held constant at 120 mIU/min/m² body surface area (BSA) for 110 consecutive minutes. Blood glucose concentration was determined every 5 min using StatStrip (Nova Biomedical, Waltham, MA, USA). Blood glucose concentration was clamped at ~5 mmol/L by an infusion of variable amounts of glucose. The total body glucose disposal rate (M-value) was calculated from the final 30 min (steady state) and was used as a measure of insulin sensitivity after adjustment to body weight. Insulin clamps at follow-up visit (day 180) were performed similarly, with two intravenous cannulas—one in an antecubital vein for the infusion of insulin and glucose and the other retrograde into a

TABLE 1 Baseline study participant characteristics

Characteristics	All patients (n = 150)	Subgroups				P-value
		Intervention group (n = 75)		Control group (n = 75)		
		Consent to clamp: Yes (n = 16)	Consent to clamp: No (n = 59)	Consent to clamp: Yes (n = 15)	Consent to clamp: No (n = 60)	
Age, mean \pm SD	61.1 \pm 15.2	58 \pm 17	61 \pm 15	64 \pm 11	62 \pm 16	.665
Sex, M/F	110/40	12/4	41/18	10/5	47/13	.663
BMI	30.1 \pm 7.4	29.2 \pm 5.9	29.4 \pm 6.5	33.3 \pm 8.1	29.9 \pm 8.1	.428
APACHE II, mean \pm SD	22 \pm 6	22 \pm 5	23 \pm 5	27 \pm 7	22 \pm 7	.045
Days from ICU admission to recruitment	1.2 (IQR, 0.8–1.8)	1.4 \pm 0.8	1.3 \pm 0.8	1.4 \pm 0.7	1.2 \pm 0.8	.895
History of diabetes, n (%)	34 (23%)	6 (38%)	11 (19%)	7 (47%)	10 (17%)	.003
Preadmission Charlson comorbidity score, median (IQR)	3 (IQR, 1–4)	2.9 \pm 2.0	2.7 \pm 2.4	3.7 \pm 2.8	3.2 \pm 2.2	.405
RAPA score, median (IQR)	1 (IQR, 1–4)	2.7 \pm 2.3	2.4 \pm 2.0	2.9 \pm 2.3	3.0 \pm 2.4	.556
Diagnostic category, trauma/surgical/medical	51/19/81	8/3/5	20/3/36	4/1/10	19/12/29	.087
Sepsis or septic shock on admission, yes/no (%yes)	37 (25%)	5(31%)	14 (24%)	5(33%)	13 (22%)	.742

Abbreviations: APACHE, Acute Physiology and Chronic Health Evaluation; BMI, body mass index; F, female; ICU, intensive care unit; IQR, interquartile range; M, male; RAPA, Rapid Assessment of Physical Activity.

dorsal hand vein for sampling of arterialized blood using the heated-hand technique.

Calculations and statistics

Differences between groups were tested using two-sided Welch *t*-test, Wilcoxon rank sum test, or linear mixed-effect model with random intercept, when appropriate, and *P* < .05 is considered significant. All calculations were performed in R and R Markdown, version 4.0.3.

RESULTS

We enrolled 150 patients into the trial, out of which 31 consented to undergo serial insulin clamps. Baseline characteristics of enrolled participants are given in Table 1.

Patients in intervention and control arms stayed for a median of 12 (interquartile range [IQR], 7–21) and 12 (IQR, 6–19) days in the ICU (*P* = .76 log-rank test) and received 137 \pm 65 and 137 \pm 88 g/day carbohydrate (*P* = .97) and 80 \pm 24 vs 50 \pm 10 min (*P* < 0.001) of rehabilitation a day. In total, there were 5659 and 5595 blood glucose measurements in the study. There was no difference in blood glucose control between groups, as average blood glucose was 8.61 \pm 2.82 vs 8.73 \pm 2.67 (*P* = .75) in the intervention vs control groups, respectively. There were 11 (0.2%) and 16 (0.3%) blood glucose values below 3.4 mM in intervention and control arms, respectively (odds ratio of hypoglycemia, 0.7; 95% CI, 0.3–1.6; *P* = .44). To control blood glucose, 31 (41%) and 35 (47%) patients needed insulin infusion during their ICU

stay (odds ratio of needing insulin in intervention arm, 0.81; 95% CI, 0.4–1.6; *P* = .62). The median daily dose in those who received insulin was 53 IU (IQR, 25–95) and 62 IU (26–96) of insulin in intervention and control arms, respectively (*P* = .44). Mean daily dose of insulin in all patients, adjusted to actual body weight, was 0.25 \pm 0.35 and 0.27 \pm 0.27 IU/kg/day (*n* = 150, *P* = .67), whereas mean adjusted dose in patients receiving insulin was 0.60 \pm 0.28 vs 0.58 \pm 0.34 IU/kg/day (*n* = 66, *P* = .83).

Insulin-mediated glucose disposal

As shown in Figure 1, insulin-mediated glucose disposal during hyperinsulinemic clamp improved significantly in both groups throughout the course of critical illness and continued during the recovery phase to reach levels measured for healthy individuals.⁹ To rule out the effect of nonsurvivors, we have also separately analyzed only patients who survived ICU until day 7, and the improvement of insulin sensitivity remained significant (see Table S2). There were no significant differences between intervention and control groups.

DISCUSSION

There are two main findings of this study. First, the early-mobility program does not significantly improve glucose control or reduce insulin requirements in critically ill patients. This is despite the exercise intervention having been successfully delivered, and there is a clear and significant separation of rehabilitation duration between treatment

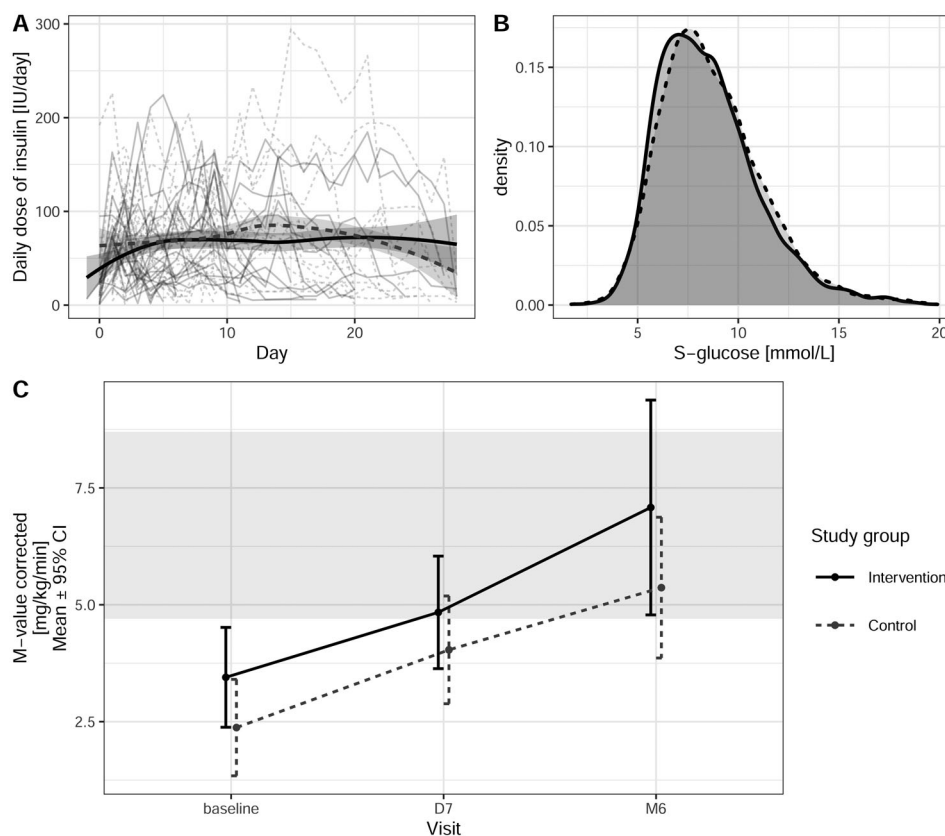


FIGURE 1 (A) Mean insulin doses (IU/day) in all patients, with 95% CIs. (B) Density diagram of blood glucose levels. (C) Prediction of difference in study groups of M-value corrected over different time visits. M-value is expressed as glucose infusion rate space corrected (mg/kg/min). The gray-shaded zone represents the published⁹ reference range in an age-matched population

groups, which mostly consists of 29 min/day of FESCE. There are a few possible explanations of these results, which contrast with those of previous studies showing that early mobilization could decrease insulin requirements in ICU patients.¹⁰ In healthy volunteers, unloaded FESCE increased energy expenditure similarly to 25-W aerobic exercise,⁹ but across-leg metabolic characteristics differ from volitional cycling; it is possible that FESCE also fails to activate mechano-signaling pathways⁶ that would activate glucose uptake. In addition, it seems from glucose profiles that the glucose control strategy was quite liberal compared with that in Patel's study.¹⁰ This, together with the fact that 23% of our cohort had preexisting diabetes, resulted in relatively high insulin requirements in those who needed insulin treatment (~ 0.6 IU/kg/day), whereas in Patel's study,¹⁰ the effect of early mobilization was seen in only the low-insulin subgroup (<0.15 IU/kg/day). In fact, we have seen a trend to a reduction of the proportion of patients needing insulin infusion in the intervention arm, and it should be emphasized that with 150 participants and 47% insulin treatment in the control group, our study was only powered to detect (at $\alpha = .05$ and $\beta = .2$) a reduction of the need for insulin treatment below 24% (or <18 of 75 patients) in the intervention group. Last, the dose of exercise in the control group (50 min/day) in our study was unusually and unexpectedly high, possibly owing to the Hawthorne effect.¹¹

The second important and innovative finding of this study is that we—to our knowledge, for the very first time—assessed by serial euglycemic hyperinsulinemic clamps the evolution of insulin sensitivity in acute and protracted critical illness and then 6 months afterward. We have seen clear and significant increases of insulin-mediated insulin sensitivity over time that were not significantly affected by treatment-group allocation. After 6 months, high-dose insulin-mediated glucose disposal was significantly better than during protracted critical illness and reached values comparable to those in patients with type 2 diabetes¹² or cancer¹³ but remained lower than those in lean, healthy individuals of similar age in some¹⁴ but not all⁹ studies. It should be emphasized that although most baseline characteristics of patients consenting to insulin clamps were not different from those in the overall study population, there seems to be a selection bias toward patients with diabetes.

In conclusion, insulin sensitivity increases during the transition from the acute to the chronic phase of critical illness and further improves after 6 months. An early-mobility program based on functional electrical stimulation-assisted supine cycle ergometry does not significantly influence glucose control or insulin requirements in mechanically ventilated, critically ill patients.

ACKNOWLEDGMENTS

The authors thank Dr Jana Kukulová, RN for monitoring the database, the team of research nurses—namely, Irena Kozáková, RN; Šárka Gregorová, RN; Šárka Marešová, RN; Kateřina Ťopková, RN; and Jana Potočková, RN—for their excellent work and assistance, and all the study participants and their families. This project was funded solely and exclusively from grant AZV 16–28663A of Czech Ministry of Health Grant Agency (Agentura pro zdravotnický výzkum).

CONFLICT OF INTEREST

None declared.

FUNDING INFORMATION

This project was funded solely and exclusively from grant AZV 16–28663A of Czech Ministry of Health Grant Agency (Agentura pro zdravotnický výzkum).

AUTHOR CONTRIBUTIONS

Petr Waldauf and Tomáš Urban equally contributed to the conception and design of the research; František Duška, Jan Gojda, and Marcela Grünerová-Lippertová contributed to the design of the research; Petr Waldauf, Bob Bakalář, Barbora Blahutová, and Kateřina Jiroutková contributed to the acquisition and analysis of the data; all authors contributed to the interpretation of the data; and František Duška drafted the manuscript. All authors critically revised the manuscript, agree to be fully accountable for ensuring the integrity and accuracy of the work, and read and approved the final manuscript.

ORCID

Barbora Blahutová MD  <https://orcid.org/0000-0003-1617-0656>

Kamila Řasová PhD  <https://orcid.org/0000-0002-3201-1770>

František Duška MD, PhD  <https://orcid.org/0000-0003-1559-4078>

REFERENCES

1. Little RA, Henderson A, Frayn KN, Galasko CS, White RH. The disposal of intravenous glucose studied using glucose and insulin clamp techniques in sepsis and trauma in man. *Acta Anaesthesiol Belg.* 1987;38(4):275–279.
2. van Steen SC, Rijkenberg S, van der Voort PHJ, DeVries JH. The association of intravenous insulin and glucose infusion with intensive care unit and hospital mortality: a retrospective study. *Ann Intensive Care.* 2019;9(1):29.
3. Finfer S, Chittock DR, Su SY-S, et al. Intensive versus conventional glucose control in critically ill patients. *N Engl J Med.* 2009;360(13):1283–1297.
4. Brealey D, Singer M. Hyperglycemia in critical illness: a review. *J Diabetes Sci Technol.* 2009;3(6):1250–1260.

5. Durham WJ, Miller SL, Yeckel CW, et al. Leg glucose and protein metabolism during an acute bout of resistance exercise in humans. *J Appl Physiol.* 2004;97(4):1379–1386.
6. Corpeno Kalamgi R, Salah H, Gastaldello S, et al. Mechano-signalling pathways in an experimental intensive critical illness myopathy model. *J Physiol.* 2016;594(15):4371–4388.
7. Waldauf P, Gojda J, Urban T, et al. Functional electrical stimulation-assisted cycle ergometry in the critically ill: protocol for a randomized controlled trial. *Trials.* 2019;20(1):724.
8. Gojda Jan, Waldauf Petr, Hrušková Natálie, Blahutová Barbora, Krajčová Adéla, Urban Tomáš, Tůma Petr, Řasová Kamila, Duška František. Lactate production without hypoxia in skeletal muscle during electrical cycling: Crossover study of femoral venous-arterial differences in healthy volunteers. *PLOS ONE.* 2019;14(3):e0200228. <http://doi.org/10.1371/journal.pone.0200228>.
9. Tam CS, Xie W, Johnson WD, Cefalu WT, Redman LM, Ravussin E. Defining insulin resistance from hyperinsulinemic-euglycemic clamps. *Diabetes Care.* 2012;35(7):1605–1610.
10. Patel BK, Pohlman AS, Hall JB, Kress JP. Impact of early mobilization on glycemic control and ICU-acquired weakness in critically ill patients who are mechanically ventilated. *Chest.* 2014;146(3):583–589.
11. McCarney R, Warner J, Illife S, van Haselen R, Griffin M, Fisher P. The Hawthorne Effect: a randomized, controlled trial. *BMC Med Res Methodol.* 2007;7:30.
12. Henry RR, Aroda VR, Mudaliar S, Garvey WT, Chou HS, Jones MR. Effects of colesevelam on glucose absorption and hepatic/peripheral insulin sensitivity in patients with type 2 diabetes mellitus. *Diabetes Obes Metab.* 2012;14(1):40–46.
13. Tewari N, Awad S, Duška F, et al. Postoperative inflammation and insulin resistance in relation to body composition, adiposity and carbohydrate treatment: a randomised controlled study. *Clin Nutr.* 2019;38(1):204–212.
14. Gudbjörnsdóttir S, Sjöstrand M, Strindberg L, Wahren J, Lönnroth P. Direct measurements of the permeability surface area for insulin and glucose in human skeletal muscle. *J Clin Endocrinol Metab.* 2003;88(10):4559–4564.

SUPPORTING INFORMATION

Additional supporting information may be found in the online version of the article at the publisher's website.

How to cite this article: Waldauf Petr, Urban Tomáš, Krajčová Adéla, et al. Can functional electrical stimulation-assisted cycle ergometry replace insulin infusion in patients? A nested substudy in a randomized controlled trial with 6 months' follow-up. *J Parenter Enteral Nutr.* 2022;46:249–253. <https://doi.org/10.1002/jpen.2213>

Příloha 8

Krajčová A, Skagen C, Džupa V, **Urban T**, Rustan AC, Jiroutková K, Bakalář B, Thoresen GH, Duška F.

Effect of noradrenaline on propofol-induced mitochondrial dysfunction in human skeletal muscle cells.

Intensive Care Med Exp. 2022 Nov 8;10(1):47. doi: 10.1186/s40635-022-00474-3. PMID: 36346511; PMCID: PMC9643307.

RESEARCH ARTICLES

Open Access



Effect of noradrenaline on propofol-induced mitochondrial dysfunction in human skeletal muscle cells

Adéla Krajčová¹, Christine Skagen², Valér Džupa³, Tomáš Urban¹, Arild C. Rustan², Kateřina Jiroutková¹, Bohumil Bakalář¹, G. Hege Thoresen^{2,4} and František Duška^{1*} 

*Correspondence:
frantisek.duska@lf3.cuni.cz

¹ Department of Anaesthesia and Intensive Care of the Third Faculty of Medicine and Královské Vinohrady University Hospital, OXYLAB-Laboratory for Mitochondrial Physiology, Charles University, Prague, Czech Republic

² Section for Pharmacology and Pharmaceutical Biosciences, Department of Pharmacy, University of Oslo, Oslo, Norway

³ Department of Orthopaedics and Traumatology of the Third Faculty of Medicine and Královské Vinohrady University Hospital, Charles University, Prague, Czech Republic

⁴ Department of Pharmacology, Institute of Clinical Medicine, University of Oslo, Oslo, Norway

Abstract

Background: Mitochondrial dysfunction is a hallmark of both critical illness and propofol infusion syndrome and its severity seems to be proportional to the doses of noradrenaline, which patients are receiving. We comprehensively studied the effects of noradrenaline on cellular bioenergetics and mitochondrial biology in human skeletal muscle cells with and without propofol-induced mitochondrial dysfunction.

Methods: Human skeletal muscle cells were isolated from vastus lateralis biopsies from patients undergoing elective hip replacement surgery ($n = 14$) or healthy volunteers ($n = 4$). After long-term (96 h) exposure to propofol (10 $\mu\text{g}/\text{mL}$), noradrenaline (100 μM), or both, energy metabolism was assessed by extracellular flux analysis and substrate oxidation assays using [¹⁴C] palmitic and [¹⁴C(U)] lactic acid. Mitochondrial membrane potential, morphology and reactive oxygen species production were analysed by confocal laser scanning microscopy. Mitochondrial mass was assessed both spectrophotometrically and by confocal laser scanning microscopy.

Results: Propofol moderately reduced mitochondrial mass and induced bioenergetic dysfunction, such as a reduction of maximum electron transfer chain capacity, ATP synthesis and profound inhibition of exogenous fatty acid oxidation. Noradrenaline exposure increased mitochondrial network size and turnover in both propofol treated and untreated cells as apparent from increased co-localization with lysosomes. After adjustment to mitochondrial mass, noradrenaline did not affect mitochondrial functional parameters in naïve cells, but it significantly reduced the degree of mitochondrial dysfunction induced by propofol co-exposure. The fatty acid oxidation capacity was restored almost completely by noradrenaline co-exposure, most likely due to restoration of the capacity to transfer long-chain fatty acid to mitochondria. Both propofol and noradrenaline reduced mitochondrial membrane potential and increased reactive oxygen species production, but their effects were not additive.

Conclusions: Noradrenaline prevents rather than aggravates propofol-induced impairment of mitochondrial functions in human skeletal muscle cells. Its effects on bioenergetic dysfunctions of other origins, such as sepsis, remain to be demonstrated.

Keywords: Propofol infusion syndrome, Noradrenaline, Mitochondrial dysfunction, Skeletal muscle, Critical illness

Introduction

Mitochondrial dysfunction in skeletal muscle is a hallmark of sepsis [1], ICU-acquired skeletal muscle dysfunction, acute lung injury, acute renal failure, and critical illness-related immune function dysregulation [2]. An association has been found 20 years ago [1] between the degree of mitochondrial dysfunction and the dose of noradrenaline that the patients were receiving.

The effects of drugs frequently used in ICU on cellular bioenergetics are understudied, but propofol is known to induce mitochondrial dysfunction [3–8], which, in its extreme form may result in propofol infusion syndrome (PRIS), a rare but potentially lethal complication [9–11]. Typical features of the syndrome include metabolic acidosis, arrhythmias, Brugada-like pattern on electrocardiogram, hypertriglyceridemia, fever, rhabdomyolysis, hepatomegaly, cardiac and/or renal failure [9–11]. The risk of the syndrome increases with rising dose and duration of propofol administration, low carbohydrate intake, inborn mitochondrial diseases, critical illness and concomitant treatment with corticosteroids [9, 12, 13]. In addition, most patients with PRIS were simultaneously treated with high doses of intravenous catecholamines leading to concern that they might be one of the triggering factors of the syndrome and could be associated with mortality [9, 12]. It remains unclear whether high doses of noradrenaline could have causally contributed to the development of PRIS or whether it is an epiphenomenon.

Noradrenaline is the first-choice vasopressor in critically ill patients [14–16] and propofol is used ubiquitously in ICUs. Therefore, in this study we sought out to investigate the effects on cellular bioenergetics of 4 days of exposure to pharmacological concentrations of propofol and noradrenaline.

Materials and methods

Study subjects

Skeletal muscle tissue biopsies were obtained from patients undergoing elective hip replacement surgery at the Department of Orthopaedic Surgery of Královské Vinohrady University Hospital in Prague ($n = 14$). Specimens were taken by open technique from *vastus lateralis* muscle (sample ~ 300 mg) during surgery. In addition, for [$1\text{-}^{14}\text{C}$]palmitic acid and [^{14}C (U)]lactic acid experiments, samples from *vastus lateralis* muscle were obtained under local anaesthesia by Bergström technique ($n = 4$) at Norwegian School of Sport Sciences, Oslo, in cooperation with Department of Pharmacy, University of Oslo. The study protocols were approved by respective REBs in both institutions. All subjects provided a prospective written informed consent. Detailed characteristics of skeletal muscle donors are described in Additional file 1: see Table S1.

Isolation and cultivation of human skeletal muscle cells

Skeletal muscle cells were isolated and cultured on gelatin-coated flasks or collagen-coated 24-well tissue culture plates as previously described [17] (for details see Additional file 1). Upon 80–90% confluency, differentiation of cells was induced by reducing serum concentration in cell culture medium [17]. Differentiated multinucleated myotubes were then treated with either 10 $\mu\text{g}/\text{mL}$ propofol, 0.1 mM noradrenaline (NA) or both agents for 96 h. The cells then underwent several experimental procedures, as

described below. For the confocal laser scanning microscopy experiments, we used proliferating myoblasts. All experiments were performed within 5 passages after isolation of cells. All chemicals were purchased from Merck Millipore (Darmstadt, Germany) or Life Technologies (Gaithersburg, MD, US), unless otherwise stated.

Viability assays and drug preparation is described in the Additional file 1. Initially, we tested a range of propofol concentrations, from those resembling propofol levels in human plasma during sedation and anaesthesia (2.5 and 10 $\mu\text{g}/\text{mL}$) [18, 19] to supratherapeutic concentrations. Given that high propofol concentrations (10 $\mu\text{g}/\text{mL}$) impair cell viability and there is no significant difference between the therapeutic concentrations (Additional file 1: see Figs. S1, S2), we used only 10 $\mu\text{g}/\text{mL}$ for further experiments. Similarly, we studied the effect of a range of noradrenaline concentrations (0.5; 1; 10 and 100 μM). Noradrenaline had no significant impact on cell survival in a dose-dependent manner (Additional file 1: see Fig. S3) and hence we used 100 μM noradrenaline for further experiments.

Cellular bioenergetics

We used XF-24 Extracellular Flux Analyzer (Agilent Technologies Inc., Santa Clara, CA, US) to measure oxygen consumption rate (OCR) in living cells seeded on 24-well plate at 37 °C [20–22] at baseline and after a sequential addition of up to four compounds [20–22]. We performed three types of assays (measurements in tri- or tetraplicates from 7 subjects for each protocol): Global mitochondrial parameters, i.e. basal respiration, ATP production, maximal respiratory capacity and non-mitochondrial respiration, were determined by sequential injection of F_0F_1 ATPase inhibitor oligomycin [1 μM], an uncoupler of the respiratory chain carbonyl cyanide-4-(trifluoromethoxy)phenylhydrazine (FCCP; [1 μM]) and complex IV inhibitor antimycin A [4 μM] (see Fig. 1, part A and B; for detailed information see Additional file 1). Exogenous fatty acid oxidation (FAO) was determined in carnitine-supplemented medium by the addition of an uncoupler FCCP [1 μM] followed by a stepwise addition of sodium palmitate (to a final concentration of 200 μM ; see Fig. 1, part C) and FAO inhibitor etomoxir [40 μM]. Endogenous fatty acid oxidation was determined in palmitate-free medium by sequential addition of FCCP [1 μM] and etomoxir [40 μM] (see Fig. 1, part D). In both protocols, FAOs were calculated as the decrement of OCR after the addition of etomoxir. Where appropriate, OCR was normalized to citrate synthase (CS) activity determined spectrophotometrically (CS Assay kit, Merck Millipore, Darmstadt, Germany) [23] in cell pellets.

Substrate oxidation assays and acid-soluble metabolites

Fully differentiated myotubes were incubated with either 100 μM [$^{14}\text{C}(\text{U})$]lactic acid (0.5 $\mu\text{Ci}/\text{ml}$) or 100 μM [$1\text{-}^{14}\text{C}$]palmitic acid (0.5 $\mu\text{Ci}/\text{ml}$) in DMEM-GlutaMAX™ (low glucose) containing 10 mM HEPES, 10 μM BSA and 1 mM L-carnitine for 4 h. Palmitic acid was bound to BSA at a ratio of 2.5:1. Following the 4-h incubation period, the cells were lysed and medium containing radiolabelled palmitic acid was collected and saved for oxidation and acid-soluble metabolites (ASM) measurements. For the lactate experiments, cell-associated radioactivity plus CO_2 production reflects total cellular uptake of [$^{14}\text{C}(\text{U})$]lactic acid, while cell-associated radioactivity plus CO_2 plus ASM reflects total cellular uptake of [^{14}C]palmitic acid.

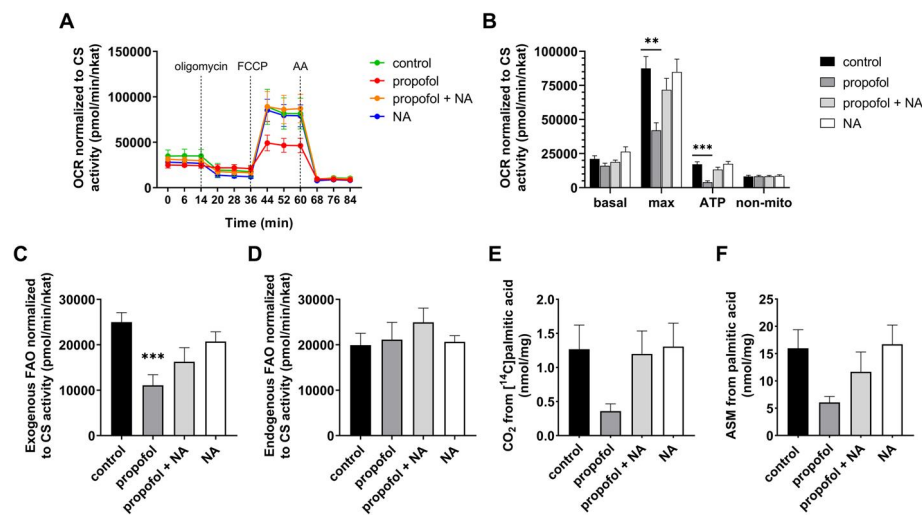


Fig. 1 Extracellular flux analysis and substrate oxidation assays. **A** Real-time measurement of OCR at baseline and after sequential injection of oligomycin, FCCP and antimycin A. Each data-point represents the mean of 7 subjects measured in tri- or tetraplicates. Values are normalized to mitochondrial content (CS activity). **B** Global mitochondrial parameters. Basal respiration, maximal respiratory capacity, ATP production and non-mitochondrial respiration determined from OCRs shown in part A. **C** Exogenous oxidation of fatty acids after palmitate addition to the medium during measurement. **D** Endogenous oxidation of fatty acids in palmitate-free medium. **E** CO_2 production from $[^{14}\text{C}]$ palmitic acid (complete oxidation). **F** Oxidation of $[^{14}\text{C}]$ palmitic acid to ASM (incomplete oxidation). Error bars in each graph indicate standard error of the mean. $**p < 0.01$, $***p < 0.001$ vs. control group. AA antimycin A, FCCP carbonyl cyanide-4- (trifluoromethoxy) phenylhydrazone, FAO fatty acid oxidation, NA noradrenaline, OCR oxygen consumption rate

Analysis of cell-associated radioactivity and CO_2 formation

100 μl medium containing radioactive substrates was transferred to a multi-well plate, sealed and frozen at -20°C following the 4 h incubation. CO_2 production was measured by adding 40 μl of 1 M perchloric acid (HClO_4) to the frozen medium, where the CO_2 was captured by a 96-well UniFilter-96 GF/B microplate that was mounted on top of the multi-well plate [24]. The mixture was incubated at room temperature for 3 h to trap radiolabelled CO_2 . The CO_2 produced during the 4 h of incubation with $[1-^{14}\text{C}]$ palmitic and $[^{14}\text{C}(\text{U})]$ lactic acid was captured by the sodium bicarbonate buffer system in the cell medium. After adding HClO_4 to the frozen medium, CO_2 was released and captured in the UniFilter-96 GF/B microplate. The cell lysates were used to measure the cell-associated radioactivity. Radioactivity was measured by liquid scintillation (2450 MicroBeta [24] scintillation counter, PerkinElmer).

Analysis of acid-soluble metabolites

The remaining radioactive medium containing $[^{14}\text{C}]$ palmitic acid was used to measure ASM, which mainly consist of tricarboxylic acid cycle metabolites and reflect incomplete FAO. The collected radiolabelled incubation medium (100 μl) was transferred to Eppendorf tubes, added 300 μL HClO_4 and 30 μL BSA (6%) before being centrifuged. The supernatant was then counted by liquid scintillation (Packard Tri-Carb 1900 TR, PerkinElmer).

Confocal laser scanning microscopy and live-cell imaging

Microscopy of cell lines at growth conditions (37 °C and 5% CO₂) has been performed using a 63 × oil immersion objective (*Leica TCS SP5* system, Leica Microsystems). For determination of mitochondrial mass we used MitoTracker™ Green FM (excitation at 488 nm), reflecting mitochondrial mass regardless of mitochondrial membrane potential [25, 26]. In addition, CellMask™ Deep Red Plasma Membrane Stain (excitation at 650 nm) labelling cellular plasma membrane allowed to determine the proportion of the cytoplasm filled with the mitochondrial network [27] (see Fig. 2, part A and B). Production of reactive oxygen species (ROS) [28–30] was determined by loading cells with a reduced non-fluorescent dye MitoTracker Red CM-H2XRos (excitation at 561; see Fig. 4), that fluoresces upon oxidation [29, 30]. Mitochondrial membrane potential ($\Delta\psi_m$) was determined as a ratio of fluorescence intensity after staining the cells with positively charged red dye tetramethylrhodamine ethyl ester (TMRE; excitation at 549 nm) and MitoTracker™ Green FM (Additional file 1: see Fig. S6). Co-localization of mitochondria with lysosomes during mitophagy was determined in 2D cross-sectional confocal images using the ImageJ™ tool (see Fig. 5) as the fraction of mitochondria, stained with MitoTracker™ Green FM (excitation at 488 nm), that overlapped with lysosomes, stained with LysoTracker™ Deep Red (excitation at 651 nm). Detailed protocols of confocal microscopy are in the Additional file 1. In addition, MitoTracker™ Green FM-staining of cells was used to determine mitochondrial volume by flow cytometry (BD FACSVerser flow cytometer, BD Biosciences, CA, USA).

Statistical analysis

All data sets were tested for normality of distribution. One-way ANOVA with Dunnett's post hoc test or Kruskal–Wallis with Dunn's post hoc test were used, as appropriate. Differences at $p < 0.05$ were considered significant. Images from confocal laser scanning microscopy were analysed using Image J (Fiji) software, whilst GraphPad Prism 8.0.1 (GraphPad Software Inc., La Jolla, CA, US) was used for graphs and statistics. Image brightness or contrast were not altered in any quantitative image analysis protocols.

Results

Effects on cell viability and bioenergetic profile

The concentrations of propofol (10 µg/mL) and noradrenaline (0.1 mM), which we used in all assays, did not affect the viability of the cells (Additional file 1: see Fig. S1).

Respiratory chain function indices

Basal OCR normalized to CS activity was not significantly different among the groups (see Fig. 1A). In line, there were no significant changes of [¹⁴C]lactic acid oxidation or uptake across the experimental conditions (Additional file 1: see Fig. S4). Propofol exposure led to significant reduction of both ATP production at rest

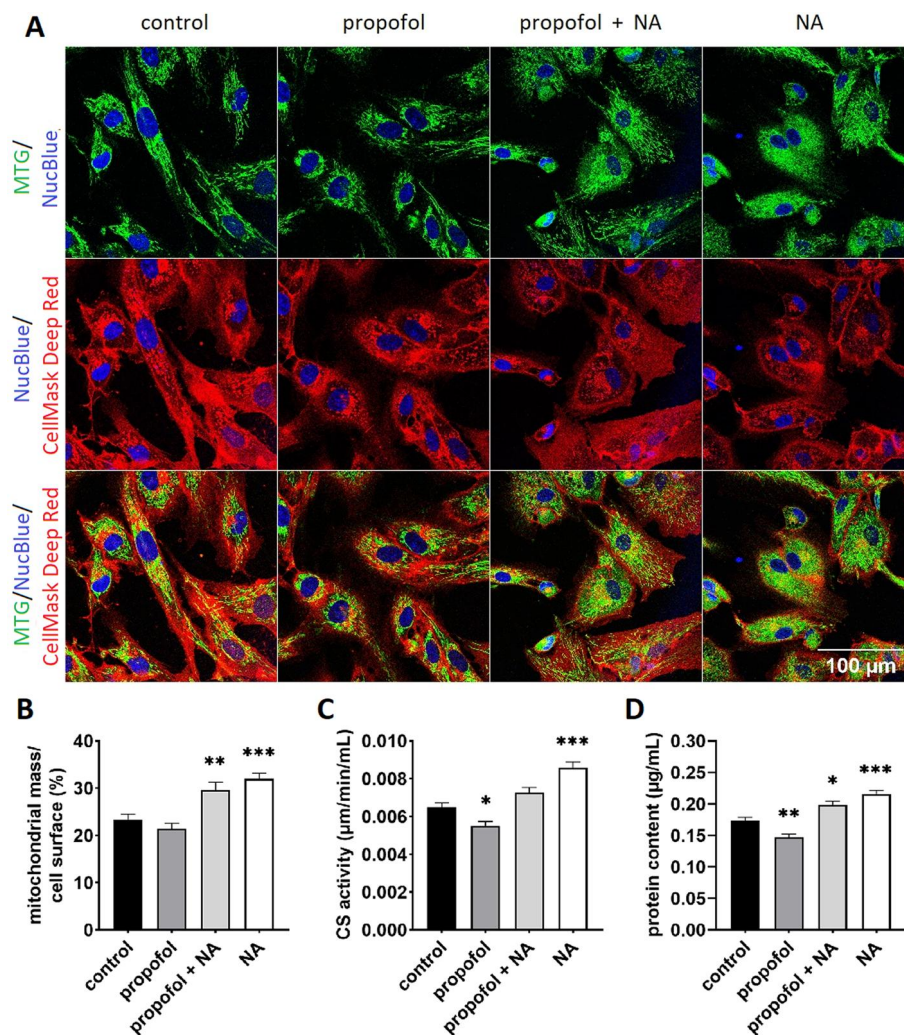


Fig. 2 **A** and **B** Analysis of mitochondrial mass by confocal imaging of exposed myoblasts. **A** Representative confocal images of each channel after dual staining with Mitotracker Green™ FM (accumulating in mitochondria) and CellMask™ Deep Red (binding into the cell membrane). Additionally, all cells were stained with nuclear blue-fluorescent probe NucBlue. Experiments were performed at least at 50 cells per each condition from 3 independent measurements (= cells established from 3 individual subjects). **B** Mitochondrial mass calculated as a fraction (%) of a cell surface area in 2D cross-sectional images. Mitochondrial mass (mitochondrial footprint) was analysed as a sum of positive pixels (binary image) per cell representing mitochondrial area using ImageJ™ tool "MINA". **C** Activity of CS enzyme measured spectrophotometrically. **D** Total protein content from frozen cell pellets was determined using Bradford assay as described elsewhere [53]. For both CS activity and protein content measurement, experiments were performed in $n = 7$ replicates in tri- or tetraplicates. Error bars indicate standard error of the mean. * $p < 0.05$, ** $p < 0.01$, *** $p < 0.001$ vs. control group. CS citrate synthase, MTG MitoTracker Green™ FM, NA noradrenaline

and of the maximum respiratory chain capacity. These effects were diminished by co-exposure to noradrenaline, whilst exposure to noradrenaline alone did not have any effects on mitochondrial functional indices (see Fig. 1B).

Fatty acid oxidation

Similar pattern of inhibition by propofol, which is mitigated by co-incubation with noradrenaline, have been observed for oxidation of exogenous palmitate by both extracellular flux analysis and by [^{14}C] palmitic acid techniques (see Fig. 1C, E–F). Uptake of [^{14}C] palmitic acid was not affected by neither compound (Additional file 1: see Fig. S4) and there was no significant alteration of endogenous FAO, either (see Fig. 1D).

Effects on mitochondrial mass

Microscopic analysis revealed that compared to control cells, noradrenaline alone or in combination with propofol significantly increased mitochondrial mass to $124 \pm 3\%$ and $114 \pm 3\%$, respectively, whilst in propofol-exposed cells mitochondrial mass was $85 \pm 4\%$ of that in control cells (see Fig. 2A, B). Measurements of CS activity (see Fig. 2C) and protein content (see Fig. 2D) confirmed these results. There were $132 \pm 4\%$ and $112 \pm 4\%$ increases compared to control cells in cells treated with noradrenaline alone and noradrenaline plus propofol, respectively, and a reduction to $85 \pm 4\%$ in cells treated with propofol alone. In 2D confocal microscopy images, mitochondria occupied $32 \pm 1\%$ and $30 \pm 2\%$ of the cell surface in noradrenaline- and noradrenaline plus propofol-exposed cells, respectively, compared to $23 \pm 2\%$ and $21 \pm 1\%$ in propofol treated and control cells, respectively. As flow cytometry with

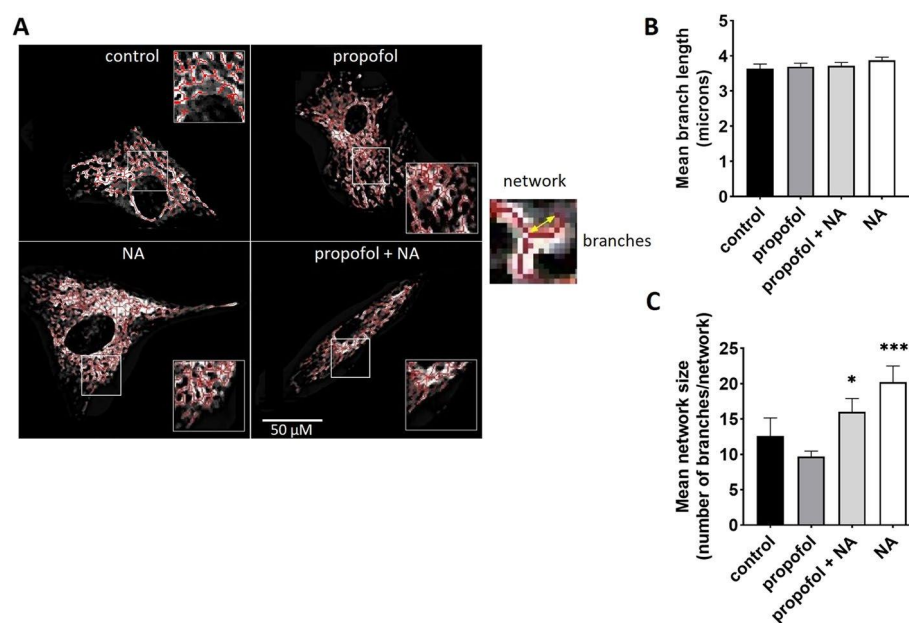


Fig. 3 Mitochondrial morphology. Confocal images of myoblasts stained with MitoTracker™ Green FM analysed with the ImageJ™ plugin “MINA”. **A** Representative skeletonized images show mitochondrial network in different groups (left). Measurements were performed at least at 50 cells per each group from 3 independent experiments (= 3 individual subjects). Yellow arrow (right) shows one of the three branches in an example of mitochondrial network. **B** and **C** Mean branch length and mean network size (= number of branches per network) were analysed in each cell separately. Error bars indicate standard error of the mean. * $p < 0.05$, *** $p < 0.001$ vs. control group. NA noradrenaline

MitoTracker™ Green FM staining suggested that these changes were mainly reflective of alterations in mitochondrial volume (Additional file 1: see Fig. S5), we explored in detail how interactions between propofol and noradrenaline affect mitochondrial morphology and turnover, reflected by mitophagy.

Effects on mitochondrial morphology

There were no changes of mean branch length across experimental conditions ($\sim 3.7 \pm 0.1$ microns for all groups), but the exposure to noradrenaline with or without propofol increased the number of branches per each individual network, and thereby led to an increase in the mean network size (see Fig. 3).

Effects on mitophagy

Since autophagosomes eventually fuse with lysosomes, co-localization analysis of mitochondria with lysosomal markers could be used to monitor mitophagy [31]. Co-localization of mitochondria with lysosomes was significantly higher in noradrenaline and noradrenaline plus propofol groups ($3.5 \pm 0.3\%$ and $3.6 \pm 0.2\%$ for noradrenaline and noradrenaline with propofol, respectively) compared to propofol-exposed ($2.8 \pm 0.4\%$) and control cells ($1.9 \pm 0.4\%$), respectively. In line, Pearson's coefficient characterizing a degree of overlap, was higher in noradrenaline-exposed cells (see Fig. 4).

Effects on reactive oxygen species production and mitochondrial membrane potential

($\Delta\Psi_m$)

Compared to control cells, all experimental exposures led to a significant increase of ROS production (to 142–162% of values in control cells; see Fig. 5) and to a reduction of the mitochondrial membrane potential (Additional file 1: see Fig. S6).

Discussion

The main finding of this study is that noradrenaline does not potentiate the adverse effects of propofol on cellular bioenergetics—a hypothesis generated by the finding of association between co-exposure to high-dose noradrenaline with mortality of PRIS [9, 13]. Our data support the alternative hypothesis [12] that the need of vasopressor support in patients with fatal PRIS is an epiphenomenon rather than causal contributor to mortality. In fact, we have found a range of effects of noradrenaline on bioenergetics that preserve mitochondrial function under stress (in our experiment induced by exposure of cells to propofol), that can be of importance for the critically ill in general. Not only because noradrenaline and propofol are among the most used drugs in intensive care units, but also because bioenergetic failure has long been known as a hallmark of acute and protracted critical illnesses [1]. Our finding sheds new light into the understanding of the effects of noradrenaline and propofol on a range of aspects of mitochondrial biology.

For our experiments we used a well-established [8] ex vivo model of human skeletal muscle—cultured myotubes differentiated from myoblasts isolated from vastus lateralis biopsies of metabolically healthy patients undergoing hip replacement surgery and healthy volunteers. We exposed those cells for 4 days to both drugs and assessed their impact on mitochondrial mass, morphology, dynamics and function. Not surprisingly

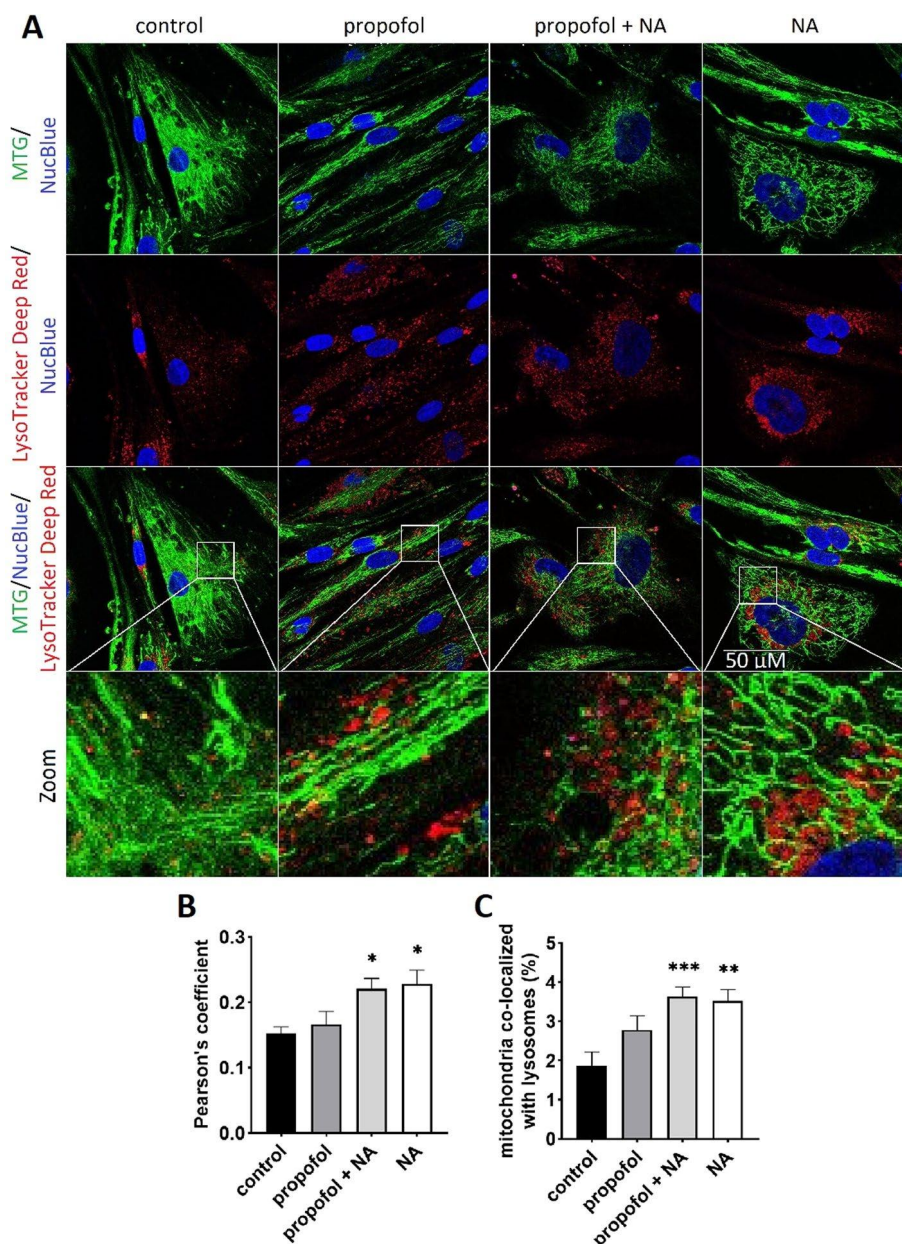


Fig. 4 Co-localization of mitochondria with lysosomes. **A** Representative confocal images of each channel after dual staining with Mitotracker Green™ FM (accumulating in mitochondria) and LysoTracker™ Deep Red (binding to acidic lysosomes). Additionally, all cells were stained with blue-fluorescent probe NucBlue to label nuclei. Experiments were performed at least at 40 cells per each condition from 3 independent measurements (= 3 individual subjects). **B** Pearson's coefficient, characterizing a degree of overlap between labelled mitochondria and lysosomes. The quantification of the co-localization was performed using ImageJ™ plugin "JACoP". **C** Percent co-localization was calculated by total area of co-localized lysosomes (red channel) over total area of mitochondria (green channel). Error bars indicate standard error of the mean. * $p < 0.05$, ** $p < 0.01$, *** $p < 0.001$ vs. control group. NA noradrenaline

and in line with our previous results [8], propofol decreased both ATP production at rest and the maximal respiratory capacity of the electron transport chain, and caused a profound inhibition of the ability to oxidize exogenous palmitate. Noradrenaline significantly counteracted those effects by several ways.

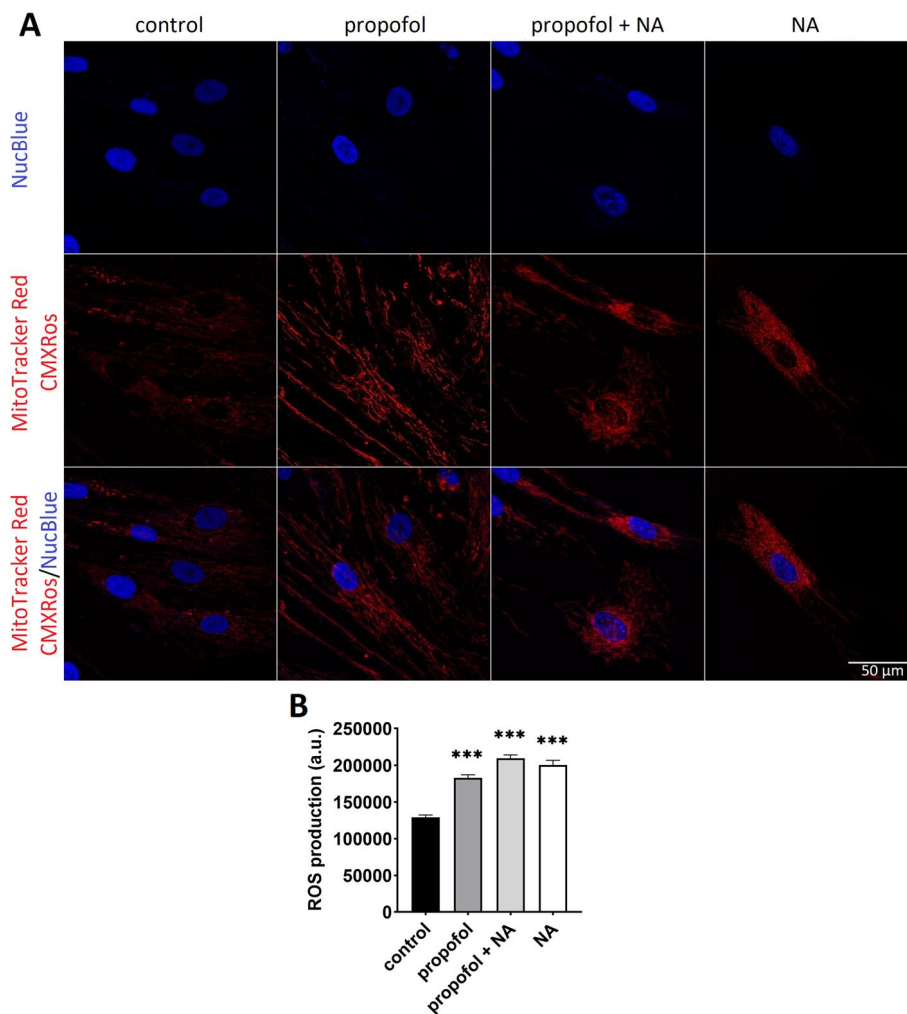


Fig. 5 ROS production. **A** Representative confocal images from myoblasts stained with MitoTracker Red CM-H2XRos to detect accumulation of mitochondrial specific-reactive oxygen species. Experiments were performed on at least 90 cells per group from $n = 3$ independent experiments (with cells from 3 individual subjects). **B** Determination of ROS production in different groups. Error bars indicate standard error of the mean. *** $p < 0.001$ vs. control group. NA noradrenaline

Firstly, noradrenaline increased mitochondrial network mass and size, most likely by increased mitochondrial turnover, as evidenced by increased mitophagy. Several studies have found that catecholamine-induced stimulation of β -adrenergic receptors promotes mitochondrial biogenesis in both skeletal muscle [32, 33] and other tissues [34, 35]. In keeping with this, noradrenaline significantly increased mitochondrial content what we confirmed by three independent techniques. In our study, we also looked at mitochondrial network architecture. Microscopic analysis revealed that in noradrenaline-exposed cells mitochondrial networks exhibited more branches rather than increased elongation compared to control cells. Increased mitochondrial amount could result either from accelerated biogenesis or a slower degradation [31]. We observed an increased co-localization of lysosomes with mitochondria which could be an indicator of a triggering mitophagy [31]. Traditionally, lysosomes have been considered acidic organelles

necessary for the autophagy and degradation of cellular components [36]. However, recent studies have shown that lysosomes could serve as the nutrient reservoirs with the potential anabolic effect in skeletal muscle and other tissues [37]. Dynamic formation of inter-organelle membrane contact sites between mitochondria and lysosomes allows a shuttle of amino acids, lipids and ions such as Ca^{2+} between the two organelles [38, 39]. The interaction of mitochondria with lysosomes might therefore play a role in improved metabolic regulation and substrate availability.

On that note, the protective effects of noradrenaline on propofol-exposed cells were still apparent even after adjustment to mitochondrial content. In particular, noradrenaline effectively counteracted propofol inhibitory effect on the oxidation of palmitoyl-carnitine, added to the media. Noradrenaline increases lipolysis in adipose tissue [40, 41], but the results of the studies of effects on intramyocellular lipolysis have been contentious [42–44]. In our study, we did not observe any increase of oxidation of endogenous fatty acids, which would suggest that noradrenaline stimulated intramyocellular lipolysis. This is further supported by the lack of effect of noradrenaline on the size and the number of lipid droplets in human myoblasts (Additional file 1: see Fig. S7). Noradrenaline is known to directly enhance the activity of carnitine palmitoyl transferase 1 (CPT1) [45], an enzyme indispensable for long-chain fatty acids transport to mitochondria, which seems to be inhibited by propofol [46–48]. Our data are consistent with noradrenaline preserving the exogenous FAO in propofol-exposed cells by preserving and activating transport of long-chain fatty acid transport to mitochondria by CPT1.

The main limitation of our study is that we only used a model of a single organ derived from biopsies of subjects that were not critically ill. This indeed severely limits the generalizability of our results. Moreover, *ex vivo* conditions may be far from representative of *in vivo* physiology. Yet, unlike other adverse effects of drugs, we believe that bioenergetic effects are important, relevant, and understudied and our study brings important data into the field. Further studies should focus of interactions between drugs frequently used in ICUs and mitochondrial dysfunction induced by critical illness itself. Also, it must be noticed that the concentrations used for noradrenaline exposure in our experiments exceeded therapeutic plasma levels during noradrenaline infusion in critically ill (up to 300 nM) [49–51]. However, noradrenaline concentration in the synaptic clefts in skeletal muscle can be much higher [52].

In conclusion, we for the first time investigated the effects on mitochondrial biology of long-term exposure of human skeletal muscle cells to propofol and noradrenaline. We have shown that noradrenaline does not worsen propofol-induced cellular dysfunction, but in fact, it is able to counteract most adverse effects of propofol on cellular bioenergetics by increasing the mitochondrial turnover and mitochondrial mass, and by enhancing the oxidation of exogenous fatty acids.

Supplementary Information

The online version contains supplementary material available at <https://doi.org/10.1186/s40635-022-00474-3>.

Additional file 1: Table S1. Study subject characteristics on biopsy day. **Figure S1.** Cell viability. Results are expressed as the percentage of cell viability relative to the control (= non-treated cells). a) Individual groups represent viability of cells exposed for 96 h to different concentrations of noradrenaline. Data are presented as the mean \pm SEM ($n=4$ subjects). Values for each experimental condition were measured in triplicates in each subject. b) Individual groups represent viability of cells exposed for 96 h to ethanol (= propofol vehicle; 0.1%),

0.1 mM noradrenaline alone and c) different concentrations ($\mu\text{g}/\text{mL}$) of either propofol alone or mixture of propofol and 0.1 mM noradrenaline. Data are presented as the mean \pm SEM ($n = 7$ subjects). Values for each experimental condition were measured in triplicates in each subject. Note: NA = noradrenaline. *** $p < 0.001$ vs. control group.

Figure S2. Kinetic graph on XF24 Analyzer demonstrates changes after propofol at various concentrations. Real-time measurement of OCR at baseline and after sequential injection of oligomycin, FCCP and Antimycin A. Each data-point represents the mean of 7 independent samples (subjects) measured in tri- or tetraplicates normalized to protein content. Error bars indicate standard error of the mean. Different colours represent different groups exposed to propofol (0; 2.5; 10 $\mu\text{g}/\text{mL}$).

Figure S3. A) Global mitochondrial parameters. Basal respiration, maximal respiratory capacity, ATP production and non-mitochondrial respiration. $N = 7$ replicates with 21–28 wells for each condition normalized to protein content. Error bars indicate standard error of the mean. B) Mitochondrial mass calculated as a fraction (%) of a cell surface area in 2D cross-sectional images. Figure S4. Uptake of CO_2 production and lactic acid metabolism. A) Uptake of [^{14}C]palmitic acid. B) [^{14}C]lactic acid oxidation. C) [^{14}C]lactic acid uptake. Note: NA = noradrenaline. Error bars in each graph indicate standard error of the mean. Note: NA = noradrenaline.

Figure S5. Flow cytometry. Histogram showing MTG intensity of individual cell groups. Data are presented as the mean \pm SEM ($n = 2-3$ experiments per each group). Note: NA = noradrenaline.

Figure S6. Mitochondrial membrane potential. A) Myoblasts after staining with MitoTracker™ Green FM (left), TMRE (in the middle) and after staining of both agents (right). Experiments were performed at least at 60 cells per each group from $n = 3$ independent experiments (cells from 3 individual subjects). B) Determination of $\Delta\psi_m$ was expressed as TMRE/MTG ratio. The mitochondrial uncoupling agent FCCP was used as a positive control. Note: MTG = MitoTracker™ Green FM; TRME = tetramethylrhodamine ethyl ester; FCCP = carbonyl cyanide-4-(trifluoromethoxy)phenylhydrazone, NA = noradrenaline. Error bars indicate standard error of the mean. * $p < 0.05$, *** $p < 0.001$ vs. control group.

Figure S7. Analysis of lipid droplets. A) Quantification of LD mass by cross-sectional area of BODIPY 493/503 normalized to cell area. B) LD size assessed by cross-sectional area of individual LDs. C) LD number normalized to cell area. Experiments were performed at least at 38 cells per each condition from 2 independent measurements ($= 2$ individual subjects). Error bars indicate standard error of the mean. *** $p < 0.001$ vs. control group.

Acknowledgements

We thank all the volunteers who consented to muscle biopsies.

Author contributions

All authors have made substantial contributions to all of the following: (1) the conception and design of the study, or acquisition of data, or analysis and interpretation of data, (2) drafting the article or revising it critically for important intellectual content, (3) final approval of the version to be submitted. All authors have read and approved the submitted version of the manuscript and agree to transfer the copyright to the journal in the event of acceptance for publication.

Funding

The study has been funded by grant NU21J-06-00078 by Czech Ministry of Health Grant Agency (AZV).

Availability of data and materials

The datasets used and/or analysed during the current study are available from the corresponding author on reasonable request.

Declarations

Ethics approval and consent to participate

The study design was in accordance with Declaration of Helsinki. All study subjects provided a prospective, written informed consent. The protocol and informed consent formularies were reviewed and approved by respective REBs in both institutions (Medical Ethics Committee at Královské Vinohrady University Hospital on 20 November 2013; decision number 270 915).

Consent for publication

Not applicable.

Competing interests

The authors declare that they have no competing interests.

Received: 22 July 2022 Accepted: 17 October 2022

Published online: 08 November 2022

References

- Brealey D, Brand M, Hargreaves I, Heales S, Land J, Smolenski R, Davies NA, Cooper CE, Singer M (2002) Association between mitochondrial dysfunction and severity and outcome of septic shock. *Lancet* 360(9328):219–223. [https://doi.org/10.1016/S0140-6736\(02\)09459-X](https://doi.org/10.1016/S0140-6736(02)09459-X)
- Supinski GS, Schroder EA, Callahan LA (2020) Mitochondria and critical illness. *Chest* 157(2):310–322. <https://doi.org/10.1016/j.chest.2019.08.2182>
- Branca D, Vincenti E, Scutari G (1995) Influence of the anesthetic 2,6-diisopropylphenol (propofol) on isolated rat heart mitochondria. *Comp Biochem Physiol C Pharmacol Toxicol Endocrinol* 110(1):41–45. [https://doi.org/10.1016/0742-8413\(94\)00078-o](https://doi.org/10.1016/0742-8413(94)00078-o)

4. Branca D, Roberti MS, Lorenzin P, Vincenti E, Scutari G (1991) Influence of the anesthetic 2,6-diisopropylphenol on the oxidative phosphorylation of isolated rat liver mitochondria. *Biochem Pharmacol* 42(1):87–90. [https://doi.org/10.1016/0006-2952\(91\)90684-w](https://doi.org/10.1016/0006-2952(91)90684-w)
5. Branca D, Roberti MS, Vincenti E, Scutari G (1991) Uncoupling effect of the general anesthetic 2,6-diisopropylphenol in isolated rat liver mitochondria. *Arch Biochem Biophys* 290(2):517–521. [https://doi.org/10.1016/0003-9861\(91\)90575-4](https://doi.org/10.1016/0003-9861(91)90575-4)
6. Rigoulet M, Devin A, Avéret N, Vandais B, Guérin B (1996) Mechanisms of inhibition and uncoupling of respiration in isolated rat liver mitochondria by the general anesthetic 2,6-diisopropylphenol. *Eur J Biochem* 241(1):280–285. <https://doi.org/10.1111/j.1432-1033.1996.0280t.x>
7. Schenkman KA, Yan S (2000) Propofol impairment of mitochondrial respiration in isolated perfused guinea pig hearts determined by reflectance spectroscopy. *Crit Care Med* 28(1):172–177. <https://doi.org/10.1097/00003246-200001000-00028>
8. Krajčová A, Løvsletten NG, Waldauf P, Frič V, Elkalaf M, Urban T, Anděl M, Trnka J, Thoresen GH, Duška F (2017) Effects of propofol on cellular bioenergetics in human skeletal muscle cells. *Crit Care Med*. <https://doi.org/10.1097/CCM.0000000000002875>
9. Kam PCA, Cardone D (2007) Propofol infusion syndrome. *Anaesthesia* 62(7):690–701. <https://doi.org/10.1111/j.1365-2044.2007.05055.x>
10. Ahlen K, Buckley CJ, Goodale DB, Pulsford AH (2006) The „propofol infusion syndrome“: the facts, their interpretation and implications for patient care. *Eur J Anaesthesiol* 23(12):990–998. <https://doi.org/10.1017/S0265021506001281>
11. Krajčová A, Waldauf P, Anděl M, Duška F (2015) Propofol infusion syndrome: a structured review of experimental studies and 153 published case reports. *Crit Care* 19(1):398. <https://doi.org/10.1186/s13054-015-1112-5>
12. Vasile B, Rasulo F, Candiani A, Latronico N (2003) The pathophysiology of propofol infusion syndrome: a simple name for a complex syndrome. *Intensive Care Med* 29(9):1417–1425. <https://doi.org/10.1007/s00134-003-1905-x>
13. Savard M, Dupré N, Turgeon AF, Desbiens R, Langevin S, Brunet D (2013) Propofol-related infusion syndrome heralding a mitochondrial disease: case report. *Neurology* 81(8):770–771. <https://doi.org/10.1212/WNL.0b013e3182a1aa78>
14. Rhodes A, Evans LE, Levy MM, Antonelli M, Ferrer R, Kumar A, Sevransky JE, Sprung CL, Nunnally ME, Rochwerger B, Rubenfeld GD, Angus DC, Annane D, Beale RJ, Bellinghan GJ, Bernard GR, Chiche J, Coopersmith C, De Backer DP, French CJ, Fujishima S, Gerlach H, Hidalgo JL, Hollenberg SM, Jones AE, Karnad DR, Kleinpell RM, Koh Y, Lisboa TC, Machado FR, Marini JJ, Marshall JC, Mazuski JE, McIntyre LA, McLean AS, Mehta S, Moreno RP, Myburgh J, Navalesi P, Nishida O, Osborn TM, Perner A, Plunkett CM, Ranieri M, Schorr CA, Seckel MA, Seymour CW, Shieh L, Shukri KA, Simpson SQ, Singer M, Thompson BT, Townsend SR, Van der Poll T, Vincent J, Wiersinga WJ, Zimmerman JL, Dellinger RP (2017) Surviving sepsis campaign: international guidelines for management of sepsis and septic shock: 2016. *Crit Care Med* 45(3):486–552. <https://doi.org/10.1097/CCM.0000000000002255>
15. De Backer D, Biston P, Devriendt J, Madl C, Chochrad D, Aldecoa C, Brasseur A, Defrance P, Gottignies P, Vincent J, SOAP II Investigators (2010) Comparison of dopamine and norepinephrine in the treatment of shock. *N Engl J Med* 362(9):779–789. <https://doi.org/10.1056/NEJMoa0907118>
16. Møller M, Claudius C, Junttila E, Haney M, Oscarsson-Tibblin A, Haavind A, Perner A (2016) Scandinavian SSAI clinical practice guideline on choice of first-line vasopressor for patients with acute circulatory failure. *Acta Anaesthesiol Scand* 60(10):1347–1366. <https://doi.org/10.1111/aas.12780>
17. Krajcova A, Ziak J, Jiroutkova K, Patkova J, Elkalaf M, Dzupa V, Trnka J, Duska F (2015) Normalizing glutamine concentration causes mitochondrial uncoupling in an in vitro model of human skeletal muscle. *JPEN J Parenter Enteral Nutr* 39(2):180–189. <https://doi.org/10.1177/0148607113513801>
18. Casati A, Fanelli G, Casaletti E, Colnaghi E, Cedrati V, Torri G (1999) Clinical assessment of target-controlled infusion of propofol during monitored anesthesia care. *Can J Anaesth* 46(3):235–239. <https://doi.org/10.1007/BF03012602>
19. Herregods L, Rolly G, Versichelen L, Rosseel M (1987) Propofol combined with nitrous oxide-oxygen for induction and maintenance of anaesthesia. *Anaesthesia* 42(4):360–365. <https://doi.org/10.1111/j.1365-2044.1987.tb03975.x>
20. Ferrick DA, Neilson A, Beeson C (2008) Advances in measuring cellular bioenergetics using extracellular flux. *Drug Discov Today* 13(5–6):268–274. <https://doi.org/10.1016/j.drudis.2007.12.008>
21. Gerencser AA, Neilson A, Choi SW, Edman U, Yadava N, Oh RJ, Ferrick DV, Nicholls DG, Brand MD (2009) Quantitative microplate-based respirometry with correction for oxygen diffusion. *Anal Chem* 81(16):6868–6878. <https://doi.org/10.1021/ac900881z>
22. Brand MD, Nicholls DG (2011) Assessing mitochondrial dysfunction in cells. *Biochem J* 435(2):297–312. <https://doi.org/10.1042/BJ20110162>
23. Srere PA (1969) Citrate Synthase. *Methods Enzymol* 13:3–11
24. Wensaas AJ, Rustan AC, Lövdstedt K, Kull B, Wikström S, Drevon CA, Hallén S (2007) Cell-based multiwell assays for the detection of substrate accumulation and oxidation. *J Lipid Res* 48(4):961–967. <https://doi.org/10.1194/jlr.D600047-JLR200>
25. Poot M, Zhang YZ, Krämer JA, Wells KS, Jones LJ, Hanzel DK, Lugade AG, Singer VL, Haugland RP (1996) Analysis of mitochondrial morphology and function with novel fixable fluorescent stains. *J Histochem Cytochem* 44(12):1363–1372. <https://doi.org/10.1177/44.12.8985128>
26. Doherty E, Perl A (2017) Measurement of mitochondrial mass by flow cytometry during oxidative stress. *React Oxy Species* 4(10):275–283. <https://doi.org/10.20455/ros.2017.839>
27. Corona JC, de Souza SC, Duchon MR (2014) PPAR γ activation rescues mitochondrial function from inhibition of complex I and loss of PINK1. *Exp Neurol* 253:16–27. <https://doi.org/10.1016/j.expneurol.2013.12.012>
28. Rieger B, Krajčová A, Duwe P, Busch KB (2019) ALCAT1 overexpression affects supercomplex formation and increases ROS in respiring mitochondria. *Oxid Med Cell Longev* 2019:9186469. <https://doi.org/10.1155/2019/9186469>
29. Hao L, Nishimura T, Wo H, Fernandez-Patron C (2006) Vascular responses to α 1-adrenergic receptors in small rat mesenteric arteries depend on mitochondrial reactive oxygen species. *Arterioscler Thromb Vasc Biol* 26(4):819–825. <https://doi.org/10.1161/01.ATV.0000204344.90301.7c>

30. Bailey SR, Mitra S, Flavahan S, Flavahan NA (2005) Reactive oxygen species from smooth muscle mitochondria initiate cold-induced constriction of cutaneous arteries. *Am J Physiol Hear Circ Physiol* 289(1 58-1):243–250. <https://doi.org/10.1152/ajpheart.01305.2004>
31. Ding WX, Yin XM (2012) Mitophagy: mechanisms, pathophysiological roles, and analysis. *Biol Chem* 393(7):547–564. <https://doi.org/10.1515/hsz-2012-0119>
32. Skagen C, Nyman TA, Peng X, O'Mahony G, Kase ET, Rustan AC, Thoresen GH (2021) Chronic treatment with terbutaline increases glucose and oleic acid oxidation and protein synthesis in cultured human myotubes. *Curr Res Pharmacol Drug Discov* 11;2:100039. <https://doi.org/10.1016/j.crphar.2021.100039>
33. Scholpa NE, Simmons EC, Tilley DG, Schnellmann RG (2019) β_2 -adrenergic receptor-mediated mitochondrial biogenesis improves skeletal muscle recovery following spinal cord injury. *Exp Neurol* 322:113064. <https://doi.org/10.1016/j.expneurol.2019.113064>
34. Kohlie R, Perwitz N, Resch J, Schmid SM, Lehnert H, Klein J, Iwen KA (2017) Dopamine directly increases mitochondrial mass and thermogenesis in brown adipocytes. *J Mol Endocrinol* 58(2):57–66. <https://doi.org/10.1530/JME-16-0159>
35. Napolitano G, Barone D, Di Meo S, Venditti P (2018) Adrenaline induces mitochondrial biogenesis in rat liver. *J Bioenerg Biomembr* 50(1):11–19. <https://doi.org/10.1007/s10863-017-9736-6>
36. Yim WWY, Mizushima N (2020) Lysosome biology in autophagy. *Cell Discov* 6:6. <https://doi.org/10.1038/s41421-020-0141-7>
37. Sawan SA, Mazzulla M, Moore DR, Hodson N (2020) More than just a garbage can: emerging roles of the lysosome as an anabolic organelle in skeletal muscle. *Am J Physiol Cell Physiol* 319(3):C561–C568. <https://doi.org/10.1152/ajpcell.00241.2020>
38. Todkar K, Ilamathi HS, Germain M (2017) Mitochondria and lysosomes: discovering bonds. *Front Cell Dev Biol* 7:5:106. <https://doi.org/10.3389/fcell.2017.00106>
39. Wong YC, Kim S, Peng W, Krainc D (2019) Regulation and function of mitochondria-lysosome membrane contact sites in cellular homeostasis. *Trends Cell Biol* 29(6):500–513. <https://doi.org/10.1016/j.tcb.2019.02.004>
40. Zhou A, Kondo M, Matsuura Y, Kameda K, Morimoto C, Tsujita T, Okuda H (1995) Mechanism of norepinephrine-induced lipolysis in isolated adipocytes: evidence for its lipolytic action inside the cells. *Pathophysiology* 2(1):29–34. [https://doi.org/10.1016/0928-4680\(95\)00004-K](https://doi.org/10.1016/0928-4680(95)00004-K)
41. Li Y, Li Z, Ngandiri DA, Llerins Perez M, Wolf A, Wang Y (2022) The molecular brakes of adipose tissue lipolysis. *Front Physiol* 113:826314. <https://doi.org/10.3389/fphys.2022.826314>
42. Quisth V, Enoksson S, Blaak E, Hagström-Toft E, Arner P, Bolinder J (2005) Major differences in noradrenaline action on lipolysis and blood flow rates in skeletal muscle and adipose tissue in vivo. *Diabetologia* 48(5):946–953. <https://doi.org/10.1007/s00125-005-1708-4>
43. Navegantes LCC, Sjöstrand M, Gudbjörnsdóttir S, Strindberg L, Elam M, Lönnroth P (2003) Regulation and counterregulation of lipolysis in vivo: different roles of sympathetic activation and insulin. *J Clin Endocrinol Metab* 88(11):5515–5520. <https://doi.org/10.1210/jc.2003-030445>
44. Hagström-Toft E, Enoksson S, Moberg E, Bolinder J, Arner P (1998) β -Adrenergic regulation of lipolysis and blood flow in human skeletal muscle in vivo. *Am J Physiol* 275(6):E909–16. <https://doi.org/10.1152/ajpendo.1998.275.6.e909>
45. Jin Y, Li S, Zhao Z, An JJ, Kim RY, Kim YM, Baik J, Lim S (2004) Carnitine palmitoyltransferase-1 (CPT-1) activity stimulation by cerulenin via sympathetic nervous system activation overrides cerulenin's peripheral effect. *Endocrinology* 145(7):3197–3204. <https://doi.org/10.1210/en.2004-0039>
46. Wolf AR, Potter F (2004) Propofol infusion in children: when does an anesthetic tool become an intensive care liability? *Paediatr Anaesth* 14(6):435–438. <https://doi.org/10.1111/j.1460-9592.2004.01332.x>
47. Timpe EM, Eichner SF, Phelps SJ (2006) Propofol-related infusion syndrome in critically ill pediatric patients: coincidence, association, or causation? *J Pediatr Pharmacol Ther* 11(1):17–42. <https://doi.org/10.5863/1551-6776-11.1.17>
48. Mirrakhimov A, Voore P, Halytskyy O, Khan M, Ali A (2015) Propofol infusion syndrome in adults: a clinical update. *Crit Care Res Pr* 2015(260385):1–10. <https://doi.org/10.1155/2015/260385>
49. Johnston AJ, Steiner LA, O'Connell M, Chatfield DA, Gupta AK, Menon DK (2004) Pharmacokinetics and pharmacodynamics of dopamine and norepinephrine in critically ill head-injured patients. *Intensive Care Med* 30(1):45–50. <https://doi.org/10.1007/s00134-003-2032-4>
50. Beloeil H, Mazoit JX, Benhamou D, Duranteau J (2005) Norepinephrine kinetics and dynamics in septic shock and trauma patients. *Br J Anaesth* 95(6):782–788. <https://doi.org/10.1093/bja/aei259>
51. Goldstein DS, Zimlichman R, Stull R, Keiser HR, Kopin IJ (1986) Estimation of intrasynaptic norepinephrine concentrations in humans. *Hypertension* 8(6):471–475. <https://doi.org/10.1161/01.HYP8.6.471>
52. Hoeldtke R, Cilmi K, Reichard G Jr, Boden G, Owen O (1983) Assessment of norepinephrine secretion and production. *J Lab Clin Med* 101(5):772–782
53. Bradford MM (1976) A rapid and sensitive method for the quantitation of microgram quantities of protein utilizing the principle of protein-dye binding. *Anal Biochem* 72(1–2):248–254. [https://doi.org/10.1016/0003-2697\(76\)90527-3](https://doi.org/10.1016/0003-2697(76)90527-3)

Publisher's Note

Springer Nature remains neutral with regard to jurisdictional claims in published maps and institutional affiliations.